1968

A theoretical and experimental study of internal standardization in analytical emission spectroscopy

William Berkey Barnett
Iowa State University

69-4210

BARNETT, William Berkey, 1941-

A THEORETICAL AND EXPERIMENTAL STUDY OF INTERNAL STANDARDIZATION IN ANALYTICAL EMISSION SPECTROSCOPY.

Iowa State University, Ph.D., 1968
Chemistry, analytical

University Microfilms, Inc., Ann Arbor, Michigan

A THEORETICAL AND EXPERIMENTAL STUDY OF INTERNAL STANDARDIZATION IN ANALYTICAL EMISSION SPECTROSCOPY

by

William Berkey Barnett

A Dissertation Submitted to the
Graduate Faculty in Partial Fulfillment of
The Requirements for the Degree of
DOCTOR OF PHILOSOPHY

Major Subject: Analytical Chemistry

Approved:

Signature was redacted for privacy.

In Charge of Major Work

Signature was redacted for privacy.

Head of Major Department

Signature was redacted for privacy.

Dean of Graduate College

Iowa State University
Ames, Iowa
1968

TABLE OF CONTENTS

INTRODUCTION

The basis of modern analytical atomic spectroscopy was introduced in 1925 by Gerlach (1) when he reported on the use of an internal standard to replace the then current external standard technique. This procedure involved measuring the ratio of the intensity of the analytical line to the intensity of a line of a second constituent which is also present in the sample under cons eration and using this ratio to calculate concentration. In the four decades following Gerlach's innovation, quantitative analytical spectroscopy grew in sophistication and application so that today it is one of the most important methods available to the analyst. During the same period, the practitioners of the science evolved a series of "rules" which were intended to assure the selection of the best possible analytical line pair in every situation. These criteria are summarized in a variety of text books and papers in the field (2, pp. 90-104; 3, pp. 200-212; 4, pp. 56-58; 5) and divide themselves naturally into two groupings: those concerned with the choice of the internal standard element and those concerned with the choice of the specific lines to be used.

The criteria traditionally accepted as being important in the selection of the internal standard element are listed

below:

1. If the internal standard element is to be added to the sample, its original concentration should be negligibly low.
2. If added to the sample, the internal standard should be in a high state of purity with respect to the elements being determined.
3. The volatilization rate of the internal standard element and the analysis element should be similar
4. The ionization energy of the internal standard and analysis elements should be comparable.
5. The atomic weights of the two elements should be roughly the same.

The choice of the internal standard line involves four additional factors:

6. Both the internal standard and analysis lines should have the same excitation energies.
7. Both lines should be free of self-absorption.
8. When photographic methods of recording are used, both lines should be of approximately the same wavelength.
9. Both lines should be of approximately the same intensity, especially when photographic methods are used.

Fulfillment of these nine conditions, in light of present knowledge, constitutes the ideal case. In practical analytical work, however, it is not usually possible to take all conditions into account, making compromises a necessity.

The information summarized in the publications cited above is deficient in two respects: (a) there is little indication of which factors are most important when inevitable compromises become necessary or what the effect of a "mismatch" will be; and (b) the partition function behavior of the two elements and its effect on the analytical ratio has been totally ignored. Consideration of this latter factor is especially important since it affects the excitation (Boltzmann) and ionization (Saha-Eggert) equations.

Several authors have recognized that there is a lack of information and have attempted to alert the practicing analyst to the implications of some of the factors involved. Boumans (6), for example, has computed correction factors to be added to excitation and ionization potentials to compensate for the contribution of partition functions to the analytical intensity ratio when the spectra are excited in a dc arc. Margoshes (7) also considered many of these same problems and emphasized particularly the importance of ionization, a factor which had previously been relegated to one of minor importance by Ahrens and Taylor (2, p. 91).

The difficulty of quantitatively studying the relevant factors is a result of the complexity of the processes normally occurring in spectral excitation sources. The dc arc, for example, suffers from the problems of instability, selective vaporization, spatial inhomogeneity, and chemical complexity in the plasma column. The high voltage ac condensed spark has the additional disadvantage of wide variation in temperature during the course of a single spark train. As a result, an attempt to correlate the results of calculations using the Boltzmann or Saha-Eggert equations to such an experimental situation must be considered semi-empirical at best.

In recent years the application of the induction-coupled plasma to analytical spectroscopy (8,9) provided a source which simplifies the experimental situation: the discharge is relatively stable with time; the plasma is composed of a pure argon atmosphere without electrode contamination to complicate the chemistry; the sample can be fed into the discharge in solution form offering good control of both flow rate and composition; and, by a simple profiling technique, it is possible to study the behavior of an analytical line pair as temperature and electron density change. These simplifications also make it feasible to construct a computer-based model of the same source utilizing well accepted theoretical principles. In this way the question of choosing a good analysis line pair can be approached simultaneously

from two directions. This dual study constitutes the subject of this dissertation.

BASIC THEORETICAL CONSIDERATIONS

In analytical emission spectroscopy, the relative concentrations (c) of the analysis element (X) and internal standard element (R) are assumed to be some function of the spectral intensity ratio $I_{(X)}/I_{(R)}$:

$$\frac{c_{(X)}}{c_{(R)}} = f(I_{(X)}/I_{(R)}). \qquad (1)$$

In the usual case, where a series of standards are utilized to construct an analytical curve, the functional relationship of Equation 1 is immaterial. In most cases, a simple proportionality constant adequately describes the actual result.

The problem facing the analyst is the choice of an analytical and internal standard line so that under the influence of all experimental variables, except concentration, the intensity ratio will remain constant. Some of the possible variables include detector (photographic or photoelectric) response, changes in system optics, and temperature or electron density fluctuations in the source. The latter two variables will be the major concern of this dissertation.

Theoretically, it is possible to derive an equation describing the emitted intensity of an atomic spectral line

from a source. Several authors (10,11,12) have presented versions of this derivation which require only the assumption of local thermodynamic equilibrium existing in the discharge. Additional writers (13,14,15,16) have concluded that for many discharges at atmospheric pressure, this is a valid assumption.

If this assumption is accepted, the basic equation for the measured intensity ($I_{qp(X^o)}$) of a line of un-ionized element X undergoing a transition from electronic state q to p is

$$I_{qp(X^o)} = C\, n_{(X^o)}\, A_{qp}\, h\, \nu_{qp}\, \frac{g_q}{Q_{(X^o)}} \exp(-E_q/kT). \qquad (2)$$

In this expression C represents an instrumental parameter, $n_{(X^o)}$ the density of neutral atoms of element X in the discharge (in this dissertation $n_{(X)}$ is assumed to be proportional to $N_{(X)}$, the total amount of X in the source), A_{qp} the Einstein transition probability for the q to p transition, h is Planck's constant, ν_{qp} the frequency of the emitted line, g_q the statistical weight of state q, $Q_{(X^o)}$ the total partition function of element X in its un-ionized state, E_q the energy of state q, k is Boltzman's constant and T the temperature in degrees Kelvin. A similar expression for the internal standard element (R) is as follows:

$$I_{sr(R^o)} = C\, n_{(R^o)}\, A_{sr}\, h\, \nu_{sr}\, \frac{g_s}{Q_{(R^o)}} \exp(-E_s/kT). \qquad (3)$$

Since it is experimentally difficult to measure absolute intensities and because the present study deals with intensity ratio behavior, Equation 2 can be divided by Equation 3 to yield

$$\frac{I_{qp(X^o)}}{I_{sr(R^o)}} = \frac{n_{(X^o)}\ A_{qp}\ \nu_{qp}\ g_q\ Q_{(R^o)}}{n_{(R^o)}\ A_{sr}\ \nu_{sr}\ g_s\ Q_{(X^o)}} \exp[(E_s - E_q)/kT]. \qquad (4)$$

An equivalent expression could also be written for the intensity ratio of two ion lines by substituting $n_{(X^+)}$ and $n_{(R^+)}$ for $n_{(X^o)}$ and $n_{(R^o)}$ along with $Q_{(R^+)}$ and $Q_{(X^+)}$ for $Q_{(R^o)}$ and $Q_{(X^o)}$.

Examination of Equation 4 suggests several possible causes of intensity ratio deviation during excitation temperature fluctuations and thus areas of investigation for the present study: relationship of the excitation energies of the two lines, the partition function ratio, and the variation of $n_{(X^o)}/n_{(R^o)}$ (or $n_{(X^+)}/n_{(R^+)}$) as a result of ionization. Other possibilities which will not be considered explicitly in this chapter include variations in $n_{(X)}/n_{(R)}$ due to chemical reactions and, since the above equations assume that the emitted intensity is the observed intensity, the role of self-absorption.

Excitation Energy

The simplest and most obvious experimental variable emerging from Equation 4 is the excitation energy difference between the two lines. Also, "matching" the excitation energy of the analytical and internal standard lines is the most widely recognized prerequisite for a good pair.

"How much difference between the two excitation energies is allowable?" constitutes a common question. One often accepted "rule of thumb" suggests that any mismatch of 1 ev or less is acceptable. A more quantitative answer is given by assuming two lines of the same element. In this case $n_{(X^o)} = n_{(R^o)}$ and $Q_{(R^o)} = Q_{(X^o)}$ (or $n_{(X^+)} = n_{(R^+)}$ and $Q_{(R^+)} = Q_{(X^+)}$ and thus cancel out. Since all other terms except the exponential term are constants, Equation 4 reduces to

$$\frac{I_{qp(X^o)}}{I_{sr(X^o)}} = C' \exp[(E_s - E_q)/kT] \qquad (5)$$

which only contains one temperature dependent term. By taking the natural logarithms of both sides and differentiating, it is possible to show that

$$\frac{d\left[\frac{I_{qp(X^o)}}{I_{sr(X^o)}}\right]}{\frac{I_{qp(X^o)}}{I_{sr(X^o)}}} = -\frac{(E_s - E_q)}{kT^2}\, dT. \qquad (6)$$

This equation says that the relative variation of the intensity ratio is directly proportional to the difference in excitation energies and the fluctuations in temperature and inversely proportional to the square of temperature. As $(E_s - E_q)$ approaches zero, the relative error in the intensity ratio also approaches zero forming the basis of the widely accepted practice of matching excitation energies of the analysis and internal standard lines. It is also apparent that at higher temperatures, a greater excitation energy difference can be tolerated (assuming a constant error in temperature) for the same uncertainty in the intensity ratio.

The Partition Function

The second temperature-dependent term in this equation involves the partition functions, $Q_{(R^o)}/Q_{(X^o)}$. The total partition function of an atom (or ion) is defined (17, p. 342) by the equation

$$Q_{(X^o)} = Q_\epsilon \frac{(2 \pi m_{a(X^o)})^{3/2} (k T)^{5/2} N_{(X^o)}}{p_{(X^o)} h^3} \qquad (7)$$

with k, T, and h having the same significance as in previous equations, $m_{a(X^o)}$ being the mass of the atom in grams, N the total number of X^o, p the partial pressure of X^o and Q_ϵ the electronic partition function as a summation over all electronic energy levels of an atom or ion as follows:

$$Q_\epsilon = g_1 + g_2\exp(-E_2/kT) + g_3\exp(-E_3/kT) + \ldots \quad (8)$$

Here the g's are the statistical weights of the electronic energy levels with energies E. The ratio $Q_{(R^o)}/Q_{(X^o)}$ now yields

$$\frac{Q_{(R^o)}}{Q_{(X^o)}} = \frac{m_{a(R^o)}^{3/2}}{m_{a(X^o)}^{3/2}} \frac{Q_{\epsilon(R^o)}}{Q_{\epsilon(X^o)}} . \quad (9)$$

Thus, only the electronic portion of the partition function must be considered further in a discussion of intensity ratio behavior.

The partition function can actually be considered as part of the excitation term of the element of interest since the expression

$$\frac{g_q\exp(-E_q/kT)}{Q_{(X^o)}} \quad (10)$$

defines the probability that electronic state q of atom X^o will be populated. Thus, the notion that matching the excitation energies will guarantee a constant relative population of the upper states of the two elements and, as a consequence, a constant intensity ratio is not correct. Only when the relative values of Equation 10 are constant, will that goal be achieved.

Unfortunately, it is much more difficult to obtain a match between partition function behavior than is possible

when only the excitation energy is considered. Also, since many modern sources such as the induction-coupled plasma (14) and the high frequency spark have temperatures purported to be in excess of 10000°K, this quantity is even more important and must be taken into account to adequately account for the observed behavior.

Calculations of partition functions as a function of temperature normally utilize Equation 8 and the energy values quoted by Moore (18) for the atoms and ions of interest. At lower temperatures (<8000°K) the summation proceeds until succeeding terms become insignificant. However, at higher temperatures it becomes necessary to define a cutoff point to which the sum is carried.

The normal method is to sum over all energy levels (q) for which $E_{q(X)} \leq E_{i(X)} - \Delta E_{i(X)}$, where $E_{q(X)}$ represents the energies of the levels being summed, $E_{i(X)}$ is the normally reported ionization energy of the atom or ion and $\Delta E_{i(X)}$ is the lowering of the ionization energy due to the presence of microfields caused by charged particles in the neighborhood of the element being ionized.

Several authors (19, pp. 231-261; 20,21,22) have discussed the various theories for calculating ΔE_i. The most widely applied relation has been that of Unsöld which considered that the atom of interest, located in a plasma cloud, was effectively perturbed only by its nearest neighbors. His

considerations resulted in the expression

$$\Delta E_i = 3\ e^2\ (z+1)^{2/3}\ (4\pi n_{(e^-)}/3)^{1/3} \qquad (11)$$

where z is the state of ionization (z=0 for an atom, 1 for a singly ionized atom, etc.), $n_{(e^-)}$ is the electron density of the plasma and e the electronic charge. Evaluation of the constants in this expression produced

$$\Delta E_i\ (\text{in cm}^{-1}) = 5.61 \times 10^{-3}\ (z+1)^{2/3} n_{(e^-)}^{1/3}. \qquad (12)$$

This expression was easily applied since only a knowledge of the electron density was needed.

In a later paper, Olsen (23) emphasized that below a critical electron density ($n_{(e^-)}$) of $\sim 10^{19}$ cm^{-3}, true of all laboratory plasmas, only the effect of the Debye polarization should be considered. This led to values smaller than Unsöld's equation by an average factor of four. In practice, the Debye radius (r_D) is first calculated (19, p. 429; 23) from

$$r_D = \left[\frac{kT}{4\pi\ e^2 \sum_j n_{(X_j)} z^2_{(X_j)}} \right]^{\frac{1}{2}} \qquad (13)$$

where e is the charge on the electron, the summation is over the density of all particles $n_{(X_j)}$ with charge $z_{(X_j)}$, and r_D is in cm. The value of ΔE_i is then given by

$$\Delta E_{i(X_j)} = (z_{(X_j)} + 1) \frac{e^2}{r_D} . \qquad (14)$$

This problem was also treated theoretically by Ecker and Kröll (24) who obtained a similar conclusion.

In the literature of analytical emission spectroscopy, the partition function has usually been ignored completely or approximated by the statistical weight (g) of the ground state. In other cases the partition function was "just a number" needed in order to apply some equation. However, Boumans (6, pp. 99-102) accounted for the partition function in dc arc excitation over a temperature range of 4500 - 6500°K by computing a correction factor for the excitation potential. Thus an effective excitation potential was obtained and lines could be matched on this basis. These corrections, calculated for 54 elements, ranged from 0.05 to 0.95 ev. Since these corrections approximate the magnitude of mismatch allowed in some analytical situations, Boumans concluded that the normal correction was too small to arouse much interest from practicing analytical spectroscopists for line pair selection.

Ionization

Ionization in spectral sources has been treated in various ways depending on the temperatures involved. Some authors, for example Boumans (6, pp. 156-170), Margoshes (7),

Mavrodineanu and Boiteux (12), and Corliss and Bozman (13, pp. viii-xi), only considered the case of single ionization for flame or arc discharges. Others, Olsen (23,25,26), Drellishak (20,27) and Dewan (28), were concerned with sources at higher temperatures and thus accounted for multiple ionizations. Dewan also considered non-equilibrium conditions. Since many laboratory sources possess temperatures adequate to produce a significant number of doubly ionized atoms, two stages have been included in the treatment presented here. Extension to include three or four stages is readily made but, since these extensions tend to obscure the functional relationships, they were not considered.

The basic concept of thermal ionization, introduced by Eggert (29) and Saha (30,31), is simply an application of the mass action law to ionization equilibria. In this case one is considering reactions of the type

$$X \rightleftarrows X^+ + e^- \quad \text{and} \quad X^+ \rightleftarrows X^{++} + e^- \tag{15}$$

for which equilibrium constants can be written:

$$K_{(X^o \rightarrow X^+)} = \frac{n_{(X^+)} n_{(e^-)}}{n_{(X^o)}} \tag{16}$$

$$K_{(X^+ \rightarrow X^{++})} = \frac{n_{(X^{++})} n_{(e^-)}}{n_{(X^+)}} \tag{17}$$

In all cases n designates the density (number/cm^3) of the nuclide which is subscripted. The behavior of these

equilibrium constants as a function of temperature is shown by the Saha-Eggert equation:

$$K_{(X^o \rightarrow X^+)} = \frac{(2\pi m_{(e^-)} kT)^{3/2}}{h^3} \frac{2Q_{(X^+)}}{Q_{(X^o)}} \exp(-E_{i(X^o)}/kT) \qquad (18)$$

$$K_{(X^+ \rightarrow X^{++})} = \frac{(2\pi m_{(e^-)} kT)^{3/2}}{h^3} \frac{2Q_{(X^{++})}}{Q_{(X^+)}} \exp(-E_{i(X^+)}/kT). \qquad (19)$$

Here k, T, h, and Q have the same meaning as in previous equations, $m_{(e^-)}$ represents the mass of the electron and E_i the ionization energy of the reaction in question.

An inspection of Equation 4 indicates that it is the behavior of the ratio $n_{(X^o)}/n_{(R^o)}$ (or $n_{(X^+)}/n_{(R^+)}$) in terms of the total ratio $n_{(X)}/n_{(R)}$ which is of interest. If Equations 16 and 17 are considered with the relationship

$$n_{(X)} = n_{(X^o)} + n_{(X^+)} + n_{(X^{++})} \qquad (20)$$

then it is possible to derive expressions for the two cases:

$$\frac{n_{(X^o)}}{n_{(R^o)}} = \frac{n_{(X)}(n^2_{(e^-)} + K_{(R^o \rightarrow R^+)} n_{(e^-)} + K_{(R^o \rightarrow R^+)} K_{(R^+ \rightarrow R^{++})})}{n_{(R)}(n^2_{(e^-)} + K_{(X^o \rightarrow X^+)} n_{(e^-)} + K_{(X^o \rightarrow X^+)} K_{(X^+ \rightarrow X^{++})})} \qquad (21)$$

$$\frac{n_{(X^+)}}{n_{(R^+)}} = \left[\frac{n_{(X)} K_{(X^o \rightarrow X^+)}}{n_{(R)} K_{(R^o \rightarrow R^+)}}\right] \left[\frac{(n^2_{(e^-)} + K_{(R^o \rightarrow R^+)} n_{(e^-)} + K_{(R^o \rightarrow R^+)} K_{(R^+ \rightarrow R^{++})})}{(n^2_{(e^-)} + K_{(X^o \rightarrow X^+)} n_{(e^-)} + K_{(X^o \rightarrow X^+)} K_{(X^+ \rightarrow X^{++})})}\right]. \qquad (22)$$

Equations 21 and 22 clearly show that ionization processes are complex and require consideration of many factors. Also, the presence in Equation 22 of the $K_{(X^o \rightarrow X^+)}/K_{(R^o \rightarrow R^+)}$ ratio indicates that the ionization contribution will be different for the case of two ion lines than for two atom lines.

One point which is frequently over-looked in discussing ionization effects is the role of the atom and ion parition functions in determining the values of the Saha-Eggert equilibrium constants. Therefore, to say that two elements with the same ionization energies will behave in a similar manner is not necessarily correct. Depending on the relative partition functions (which can change as a function of temperature), elements which may be considered "matched" in regard to their ionization energy may actually exhibit quite different ionization versus temperature behavior.

CONSTRUCTION OF THE MODEL

Even the simplified experimental source chosen for this study and outlined in the introduction requires consideration of a large number of variables. To examine the various interactions, a computer-based model was constructed which integrates the various factors and allows a number of predictions to be made (see Appendix for details and program listing).

To make the computer model manageable, the following experimental conditions and assumptions were imposed:

1. The argon plasma is fed with a water solution containing metal salts.
2. The plasma is in local thermodynamic equilibrium.
3. No self-absorption occurs.
4. All elements are present as monatomic gases.
5. The ideal gas law with the Debye-Hückel correction applies.
6. No chemical reactions occur.

7. Chloride is the common anion.
8. The plasma is composed of a uniform mixture of the elements.

The validity of some of these assumptions may well be questioned, but all of them either made the program feasible or simplified the experimental situation. As will be shown in a subsequent chapter, the resultant model is reasonably valid when judged against the ultimate standard of compatibility with actual experimental examples.

Several significant papers (20,23,25,26,27), which were concerned with the calculation of the properties of argon plasmas at or near atmospheric pressure, were very helpful in constructing the model. These papers covered a temperature range which encompassed most of the region of interest in this study. In contrast to the present work, however, these studies only needed to account for argon and its ions plus electrons whereas the present work accounted for up to

seven elements, their ions, and the electron density resulting from the presence of all seven elements. Four of these elements were considered permanent plasma constituents: argon, the primary plasma gas; hydrogen and oxygen from the sample solvent, i.e. water; and chlorine, chosen as the common anion of all samples. In addition, the two metals whose intensity ratio was being studied were present, and provision was made for a third metal in order to study the effect of the presence of an electron donor.

The chosen variables for completely describing the model plasma were pressure, temperature, and stoichiometry (the number of atoms of each constituent put into the discharge). Boumans (32) has also concluded that three independent variables must be established, but chose to measure electron density and temperature which, along with pressure, then determined the degree of ionization of the various constituents in the discharge.

To calculate electron density from the established stoichiometry, two equations in addition to those presented thus far are needed: the electroneutrality condition

$$n_{(e^-)} = \sum_i n_{(X_i^+)} + 2\sum_i n_{(X_i^{++})}; \qquad (23)$$

and the Debye-Hückel modified ideal gas law (23) to determine total particle density from the pressure surrounding the discharge

$$n_{(total)} = \frac{1}{kT}\left[p - \frac{kT}{24\pi r_D^3}\right] . \qquad (24)$$

In the above equation p is the pressure surrounding the plasma and r_D is the Debye radius calculated from Equation 13.

In the computer program, electron density was obtained at each temperature of interest by an iterative method in contrast to the relatively direct methods employed by Olsen or Drellishak, et al., but similar to the method used by Diermeier and Krempl (33). The chosen procedure allowed a straight forward consideration of the 14 Saha-Eggert equations (7 constituents with 2 each) along with Equations 23 and 24. During the construction of the program it was empirically determined that successive $n_{(e^-)}$ values oscillated about the final, self-consistent one. This fact was exploited to expedite the convergence of the iteration.

Once the plasma composition was established at a particular temperature, the program tabulated a series of descriptive parameters including: the ionization energy lowering (ΔE_i); the total particle density; the electron density ($n_{(e^-)}$); per cent and particle density of each constituent present as neutral atom, first and second ion; and the partition function (Q) of each constituent for each stage of ionization. Examination of this information gave a good picture of the plasma properties and indicated the nature of

some emission characteristics it should exhibit.

After information for a range of temperatures was generated, the program calculated, tabulated, and plotted as a function of temperature the relative behavior of eight parameters which were of interest in choosing good analytical line pairs. Some of these were: $I_{qp(X^o)}/I_{sr(R^o)}$; $I_{qp(X^+)}/I_{sr(R^+)}$; $n_{(X^o)}/n_{(R^o)}$; $n_{(X^+)}/n_{(R^+)}$; $Q_{(R^o)}/Q_{(X^o)}$; and $Q_{(R^+)}/Q_{(X^+)}$. In addition the behavior of the exponential terms for both the atom and ion cases, based on the excitation energies of the lines being considered, were calculated. The importance of these parameters is readily apparent in Equation 4.

The Partition Function Problem

To the uninitiated, calculation of partition functions for the elements appears to be one of the simplest steps in any theoretical undertaking. As was pointed out in Chapter 2, it is only necessary to sum over all energy levels of the element of interest up to the lowered ionization energy according to Equation 8. However, as frequently happens, these calculations became one of the most troublesome phases of the current study and emphasized some of the serious shortcomings in our knowledge of basic spectroscopic data.

The basic problem was that the most complete list of atomic energy levels (18) included only a fraction of the

levels of a particular element. Normally, the missing levels were reasonably high in energy, leading to few problems over the temperature range up to ~7000°K. However, large discrepancies, sometimes as high as 50 per cent, occurred in the partition function at higher temperatures.

The literature contains several suggestions for overcoming the difficulty and obtaining valid numbers. Drawin and Felenbok (19, pp. 258-260) suggested completing each observed spectral series using the Ritz formula. This formula, as presented by Kuhn (34, p. 137), requires calculation of the effective quantum number (n^*) using

$$n^* = \left[\frac{R}{\Delta}\right]^{\frac{1}{2}} \tag{25}$$

where R is the Rydberg constant (109737.3 cm^{-1}) and Δ is given by

$$\Delta = E_{i(X^o)} - E_{q(X^o)} \tag{26}$$

with $E_{i(X^o)}$ being the element ionization energy and $E_{q(X^o)}$ the energy of the particular level of interest. The Ritz formula can then be written as

$$n^* = n - \alpha - \frac{1}{n^2}\beta \ . \tag{27}$$

In practice, the last two existing members of the series in question are used to evaluate α and β which are then used to calculate the remaining members of the series. When a spectral

series is predicted for which there are no observed members, a series as closely related as possible is chosen and its degeneracy increased to account for the unobserved series. Although this method should provide a reasonably accurate extension of the series for elements with relatively simple energy level schemes, its application to elements with complex terms seemed too elaborate. An alternate scheme, suggested by Griem (15, pp. 140-142), uses the levels for all principal quantum numbers which are reasonably complete to calculate a partition function. A correction term is added based on a hydrogenic structure but accounting for the differences in degeneracy. First one selects n', representing the highest usable principal quantum number (n' will frequently be the lowest quantum number of the element), and defines n_{max} according to

$$n_{max} \leq \left[\frac{E_H}{\Delta E_{i(X)}}\right]^{\frac{1}{2}} \tag{28}$$

where E_H is the hydrogen series limit (109679 cm^{-1}) and $\Delta E_{i(X)}$ is the amount of ionization energy lowering for the system. The complete partition function is then calculated using

$$Q_{(X)} \approx \sum_q g_{q(X)} \exp(-E_{q(X)}/kT) + (2S + 1)(2L + 1) \sum_{n=n'+1}^{n_{max}} 2n^2 \exp\left[-\frac{E_{i(X)} - E_H/n^2}{kT}\right] \tag{29}$$

where the first sum is over those levels (q) which are included in the complete or nearly complete quantum levels (up to $n=n'$) and the second sum is the correction. In the second sum, S and L are the spin and orbital momenta of the next stage of ionization (i.e., the first ion, since we are concerned only with the un-ionized atom here), $E_{i(X)}$ is the ionization energy of the element and E_H and n_{max} are as defined above.

The implications of these procedures may be more fully appreciated if one considers magnesium, which has a relatively simple spectrum. All predicted terms of the Mg I isoelectronic series as given by Moore (18) are tabulated in Table 1. In addition, the degeneracy of each term, the number of observed terms, and number of terms of the series when completed to within 806 cm^{-1} (the $\Delta E_{i(X^o)}$ chosen for these comparison calculations) of the ionization energy are listed. Finally, for those terms which are not observed at all, the series to which the extra degeneracy is added are shown. Examination of this information revealed that less than half of the series have been observed at all and, significantly, none of the terms with high degeneracy (G, H, and I) which will contribute heavily to the partition function at high temperatures.

Continuing with the examination of magnesium, several calculations of its partition function are presented in Table 2. Here the results were obtained by: (a) simply summing

Table 1. Properties of the spectral series of Mg I

Series Designation	Degeneracy	# Observed Terms	# Terms After Completion	Represented by
^1S	1	5	11	
^3S	3	11	11	
^1P	3			$^1P^o$
^3P	9	1	7	
$^1P^o$	3	3	10	
$^3P^o$	9	5	10	
^1D	5	11	11	
^3D	15	12	12	
$^1D^o$	5			^1D
$^3D^o$	15			^3D
^1F	7			$^1F^o$
^3F	21			$^3F^o$
$^1F^o$	7	11	11	
$^3F^o$	21	9	9	
^1G	9			$^1F^o$
^3G	27			$^3F^o$
$^1G^o$	9			$^1F^o$
$^3G^o$	27			$^3F^o$
^1H	11			$^1F^o$
^3H	33			$^3F^o$
$^1H^o$	11			$^1F^o$

Table 1. (Continued)

Series Designation	Degeneracy	# Observed Terms	# Terms After Completion	Represented by
$^3H^o$	33			$^3F^o$
^1I	13			$^1F^o$
^3I	39			$^3F^o$

Table 2. Comparison of partition function values for Mg I computed using several methods

Temperature (°K)	Levels Only	Extended Levels	Approximation Method	Drawin & Felenbok
3500	1.001	1.001	1.001	1.001
4051	1.004	1.004	1.004	1.004
4690	1.011	1.011	1.011	1.011
5171	1.021	1.021	1.021	1.021
5701	1.037	1.038	1.037	1.037
6285	1.063	1.066	1.064	1.064
6929	1.103	1.113	1.107	1.109
7640	1.164	1.194	1.178	1.183
8423	1.257	1.340	1.301	1.310
9286	1.398	1.609	1.517	1.536
10238	1.615	2.105	1.907	1.943
11287	1.951	3.001	2.604	2.671
12444	2.468	4.571	3.818	3.935
13720	3.253	7.206	5.858	6.054
14406	3.780	9.080	7.312	7.562

over the listed levels; (b) completing each series and accounting for the unobserved series before summing; (c) by using Griem's approximation method (15); and (d) one set of literature values (19, p. 300) for comparison.

The most significant trend illustrated by Table 2 is that up to about 7000°K all of the calculations gave approximately the same result. As higher temperatures were approached greater deviations became increasingly obvious. Beyond 7000°K, the Griem and Drawin and Felenbok calculations gave parallel trends. Since Griem's computations are simpler, his method was selected for this study.

Plasma Properties as Defined by the Model

For most of the calculations which follow, an "example" plasma was defined; the flow rates and solute concentrations selected are outlined in Table 3. To gain a more detailed physical description of the type of discharge being described, the reader is referred to the papers by Greenfield, Jones and Berry (8) or Wendt and Fassel (9).

Table 3. Assumed properties of the "example" plasma

Argon flow rate	10 l/min
Solution flow rate	0.1 ml/min
Solvent	Water in all cases
Solute concentration	5.0 gms/100 ml total metal present
Anion present	Chloride in all cases

Since electron density was one of the most important descriptors of the plasma, first consideration was given to this quantity in the present study. The electron density of the "example" plasma with magnesium as the metal in the solution and, for comparison, the electron density behavior of a pure argon plasma are plotted in Figure 1. It is seen that at higher temperatures, both electron densities showed identical behavior, but at lower temperatures the "example" plasma containing magnesium had a considerably higher electron density. Thus, it is evident that the contribution of the sample is not negligible when plasma properties are discussed.

Figure 2 presents additional particle density information for the "example" plasma; again the solute metal is magnesium. This figure clearly shows that at low temperatures the sample dominates the electron production process, demonstrated by the simultaneous and equivalent rise of electron density (e^-) and Mg^+. At higher temperatures the argon dominates, as is shown by the parallel e^- and Ar^+ curves. Further examination of this figure indicates that Mg^{++} plays a very minor role, suggesting that the second ionization potential should not be important in internal standard selection unless temperatures in excess of 15000°K are anticipated.

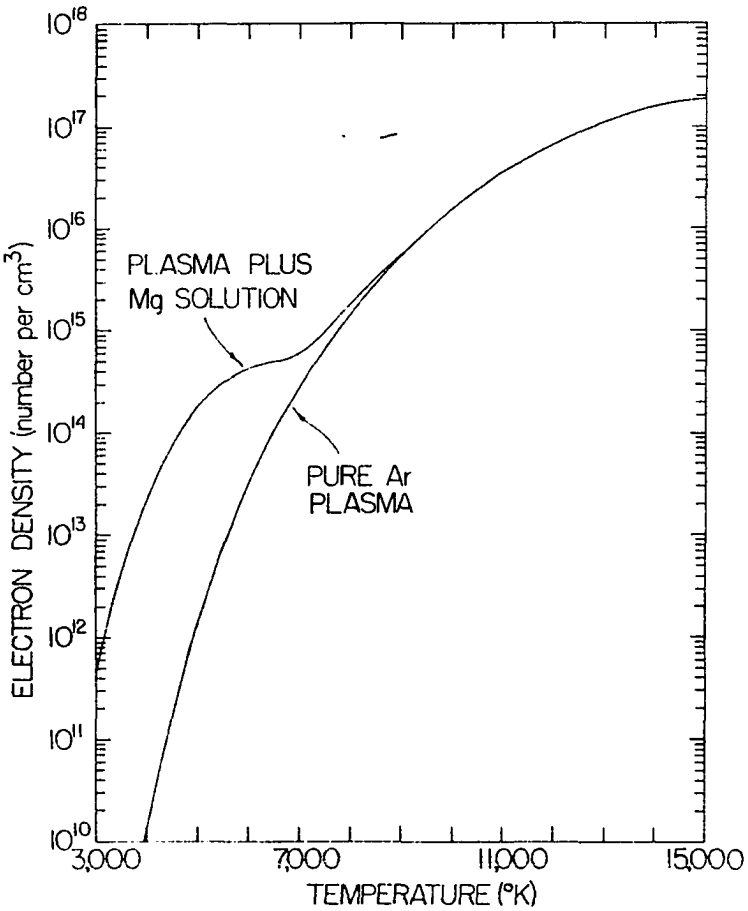

Figure 1. Comparison of the electron density variations of the solution fed plasma with the pure argon plasma

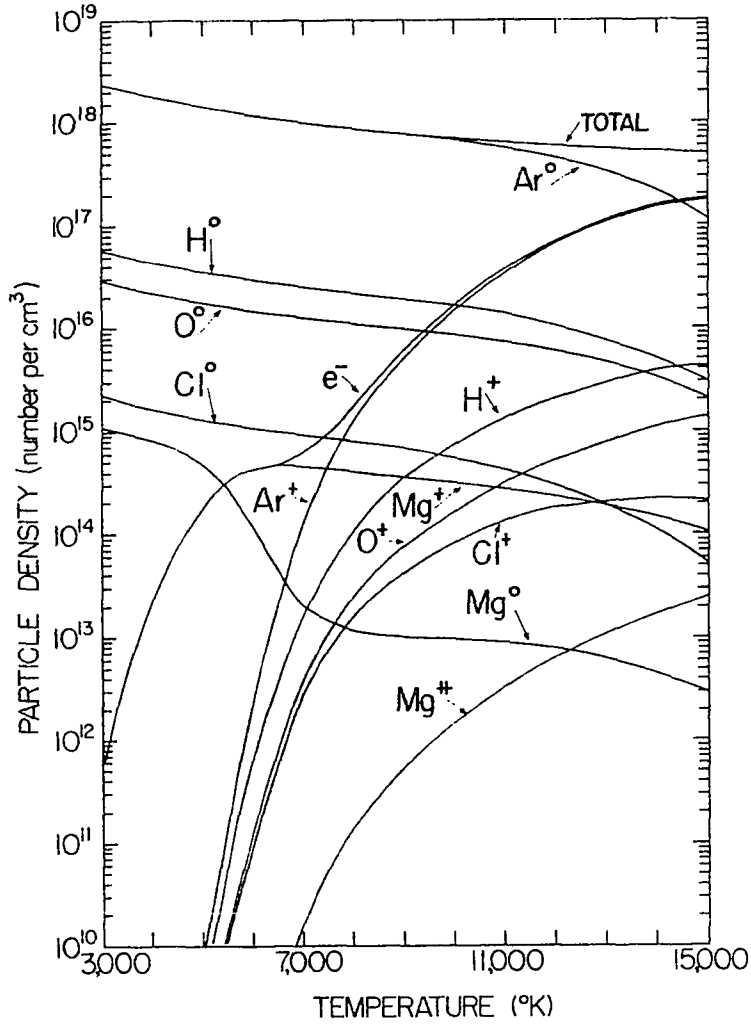

Figure 2. Density variations as a function of temperature for the solution fed, argon plasma

SAMPLE BEHAVIOR IN THE MODEL PLASMA

The manner in which a sample will behave in the model plasma is difficult to predict a priori. In this section I will present the results of a series of calculations which show how elements or their intensity ratios responded to the model plasma environment. Most of these calculations used "elements" which were fabricated to test intensity ratio behavior under carefully controlled conditions, allowing the reader to assess for himself the importance of some of the criteria previously discussed for his particular application.

The first of these calculations involved three real elements: Tl, Mg, and Cd. Figure 3 shows the percentages of each in the various states of ionization as a function of temperature. In all cases the "example" plasma, defined in the previous chapter, was used with only the solute metal being changed. The plot shows that the elements considered, which possess ionization energies encompassing the bulk of the common metals, change from almost completely un-ionized to 90% ionized over a temperature span of only 2000 degrees. Significantly this temperature occurs within the 4000 to 7000°K range which is commonly encountered in conventional arc-like discharges. Also, the temperature required for 50% ionization

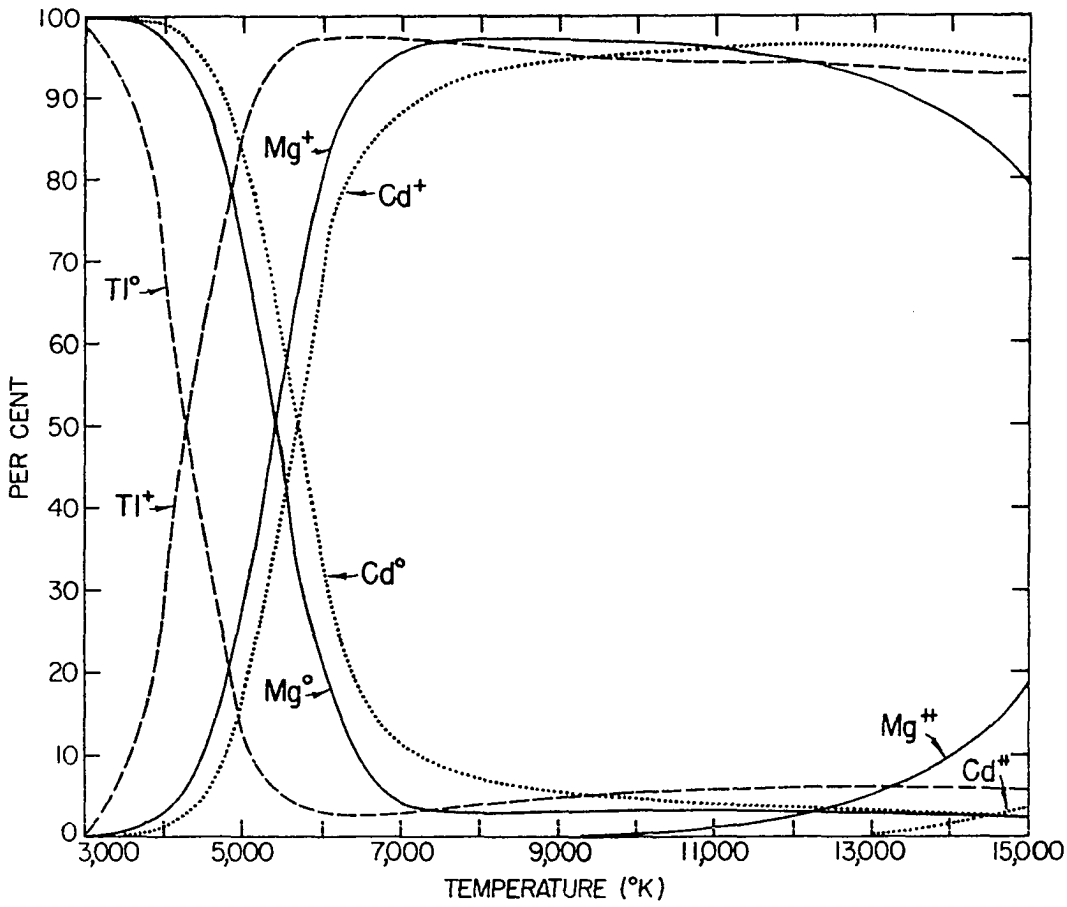

Figure 3. Percentage of several typical elements in each ionic stage versus temperature

for the three elements ranged from 4000 to 6000°K, an unexpectedly small interval for ionization energies varying from 49000 to 72000 cm^{-1}.

From these observations, several general conclusions may be drawn. Since the greatest ionization shifts occur in the 3000 to 8000°K temperature range, the atom or ion emission from any spectral source operating in this region would be subject to relatively large variations with small temperature changes. On the other hand, the atom line radiation from a source operating below 3000°K or the ion line radiation from a source above 8000°K should show greater stability. This may be one of the contributing factors to the lack of precision of the dc arc compared to the flame or high temperature spark.

Another implication inherent in the ionization behavior illustrated in Figure 3 concerns the choice of analysis and internal standard lines when ion lines are used. If the spectral source operates in the 8000 to 15000°K region, ionization behavior would not be of primary importance. If similar partition function behavior for the ions is assumed, only matching of the excitation energies of the lines, measured from the ground state of the ion, would be important.

Turning from the ionization properties of individual elements to intensity ratio behaviors, a natural starting point is with the excitation energy (exponential) term of Equation 4. As was shown in Equation 5, this factor can be

studied experimentally using two lines of the same element. This is also an easy way for the model program to calculate this behavior. In Figure 4 is shown the result over the 3000 to 15000°K temperature range for three values of $E_{q(X^o)} - E_{s(X^o)}$. The result for two ion lines would, of course, be the same.

The alert reader will recall that there is a second influence on the probability of population of an excited state and thus intensity ratio--the partition function. This term was examined for three typical neutral atom line pairs. If the ionization term $(n_{(X^o)}/n_{(R^o)})$ in Equation 4 is neglected, and $E_s - E_q = 0$, then the intensity ratio equation will reduce to

$$\frac{I_{qp(X^o)}}{I_{sr(R^o)}} = C \frac{Q_{(R^o)}}{Q_{(X^o)}} \quad . \tag{30}$$

The calculated results for the chosen element pairs are shown in Figure 5. This figure clearly illustrates the desirability of choosing internal standard element pairs which have a similar pattern in the disposition and degeneracy of their energy levels. This is the case for the Cu/Au line pair. For dissimilar patterns, such as Ca/Fe, a temperature excursion between 4000 and 8000°K can cause a four-fold change in the intensity ratio. Thus, the serious selection of internal standard element pairs requires the calculation of this behavior.

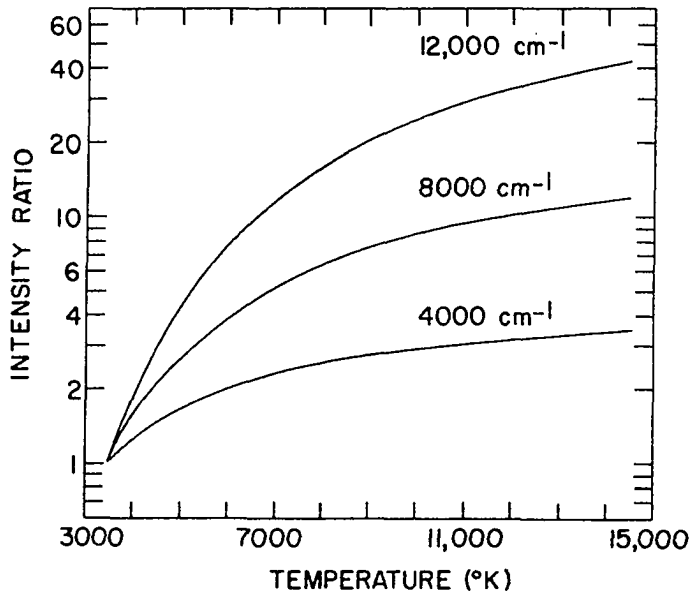

Figure 4. Intensity ratio behavior for three values of $E_{q(X^o)} - E_{s(X^o)}$

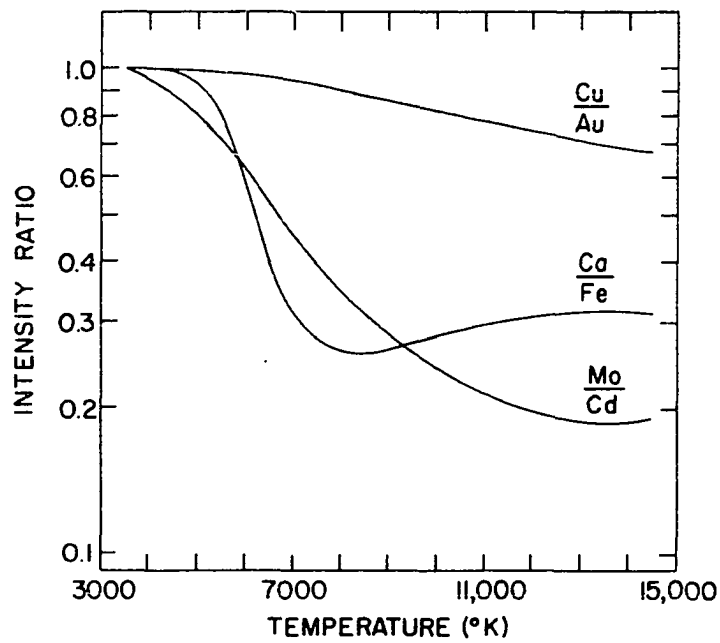

Figure 5. Intensity ratio behavior resulting from partition function variations with temperature

This is, in effect, what Boumans (6, p. 99) did when he calculated correction factors to be applied to atom excitation potentials for dc arc excitation. In this case, however, he was attempting to obtain a compensating effect by mismatching excitation potential values to correct for the partition function variation with temperature.

A comparison of Figure 5 with Figure 4 further emphasizes the importance of the partition function effect because in our examples some of the deviations approach those observed when $E_s - E_q = 8000\ cm^{-1}$. Although the chosen examples all involved neutral atom line pairs, others involving ion pairs were also studied, but the effect was usually less pronounced because the levels involved have higher energy values.

The influence of ionization on the intensity ratio behavior is even more complex than is the excitation process. There are now three factors to take into account: the relative ionization energy (E_i) of the two elements; the relative values of the $Q_{(X^+)}/Q_{(X^o)}$ and $Q_{(R^+)}/Q_{(R^o)}$ ratios which can vary with temperature; and variations in electron density in the source which will be dependent on temperature as well as the presence of other substances in the discharge. The importance of the first two factors is readily seen from Equation 18. The role played by electron density is apparent from Equations 15 and 16.

In order to systematically study these factors, fabricated "elements" and "lines" were used to which excitation energies and ionization energies could be assigned to meet the needs of the situation. Also, as Equation 8 suggests, it is possible to assign a partition function which remains constant with temperature by considering "elements" with only one energy level at 0.0 cm^{-1}. In this case $Q = 2J + 1$ and is temperature independent. Unless otherwise noted, the "example" plasma defined in Table 3 was used with 2.5 gms/100 ml of each element assumed for the total of 5.0 gms/100 ml.

In the first application of this procedure, the partition functions (Q) of neutral atom, first and second ion were all set to a value of 4.0 for both the analysis element (X) and the reference element (R). $E_{i(R^o)}$ was assigned a value of 64000 cm^{-1} while $E_{i(X^o)}$ was given values of 52000 cm^{-1}, 56000 cm^{-1}, and 60000 cm^{-1}. Excitation energies of the two "lines" in question were exactly matched.

Figures 6 and 7 show the results of these calculations for $I_{(X^o)}/I_{(R^o)}$ and $I_{(X^+)}/I_{(R^+)}$ respectively. It is immediately obvious that the two ratios behave quite differently. $I_{(X^o)}/I_{(R^o)}$ decreases rapidly, changing by a factor of 13 as temperature varies from 4300 to 6000°K, as element X begins to ionize and goes through a minimum value as element R "catches up".

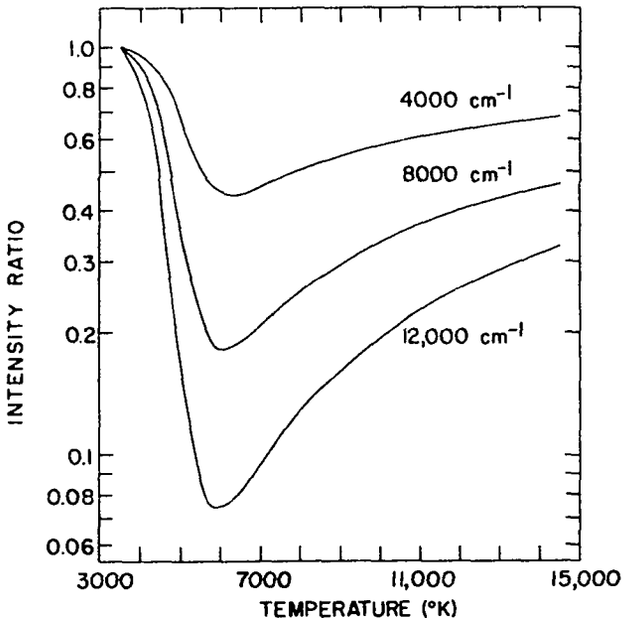

Figure 6. The behavior of $I_{(X^o)}/I_{(R^o)}$ for three different values of $E_{i(R^o)}-E_{i(X^o)}$

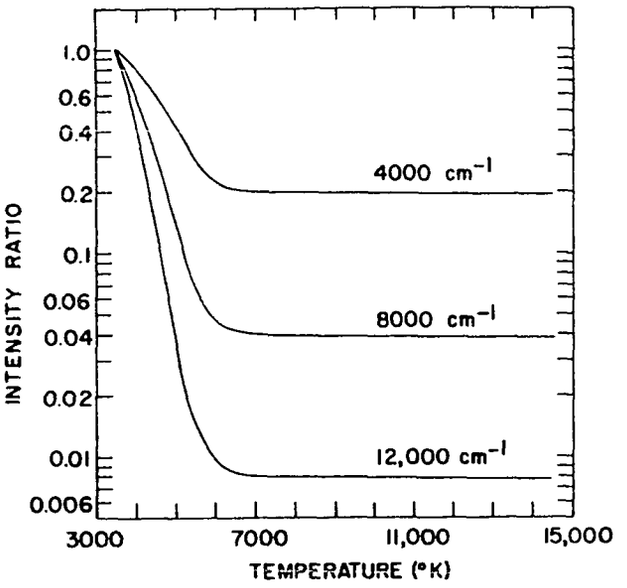

Figure 7. The behavior of $I_{(X^+)}/I_{(R^+)}$ for three different values of $E_{i(R^o)}-E_{i(X^o)}$

Figure 7 shows that $I_{(X^+)}/I_{(R^+)}$ does not parallel the neutral atom intensity ratio behavior. The very rapid decrease in $I_{(X^+)}/I_{(R^+)}$ occurs in the temperature region over which the degree of ionization of both elements is changing rapidly, but with significantly different rates. It is appropriate to note that if the $E_{i(X^+)}$ or $E_{i(R^+)}$ values were low enough (for this calculation both were assigned 180000 cm^{-1}) or if higher temperatures were reached, the shape of the curves would be modified by the influence of second ionization. For most elements examined in the course of this study, very little double ionization was observed, even at 15000°K (Figure 3 shows several examples).

One additional comparison of Figures 6 and 7 shows that the change of $I_{(X^+)}/I_{(R^+)}$ was significantly greater than $I_{(X^o)}/I_{(R^o)}$ in the 3000 to 7000 degree region. Equations 21 and 22 show that the latter contains an additional $K_{(X^o \rightarrow X^+)}/K_{(R^o \rightarrow R^+)}$ term, a ratio which varied considerably in this temperature range. Finally, it should be emphasized that the selection of different values for $E_{i(X^o)}$ and $E_{i(R^o)}$, even if $E_{i(R^o)}-E_{i(X^o)}$ were the same, would have caused the minimum point to occur at a different temperature.

The second significant factor in establishing the Saha-Eggert equilibrium constants is the relative value of the atom and ion partition functions. For this calculation I assigned $E_{i(X^o)} = E_{i(R^o)} = 60000$ cm^{-1}, set the partition

function ratio $Q_{(R^+)}/Q_{(R^o)}$ equal to 1.0 for all calculations, and gave the ratio $Q_{(X^+)}/Q_{(X^o)}$ three values: 8.0, 4.0, and 2.0. Referring to Equations 4, 21, and 22, it is apparent that since the ratio $K_{(X^o \rightarrow X^+)}/K_{(R^o \rightarrow R^+)}$ will now remain constant with temperature, the relative behavior of both $I_{(X^o)}/I_{(R^o)}$ and $I_{(X^+)}/I_{(R^+)}$ will be the same, shown in Figure 8. Examination of this figure again illustrates a very rapid intensity ratio change in the 4000 to 7000°K temperature region. Beyond 7000°K no deviation was observed, but in a situation involving real elements the ratio of atom and ion partition functions is likely to change significantly causing considerable deviation. Again the selection of 60000 cm^{-1} ionization energies was purely arbitrary and another value would have produced a curve which would have flattened at a different temperature.

Additional calculations were also made of the intensity ratio for two hypothetical elements considered earlier, i.e. the $Q_{(R^+)}/Q_{(R^o)}$ and $Q_{(X^+)}/Q_{(X^o)}$ ratios were the same and $E_{i(R^o)}$ = 64000 cm^{-1} while $E_{i(X^o)}$ = 52000 cm^{-1}, but for metal concentrations of only 0.02 gms/100 ml. In addition, for one of the calculations, 5.0 gms/100 ml of Sr, a well known electron donor, was also present. Figure 9 shows that the presence of the Sr shifted the temperature of the intensity ratio minimum almost 2000 degrees and produced a slight broadening of the latter curve. It is probable that

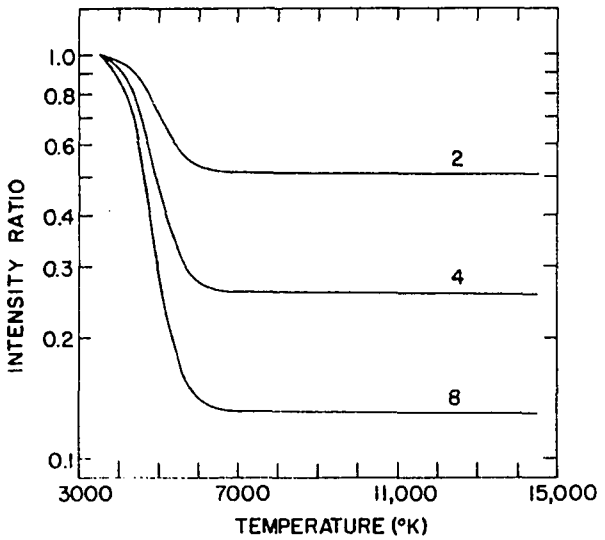

Figure 8. The behavior of $I_{(X^o)}/I_{(R^o)}$ or $I_{(X^+)}/I_{(R^+)}$ for three different values of $Q_{(X^+)}/Q_{(X^o)}$

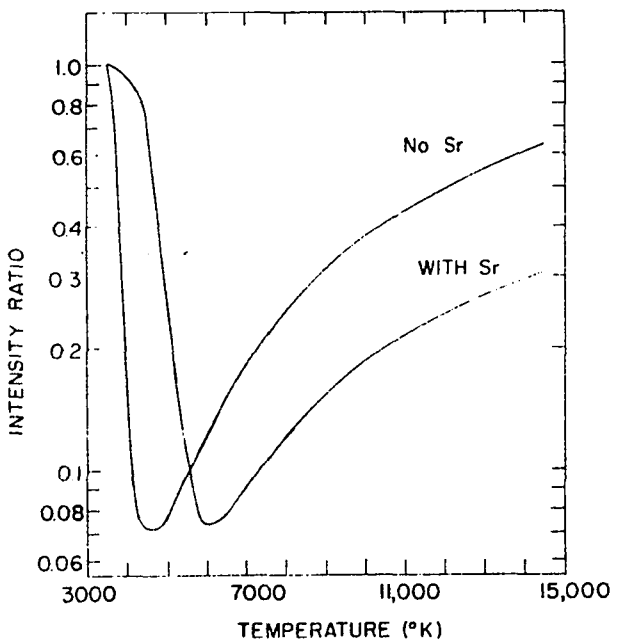

Figure 9. Illustration of the effect of $n_{(e^-)}$ on intensity ratio behavior

both of these effects would have been greater except that, as shown in Figure 1, argon ionization begins to become significant at about 7000°K nullifying the effect of the added strontium.

Application to an Analytical Situation

The preceding discussion has attempted to accomplish three primary objectives: review of the basic theory governing the intensity ratio behavior of an analytical line pair; describe the construction of a computer-based model of a simplified spectral source; and, using the model, explore line intensity or line pair intensity ratio behavior for a variety of lines and line pairs for real and hypothetical elements. In an attempt to summarize this material and relate it to problems of a more pratical nature, the author chose an actual analytical problem for consideration.

The selected example was the ASTM standard method for the dc arc analysis of nickel alloys (35, pp. 103-107). The author recognized that the model source did not duplicate the dc arc conditions, but it did allow examination of the behavior of several of the suggested analytical line pairs over a temperature range which included reported dc arc temperatures. For these calculations the "example" plasma

outlined in Table 3 was used with the solution containing 5 gms/100 ml of nickel and a proportionately lesser amount of the alloy elements.

The lines selected from the ASTM method for the calculations are outlined in Table 4. In all cases the Ni 2746.75 line was used as the internal standard. A brief examination of these data indicated that the largest excitation energy "mismatch" occurred for the Cu/Ni pair, 5817 cm^{-1}, while the ionization energy differences ranged up to 1121 cm^{-1} for the Fe/Ni combination. Thus, by traditional criteria, one is considering four reasonably well matched line pairs.

Table 4. Properties of analytical lines and elements selected for this study

Element	Wavelength (Å)	Excitation energy (cm^{-1})	Ionization energy (cm^{-1})
Co	3072.34	33946	63438
Cu	3247.54	30784	62317
Fe	2720.90	37158	63700
Mg	2852.13	35051	61669
Ni	2746.75	36601	61579

Figure 10 shows the calculated behavior of the intensity ratios for the 3000 to 9000°K temperature region. The most important feature to note, since this is a dc arc method, are the slopes of the intensity ratio versus temperature

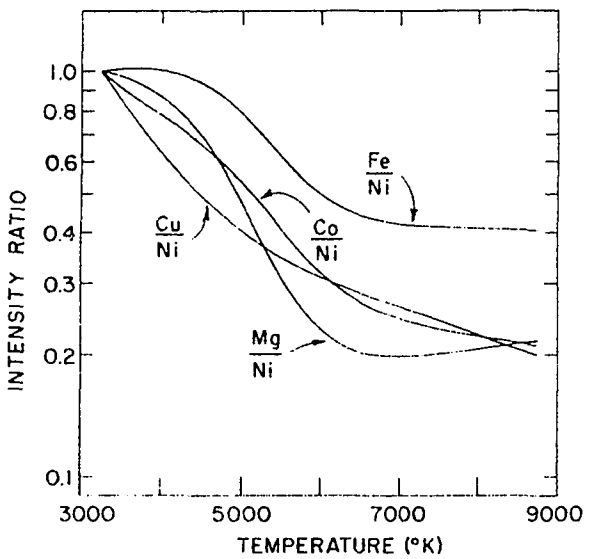

Figure 10. Intensity ratio behavior for four analytical line pairs selected from a standard method

curves in the temperature region of that source. If, for example, one assumes a median temperature of 5000 ± 250°K, per cent decrease in intensity ratio from the lower temperature to the higher would be as follows: Co/Ni 22%, Cu/Ni 15%, Fe/Ni 19%, and Mg/Ni 34%. The analytical line pair with the smallest change (Cu/Ni) should theoretically give the most precise results while the Mg/Ni pair should, by the same criterion, be the poorest choice of the four. Yet, if just the data in Table 4 are considered, the Mg/Ni line pair appears to be the best "matched" pair of the group. Clearly, the traditional criteria of just "matching" excitation and ionization energies are only part of the story. The energy

level configurations of the elements being studied, which controls their partition function behavior, is an equally important consideration. Thus the careful selection of internal standard line pairs requires the judicious balancing of the major temperature dependent factors, i.e., populations of excited states, degree of ionization, and partition function behavior.

EXPERIMENTAL FACILITIES

The experimental phase of this study employed the induction-coupled plasma torch which has recently received attention in the spectrochemical literature (8,9,36-40). Some of the advantages of this source noted in the references cited include:

1. The discharge is relatively stable with time.
2. The plasma is composed of pure argon without electrode material to complicate the chemistry.
3. The sample can be fed into the discharge as a solution offering good control of both rate of introduction and composition.
4. The temperature range covered encompasses that of many common laboratory spectral sources.

Thus, as was noted previously in the introduction, the induction-coupled plasma is far more manageable than the dc arc or ac spark for studying the excitation behavior of an analytical line pair. In addition, this source offers the opportunity for comparing experimental results with those calculated using the model.

The experimental equipment employed in this investigation consisted of three parts: the plasma generation power supply and plasma torch assembly; the aerosol production facility;

and the spectrometer and detector used for observing the emitted spectra. The principal components of this configuration are outlined in Table 5. Portions of this equipment have been adapted from that previously used by Wendt and Fassel (9).

The tuning and coupling unit, torch assembly, and aerosol generation chamber were mounted on a specially built, movable platform which allowed accurate vertical and horizontal adjustment of the plasma position relative to the optical axis (see Figure 11). For the atomic absorption portion of this study, a plane, front-surface mirror was mounted on the platform behind the plasma to reflect the primary source radiation through the discharge as shown in Figure 12.

Table 5. Experimental facilities employed

	Plasma Generation
Power supply	Variable frequency, 2.5 kw induction heater (model T-2.5-1-MC2-J-B, Lepel High Frequency Laboratories, Woodside, New York) equipped with a tuning and coupling unit to allow impedance matching and remote operation of the plasma. Operated at 31 MHz.
Coil	Solenoid type, 24 mm id, composed of two turns of 5 mm od copper tubing.
Coolant tube	Clear fused quartz, 20 mm od, 18 mm id, extending approximately 5 mm above the coil.

Table 5. (Continued)

Plasma tube	Clear fused quartz, 15 mm od, 13 mm id, centered within the coolant tube and terminating approximately 17 mm below the top of the coil.
Aerosol tube	Borosilicate glass, 5 mm id, 7 mm od, terminating approximately 100 mm below the coil.
Argon flow rates	Coolant: 18 l/min Plasma: 0.75 l/min Aerosol: 0.42 l/min
Aerosol introduction rate	Approximately 0.1 ml/min
Ignition	Graphite rod, not grounded, lowered into the high-field region until the plasma is formed and then withdrawn.
	Aerosol Generation
Power supply	Twelve watt, 870 KHz ultrasonic generator (Sonostat 631U, Siemens-Reiniger-Werke Ag., Erlangen, Germany).
Lens	A plano-concave acrylic plastic lens, 35.6 mm radius of curvature, 1.27 mm thick at the center, attached to the transducer assembly with epoxy glue.
Focusing chamber	Plexiglass, 82 mm id, equipped with 5 turns of 5 mm od copper tubing which carried cooling water to dissipate the heat generated and maintain a constant bath temperature over extended periods of operation.
Sample container	Borosilicate glass, 75 mm id, equipped with a 0.03 mm thick polyethylene bottom; 90 ml capacity; attached to a ℱ 50/50 inner glass joint.
Aerosol chamber	Borosilicate glass tube, 28 mm od, 18 mm long, sealed into a ℱ 50/50 outer glass joint.

Table 5. (Continued)

	Spectroscopic Equipment
Spectrometer	One meter, Czerney-Turner mount, scanning spectrometer (Hilger-Engis model 1000, Engis Equipment Co., Morton Grove, Illinois).
Grating	102 mm by 102 mm, 1200 rulings/mm, blazed for 5000 Å (Bausch and Lomb, Inc., Rochester, New York).
Reciprocal linear dispersion	8 Å/mm, first order.
Slits	Bilateral straight slit assembly, utilized between 10 and 25 μ wide with a height of 1 mm.
Detector	S-13 response, 13 stage, end-on photomultiplier (EMI type 6255B, Electra Megadyne, Inc., North Hollywood, Calif.). Operated at 1250 volts.
Recorder	Variable span with built in zero suppression (Speedomax G, Leeds and Northrup Co., Philadelphia, Penna.). Operated at 2.5 mv full scale.
External optics	Fused quartz lens, 15.5 cm focal length, used to focus a 1:1 image of the plasma on the spectrometer slit.
	Emission Measurements
Amplifier	Micro-microammeter with operating range of 10×10^{-4} to 3×10^{-13} ampere full scale (model 410, Keithly Instruments, Inc., Cleveland, Ohio).

Table 5. (Continued)

Absorption Measurements	
Amplifier	An ac, lock-in amplifier (model HR-8, Princeton Applied Research, Princeton, N. J.) utilized in connection with a chopper at 160 Hz.
Primary source	Calcium hollow-cathode lamp (Perkin-Elmer Corp., Norwalk, Conn.) powered by a custom built, dc power supply.
Additional optics	A second lens, 12.5 cm focal length, focused the hollow-cathode radiation at the center of the plasma via a front surface mirror.

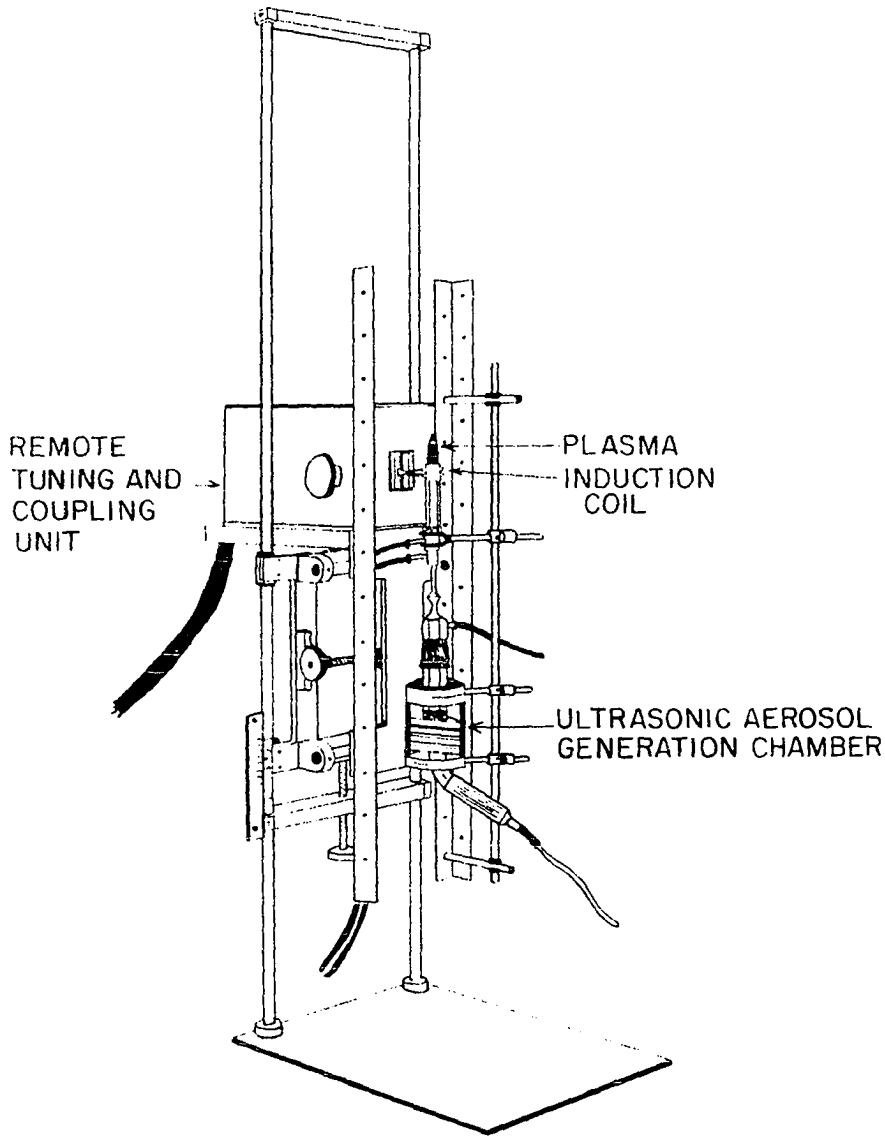

Figure 11. Movable platform used for this study with the tuning and coupling unit, torch assembly, and aerosol generation chamber mounted in place

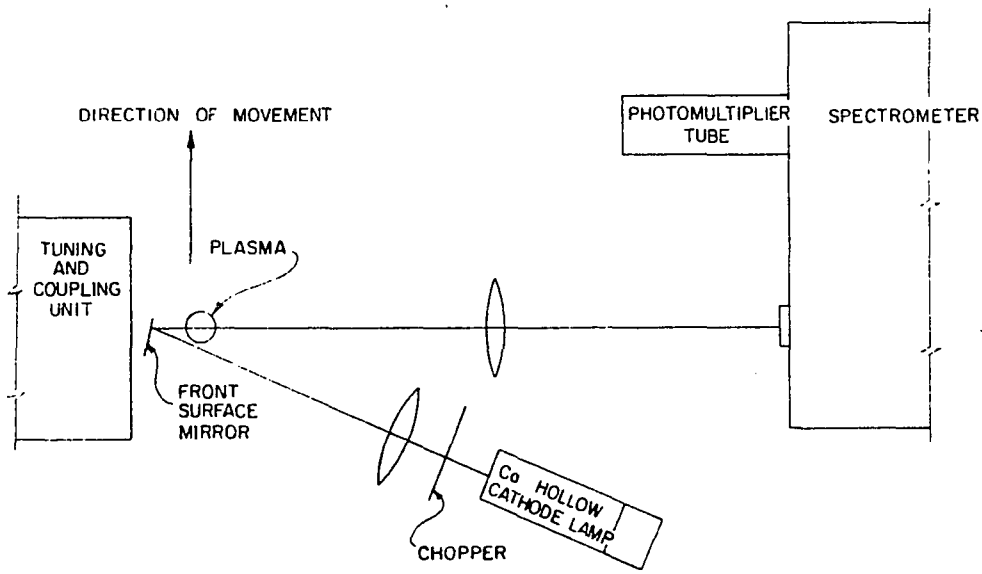

Figure 12. Optical configuration used for the atomic absorption phase of this study

PLASMA CHARACTERISTICS

The plasma chosen for this study is supported by a flow of argon, chosen for its chemical inertness and ease of ionization. Being partially ionized, the atmosphere will interact with the electrical and magnetic fields of the surrounding induction coil allowing energy to be transferred into the plasma without the need for electrodes. An aerosol containing metallic salts of the elements being studied was added to this inert plasma. In spite of the simplicity of this discharge relative to other more common laboratory excitation sources, the plasma was sufficiently complex to require a study of its own properties before it could be applied to a study of internal standardization.

Temperature

One of the most important plasma descriptors of interest in this investigation was the temperature existing in various regions of the discharge. In order to be meaningful, however, local thermodynamic equilibrium must exist or be closely approximated. Reed (14,41) has considered this question and concluded that the existence of local thermodynamic equilibrium was a valid assumption for the induction-coupled plasma. He then measured the temperature of that discharge using a technique first developed by Fowler and Milne (42) and applied

more rigorously by Olsen (26). This method depends on the fact that the intensity of a given spectral line increases with temperature, goes through a maximum, and then decreases in intensity as the neutral atom population is depleted due to ionization. Reed (14,41) observed an off-axis peak in the intensity of the Ar I 7635 Å line and interpreted the dip toward the center as a region of increasing temperature. A core temperature of approximately 16000 °K was measured in this manner.

In a later paper, Johnson (43) studied the problem further and concluded that the off-axis peak observed by Reed was a consequence of the skin-depth effect of induction heating and not the result of observing the maximum intensity for the Ar I 7635 Å line. As an alternative, Johnson measured the relative intensity of the $3p^5 4s-3p^5 4p$ and $3p^5 4s-3p^5 5p$ groups of argon neutral atom lines. From these measurements he concluded that the discharge possessed an off-axis maximum temperature of 9500 °K, considerably less than Reed's measurement. Three additional papers (44,45,46) support the lower temperature maximum for the pure argon plasma. A summary of the pure argon discharge temperature measurements is presented in Table 6. The consensus supports a core temperature in the 9000 to 10000 °K range.

The discharge employed in the present investigation was different from those discussed above in several significant

Table 6. Temperature measurements of the pure argon, induction-coupled plasma

Frequency	Power	Torch Design	Methods Used	Temperature	Ref
4.0 MHz	10 kw	20 mm id, single tube design with 9.4 to 12 l/min of argon	Fowler and Milne technique	16000 °K core maximum	14 41
4.5 MHz	6 kw	Single tube with tangential gas flow	Relative intensity of Ar I red and blue lines	Off axis maximum of 9500 °K	43
26 MHz	2-3 kw	Water cooled quartz, single tube type, 30, 22 & 16 mm id Argon flow rates of 12-18, 2-6, & 2.5-3.5 l/min	(a) Absolute intensity of Ar I 4510 Å (b) Absolute intensity of continumn (c) Relative intensity 4510 Å/continumn (d) Broadening of H_β line	9200 to 9700 °K in core region Plots indicate an off-axis maximum	44
5.8 MHz		30 mm id, single tube design with 40 l/min of argon	Absolute intensity of the Ar I 7503 Å line	10500 °K maximum off axis	45
5.1 MHz	6 kw	23 mm id, single tube design with 20 l/min of argon	Relative intensity of 4s5p lines of Ar I spectrum	8500 °K in core to 6000 °K in center 6 cm above core region	46

respects: an aqueous aerosol containing metallic salts was being introduced into the plasma in addition to the argon; a 2.5 kw induction heater operated at 31 MHz was employed; and a two tube, "laminar" gas flow plasma was used rather than the one tube, tangential flow configuration. As a result, the chosen discharge may exhibit significantly different temperature characteristics. In addition, with the aerosol introduced in the manner described, it may not "experience" the full effect of the higher core temperature. Thus, a knowledge of the "effective" temperature through the plasma center was necessary since vertical profiling was the experimental method adopted for studying relative line pair behavior.

The temperature measurement technique selected was the two-line method, discussed in detail and suggested by Pearce (16) as the most appropriate for the temperature range expected in the induction coupled plasma. The element chosen for use as the "electronic thermometer" was iron because extensive transition probability data are available for both the neutral atom and the first ion (13,47,48). For the initial experiments the iron compound added was ferrocene [$(Fe(C_5H_5)_2$], suggested by Broida and Shuler (49), in hopes that a more uniform distribution of iron in the plasma would be obtained since the sample would enter as a gas rather than an aerosol. However, the line emission

intensities were too weak for observation resulting in the use of solutions for the remainder of these experiments.

The initial temperature measurements were made with Fe II (first ion) lines, but the values obtained were not only erratic but unreasonably high (up to 26000 °K). These results suggest that the transition probability data for the ionic species may be in error. In the neutral atom spectrum of iron, a pair of lines at 3916.73 Å and 3917.18 Å possess several characteristics which made them especially attractive: being separated by only 0.45 Å, the lines could be scanned in rapid succession minimizing the possibility of plasma drift between measurement of the two intensities; the lines were completely resolved by the spectrometer (in the second order); calibration of the response of the spectrometer-detector combination was not necessary because of the wavelength proximity; the upper energy levels of the two transitions were well separated producing good sensitivity (see Table 7); and neither of the lower energy levels was in the iron ground state multiplet minimizing the self-absorption problem. All of the temperature measurements were made with this line pair.

Horizontal temperature profiles, developed with the aid of the Abel inversion method of Cremers and Birkebak (50) to calculate the radial intensity behavior of the two lines, are shown in Figure 13 for three positions above the induction

Table 7. Properties of the Fe I line pair utilized for the plasma temperature measurements[a]

Wavelength (Å)	gA Value (10^8/sec)	Energy levels (cm^{-1})
3916.73	6.4	26106 - 51630
3917.18	.11	7986 - 33507

[a]Wavelengths, gA values and energy levels from Corliss and Bozman (13).

coil. These plots indicate that a maximum temperature of 6200 °K was observed, less than the maxima observed for the pure argon plasma discussed earlier. However, the lowest point sampled in the plasma was 8 mm above the induction coil or about 14 mm above the core of the discharge. Thus, the hottest portion of the plasma was not examined. In addition, the presence of the aqueous aerosol may have reduced the plasma temperature. The 400 degree drop in the 8 mm profile between the axial center and 2 mm is in agreement with the observations on the pure argon plasma which showed off-axis maxima due to the skin depth effect. The most important feature of these profiles, however, is the horizontal temperature gradient of 1000 to 1500 degrees. This means that observation of line intensities emitted from different atoms or ions may originate from regions of different temperatures in the plasma complicating data interpretation. As a result, a vertical profile will give only an average or "effective" temperature.

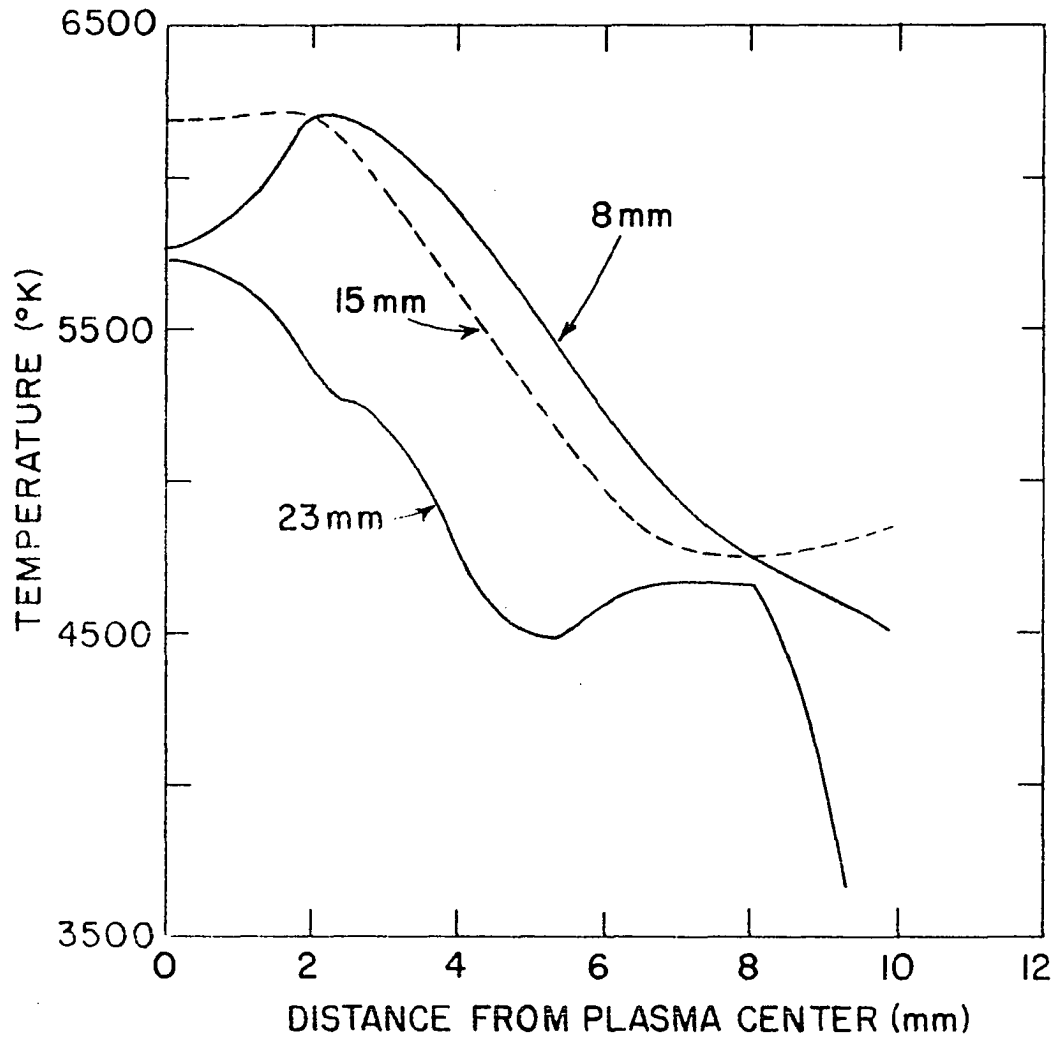

Figure 13. Horizontal temperature observations at three vertical positions in the plasma

The vertical profile shown in Figure 14 provides us with good insight of the "effective" temperature gradient along the length of the plasma. Other observations indicate that the rate of temperature change decreases above 45 mm, but direct measurement with the selected line pair was not possible because the intensity of the 3916.73 Å line was too weak in this region for making accurate intensity measurements. Other elements will have a similar neutral atom "effective" temperature profile but possibly with a magnitude of ±200 to 300 degrees because of differences in ionization energy. The "effective" temperature for ion species, while not measured explicitly, may be several hundred degrees higher. This would result if the ion population were located closer to the axial center, shown by Figure 13 to be a hotter region of the discharge.

Additional observations indicated that day to day fluctuations of the measured temperature were on the order of 200 to 300 degrees. Several experimental variables appeared to be responsible: The setting of the variable capacitor in the tuning and coupling unit (which matches the impedance of the plasma with the induction heater) was critical and yet there was no accurate method to reproduce this setting; and with the experimental facilities employed in this study, the amount of solution fed into the plasma varied, possibly on the order of ±25% from day to day,

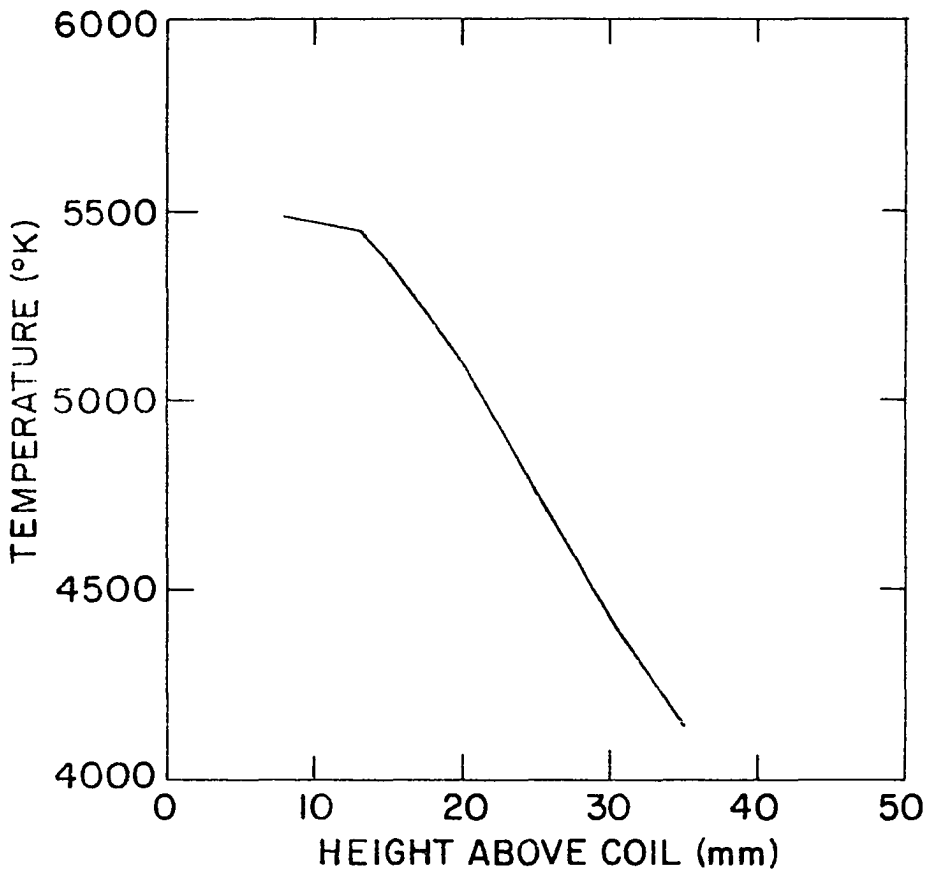

Figure 14. Vertical profile of the "effective" temperature behavior in the plasma measured using Fe I lines

changing the amount of water vaporized and the electron density contributed by the sample.

Sample Distribution

The second important plasma characteristic affecting intensity ratio behavior was the manner in which the sample was distributed within the discharge. Riemann (51), working with a different type of plasma, noted that aerosol samples tended to avoid the discharge due to the thermal barrier and traveled instead around the outside. Visual observation of our plasma indicated that the same type of phenomenon was occurring. In order to confirm this observation and gain further insights concerning sample distribution, the atomic absorption technique was utilized. Two types of profiles were measured: (a) horizontal, to indicate the uniformity of sample distribution across the discharge; and (b) vertical, to obtain an indication of the amount of sample dilution taking place and the relative behavior of the atom and ion species. A 50 ppm calcium solution served as the sample.

Figure 15 presents relative horizontal absorption profiles for the calcium atom and ion species at three vertical positions in the plasma. These plots represent the extremes of the expected behavior: off-axis maxima for both species observed at the lowest point studied, 13 mm above the coil; and a maximum close to the axis for the calcium ion absorbance

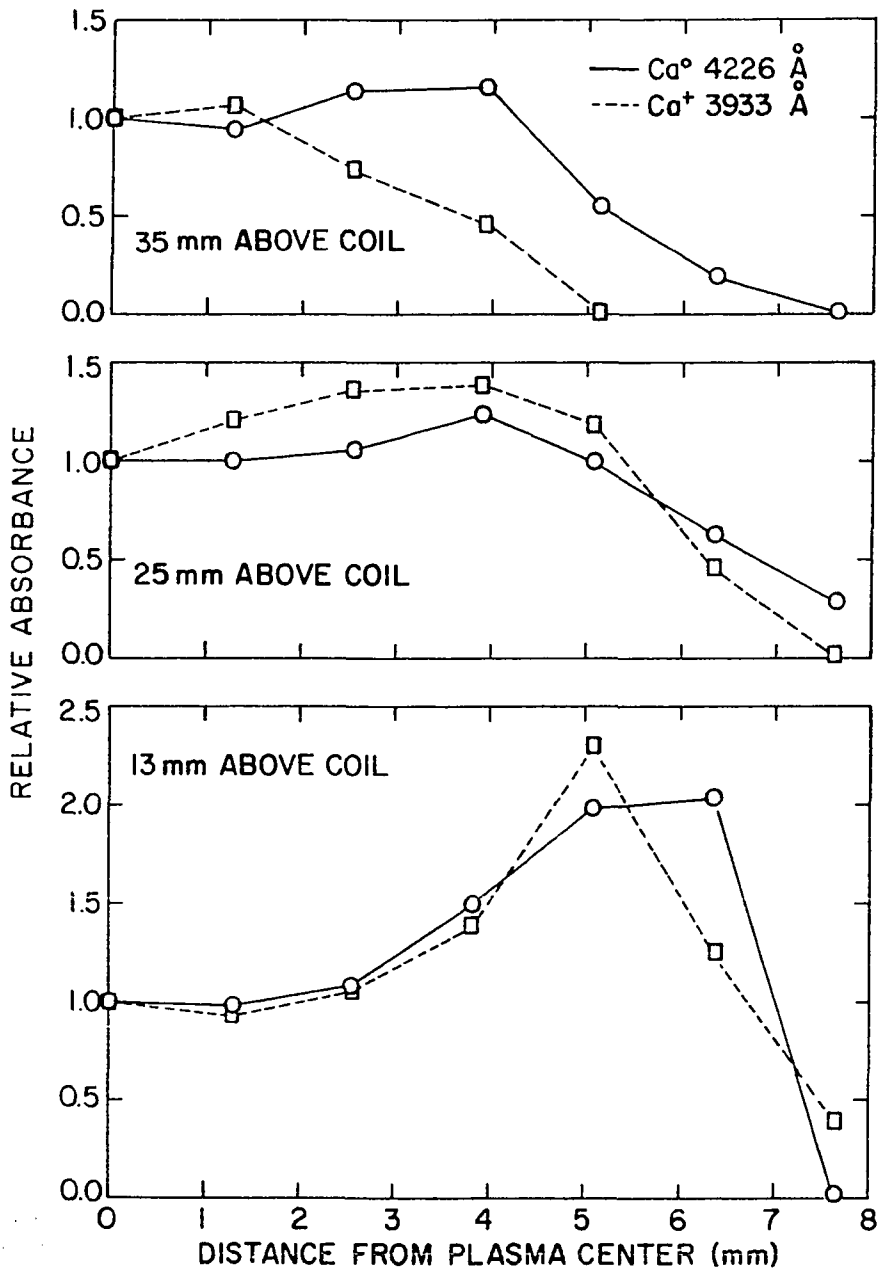

Figure 15. Horizontal profiles of relative calcium neutral atom and ion absorbance obtained at three positions above the induction coil

with an off-axis maximum of the calcium neutral atom absorbance observed at 35 mm above the coil. The behavior at 25 mm above the coil is intermediate between these two extremes.

The profile observed at 35 mm above the coil is approximately the one expected for uniform distribution of the sample across the discharge. Figure 13 indicates that the maximum temperature exists on or near the plasma axis and is adequate to ionize a majority of the sample atoms. Thus, for a uniform sample distribution, a majority of the atoms near the axial center should be ionized, producing an ion maximum at that point. The neutral atom absorbance should, as a result, exhibit its maximum at some distance from the center. The off-axis maxima observed for both species at 13 mm above the induction coil indicate that little, if any, of the sample had reached the center. Instead, the bulk of it is concentrated in a ring between 4.5 and 6.5 mm from the center.

The vertical profiles obtained of the calcium neutral atom and ion absorbance are shown in Figure 16. The neutral atom population decreases in a relatively uniform manner as would be expected from sample dilution. The ion profile is quite similar in relative behavior up to about 25 mm above the induction coil; at that point the ion population begins to increase. It was previously shown (see Figure 14) that

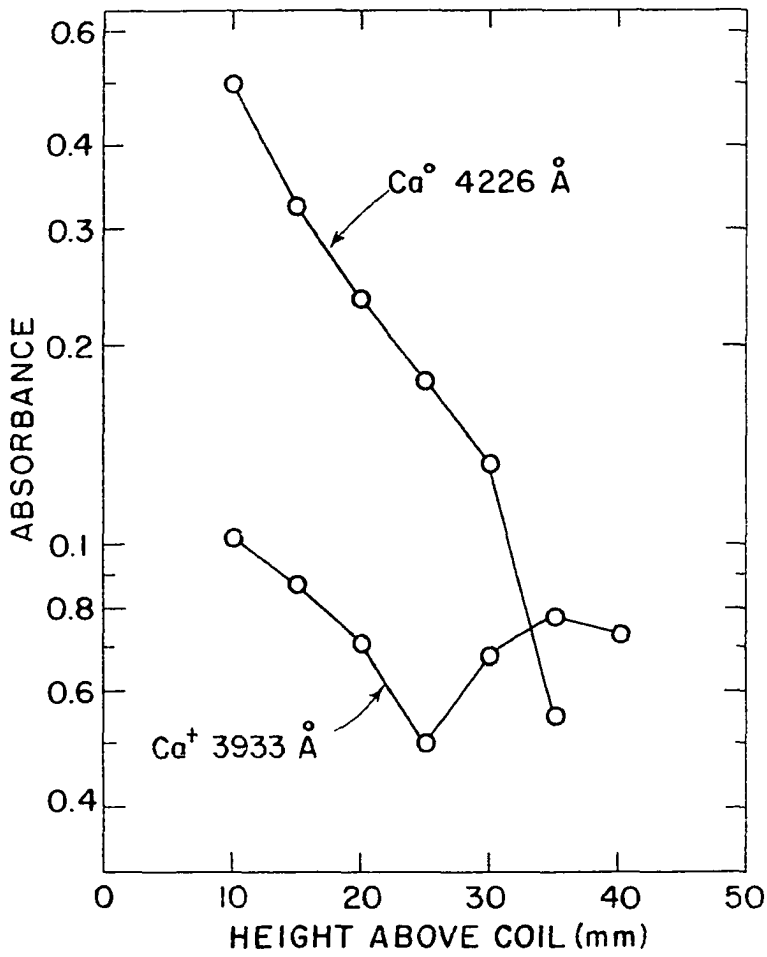

Figure 16. Vertical profiles of the absorbance of calcium neutral atom and ion species

the "effective" temperature decreases in a uniform manner; in addition, the ionization of argon effectively controls the discharge electron density in these experiments because of the low sample concentration selected. In view of these conditions, two possible explanations can account for the increase in ion population at this point: (a) the electron density in the discharge supplied by argon ionization decreases significantly or (b) additional sample is diffusing to the hotter axial center to favor the greater degree of ionization.

There are several implications inherent in these observations: first, the "effective" temperature experienced by a metallic species will not be the maximum temperature measured because most of the sample avoids that region of the discharge; second, the "effective" temperature of the ion population may be higher than that of the neutral atom or have a different profile since the ion population lies closer to the axial center of the discharge; third, the "effective" temperature of a given species will depend on the ionization properties of the element in question, which will govern the horizontal position in the discharge from which a given atom or ion population will emit the majority of its intensity; and fourth, transport phenomena will play a role in the emission characteristics and intensity ratio behavior because the sample tends to flow around the hotter axial core of the discharge.

CORRELATION OF OBSERVED INTENSITY RATIOS WITH MODEL CALCULATIONS

The intensity ratio behavior of two atom lines was described by the expression

$$\frac{I_{qp(X^o)}}{I_{sr(R^o)}} = \frac{n_{(X^o)}\ A_{qp}\ \nu_{qp}\ g_q\ Q_{(R^o)}}{n_{(R^o)}\ A_{sr}\ \nu_{sr}\ g_s\ Q_{(X^o)}} \exp\left[(E_s - E_q)/kT\right] . \qquad (31)$$

An equivalent expression can also be written for two ion lines by substituting X^+ and R^+ for X^o and R^o. Thus, the analytical intensity ratio ($I_{qp(X^o)}/I_{sr(R^o)}$) is a direct function of two temperature dependent terms, namely the partition function ratio ($Q_{(R^o)}/Q_{(X^o)}$) and the Boltzmann exponential term. In addition, the ratio $n_{(X^o)}/n_{(R^o)}$ is affected by the degree of ionization of X and R which is not only a function of temperature but of electron density as well. The latter, in turn, is related to nebulized sample density in the discharge. If we now observe intensity ratios along the length of the plasma, the experimental values will reflect their response to all of these primary variables.

In the earlier theoretical analysis, the sample/argon ratio was defined to be 0.1 ml of sample combined with 10 l of argon. A difficulty presented in the experimental portion of the investigation was the absence of an easy method for

determining the sample/argon ratio actually existing in various regions of the plasma. Knowledge of the argon flow and sample introduction rates only provided a starting point for arriving at an approximation of the possible ratio. The ratio of sample flow to total argon flow introduced into the plasma tube was approximately 0.1 ml/20 l. The estimation of the actual sample/argon ratio in the discharge was rendered uncertain by a lack of definitive data on: (a) the rate at which this ratio decreases with height; (b) the degree of mixing of the three independent argon flows in the plasma; and (c) the fraction of aerosol particles which "by pass" the plasma entirely.

In the absence of actual sample/argon ratios, it is instructive to examine the effect this parameter will have on the theoretical intensity ratio profile. Figures 17 and 18 show three dimensional projections of the calculated intensity ratios as a function of temperature and sample/argon ratio for two line pair ratios which will be considered later in the discussion of experimental examples. It is readily apparent from inspecting Figure 17, for example, that the Ca I/Fe I intensity ratio changes most rapidly in the 4000 to 5400 °K temperature range. Also, within this same region, the intensity ratio is more readily affected by changes in flow ratio than at the extreme temperatures plotted where the majority of the sample is either present

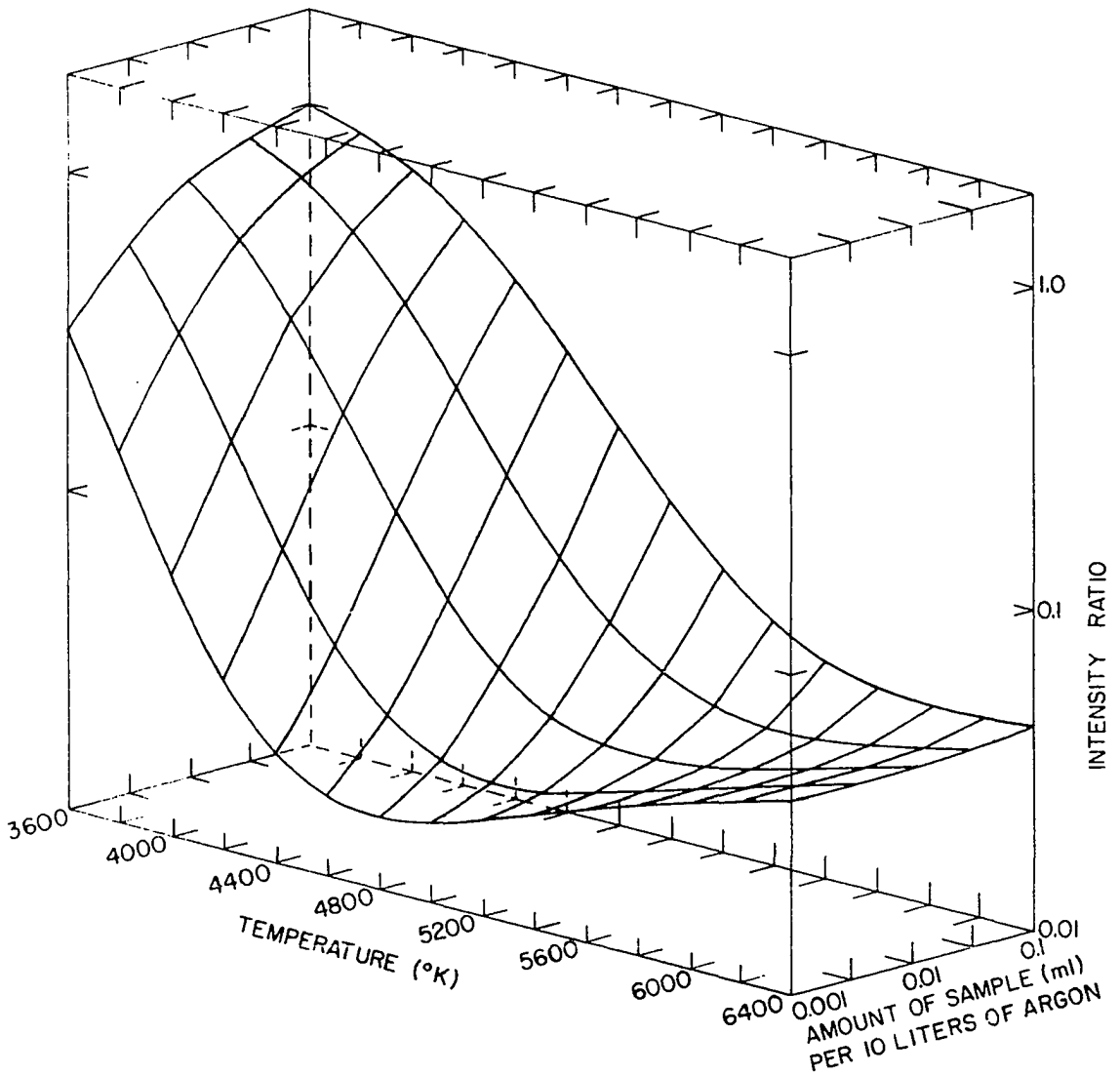

Figure 17. Three dimensional projection of the intensity ratio of Ca I 4302 Å/Fe I 3827 Å as a function of temperature and sample/argon ratio

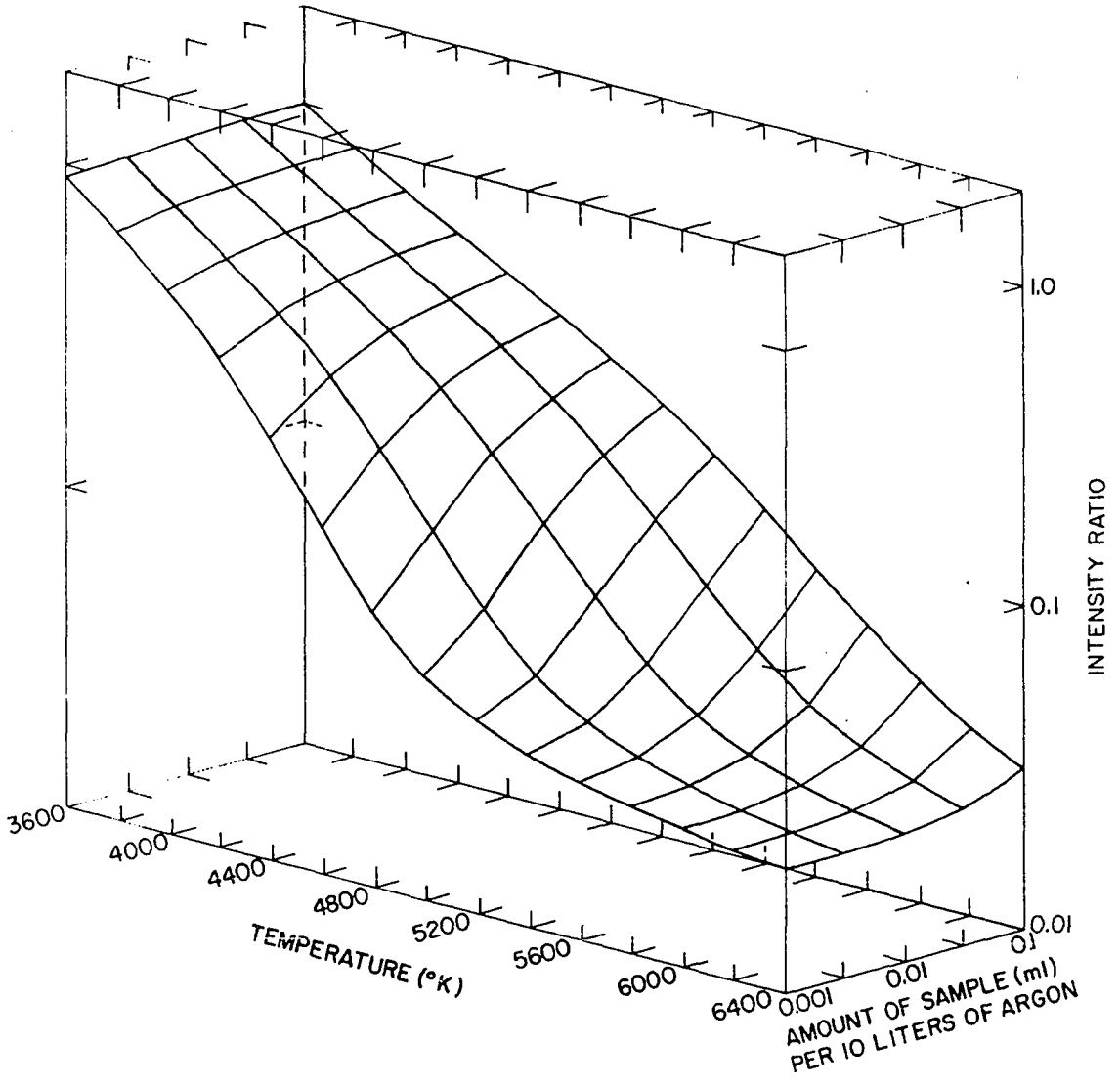

Figure 18. Three dimensional projection of the intensity ratio of Cu II 2247 Å/Au II 2110 Å as a function of temperature and sample/argon ratio

as neutral atoms or as ions. Figure 18 shows that the Cu II/ Au II line pair undergoes a less rapid change as a function of temperature and is less influenced by changes in the sample/argon ratio. No attempt was made to predict in advance the actual shape of the experimental profiles. Rather, the theoretical model was most useful for suggesting the direction and magnitude of general trends and interpretation of experimentally measured profiles.

EXPERIMENTAL EXAMPLES

One method of studying the internal standardization problem would be to consider each temperature and electron density dependent variable in Equation 31 individually. However, the complexity of relationships which develop, especially regarding the ionization term, made that an impossible task. As a result, the author chose the more pragmatic approach of calculating the effect of each contribution--ionization, partition function, and exponential--and the complete analytical intensity ratio behavior as a function of temperature at several sample/argon ratios. These calculated behaviors were then compared with and used to interpret the experimentally derived results. The examples included in this chapter are typical of the many observed in the course of this study.

Self-Absorption

Inherent in the equation for the intensity ratio of two spectral lines is the assumption that the emitted radiation is the observed radiation. However, changes produced by self-absorption are well known in emission spectroscopy. To check on its importance in the induction-coupled plasma, two examples were chosen, one consisting of neutral atom lines and the other ion lines. In each case three lines

were selected which had approximately the same excitation energy. Two of the lines had lower energy levels which were high enough to minimize the possibility of self-absorption while the third had as its lower level the ground state of the atom or ion in question. In the ion line example, the two ^4P energy levels are meta-stable, but of sufficiently high energy so that they should not be highly populated. Figures 19 and 20 illustrate the energy relationships involved and the observed results in each case. As can be easily seen, the intensity ratio of the two lines in each system not subject to self-absorption remained reasonably constant with height while the ratio involving the other line showed a large change.

The initial increase of the Fe I 2166 Å/Fe 4466 Å ratio plotted in Figure 19 suggests that self-absorption of the Fe I 2166 Å line was decreasing with height as would be expected due to sample dilution. Then, beyond 25 mm above the induction coil, the decreasing intensity ratio indicates increasing absorbance of the Fe I 2166 Å line. This increasing absorbance of the Fe I 2166 Å line could be the result of an increase in self-absorbance or due to non-specific absorption in the 2000-2200 Å region by atmospheric gases. There was considerable entrainment of air into the discharge above 25 mm which may have been sufficient to absorb radiation of this wavelength when heated.

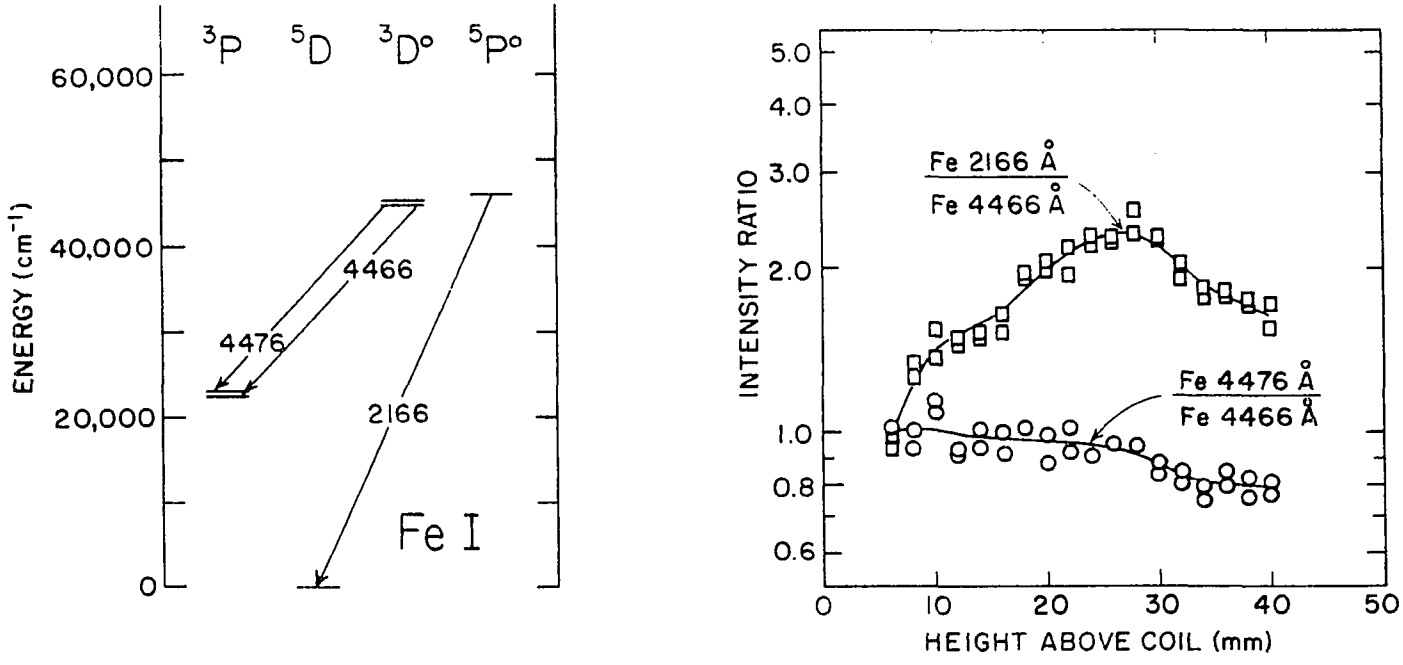

Figure 19. Energy levels and experimental evidence showing the importance of absorption processes in the plasma for neutral atom lines

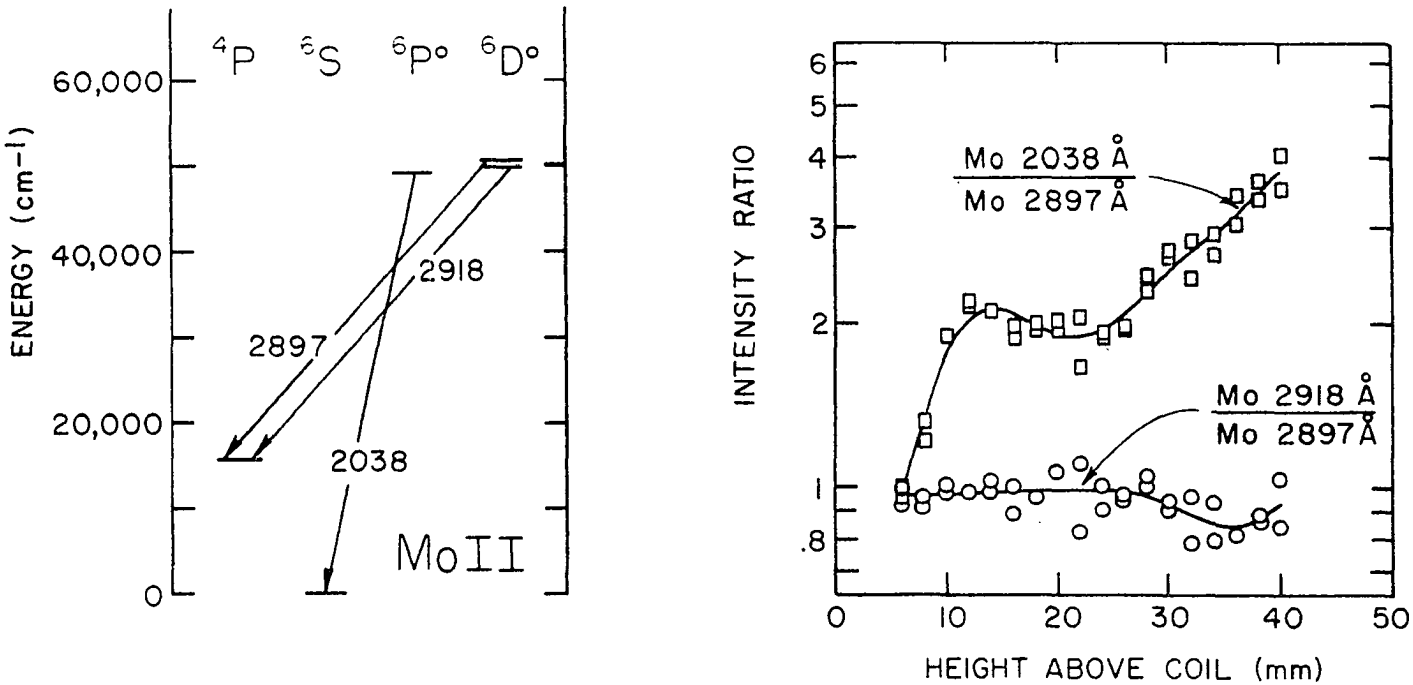

Figure 20. Energy levels and experimental evidence showing the importance of absorption processes in the plasma for ion lines

The Mo II 2038 Å/Mo II 2897 Å intensity ratio profile illustrated in Figure 20 shows a general increase with height, indicating a decrease in self-absorption of the Mo II 2038 Å line. A plateau and slight dip in the intensity ratio was observed between 15 and 25 mm above the coil which, at first thought, is surprising. This unusual behavior occurs in the same general region that the intense, luminous core region of the plasma terminates and the downward trend of the Ca II 3933 Å absorbance was reversed (see Figure 16). This behavior provides additional evidence for a sharp drop in electron density or greater inward diffusion of sample just above the core region of the plasma which causes an increase in the ion population and, consequently, self-absorption. Above 25 mm, the amount of self-absorption again decreases as the falling temperature decreases the ion population.

It is apparent that self-absorption or other types of absorption can significantly influence line pair intensity ratios. As a consequence, spectral lines whose lower energy levels were at or near the ground electronic state of the atom or ion in question or were of short wavelengths were avoided as much as possible for the remainder of the experiments carried out as part of this study. More importantly, the observed effects are obviously one additional consideration when internal standard line pairs are chosen.

As additional experimental profiles are presented, it will be evident that the deviations illustrated in Figures 19 and 20 are as significant as any which are caused by other types of "mismatching".

Neutral Atom Line Pairs

The elements, wavelengths, energy levels and ionization energies of three neutral atom line pairs chosen for detailed discussion in this paper are outlined in Table 8. By the traditional criteria used to judge line pair suitability, all three line pairs appear equally mismatched: excitation energies of the line pairs are approximately matched, but there is between 14000 and 15000 cm^{-1} difference in the ionization energy in each case.

Table 8. Properties of the neutral atom line pairs[a]

Element Pair	Wavelength (Å)	Energy Levels	Ionization Energy
Mn	4018.10	17052 - 41933	59960
Au	3122.78	9161 - 41174	74410
Mo	4811.06	30496 - 51276	57260
Cd	4678.16	30114 - 51484	72539
Ca	4302.53	15316 - 38552	49305
Fe	3827.82	12561 - 38678	63700

[a]All wavelengths, energy levels, and ionization energies in this and subsequent tables taken from Meggers, Corliss and Scribner (52) unless noted otherwise.

The experimental intensity ratio versus height profiles illustrated in Figures 21, 22 and 23 indicate that their behaviors were, however, different. The Mn I 4018 Å/Au I 3122 Å ratio decreased slightly before increasing five fold in a nearly linear manner. The Mo I 4811 Å/Cd I 4678 Å profile shows a slow increase in intensity ratio through-out the entire profile. The Ca I 4302 Å/Fe I 3827 Å intensity ratio decreased slowly and then increased to approximately the original value.

In order to account for the differences in the observed behaviors of the three neutral atom line pairs, it is necessary to look beyond the traditional criteria outlined in Table 8. Instead of considering just the differences between the ionization energies of the element pair, the Saha-Eggert equilibrium constant for each is actually the governing quantity. The reaction being considered is

$$X \rightleftarrows X^+ + e^- \tag{32}$$

for which the equilibrium constant is defined as

$$K_{(X^o \rightarrow X^+)} = \frac{n_{(X^+)} n_{(e^-)}}{n_{(X^o)}} \ . \tag{33}$$

The Saha-Eggert equation allows calculation of this equilibrium constant as a function of temperature:

$$K_{(X^o \rightarrow X^+)} = \frac{(2\pi m_{(e^-)} kT)^{3/2}}{h^3} \, 2 \, \frac{Q_{(X^+)}}{Q_{(X^o)}} \exp\left(-E_{i(X^o)}/kT\right). \tag{34}$$

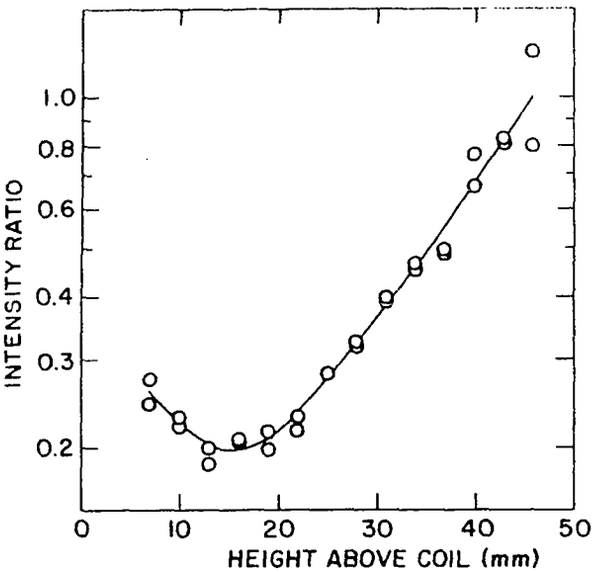

Figure 21. Experimentally observed behavior of the Mn I 4018 Å/Au I 3122 Å line pair intensity ratio

An analogous equation can also be written for the reference element (R). The meaning and implications of this equation have already been discussed in the previous theoretical analysis. The important fact to note here is that $K_{(X^o \rightarrow X^+)}$ is directly proportional to the partition function ratio and the exponential term which contains the ionization energy. Table 9 summarizes the basic quantities involved and the Saha-Eggert equilibrium constants for the six elements at 4600 °K. From an inspection of these data, it is not surprising that different behaviors were observed.

An additional difference between the three element pairs is the behavior of the partition function ratio of Equation 31, a quantity important because it is directly

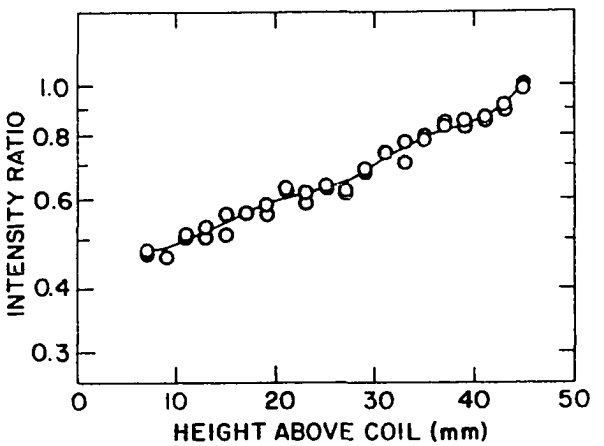

Figure 22. Experimentally observed behavior of the Mo I 4811 Å/Cd 4678 Å line pair intensity ratio

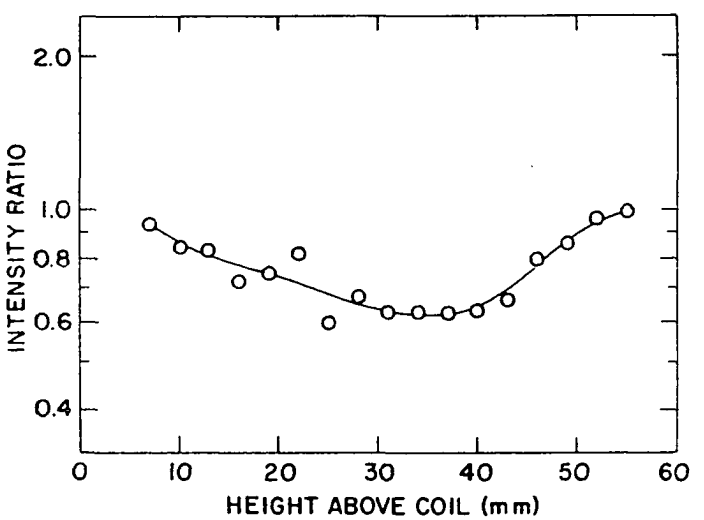

Figure 23. Experimentally observed behavior of the Ca I 4302 Å/Fe I 3827 Å line pair intensity ratio

Table 9. Partition functions, ionization energies and Saha-Eggert equilibrium constants for the neutral atom element pairs at 4600 °K

Element Pair (X/R)	$Q_{(X^o)}$ or $Q_{(R^o)}$	$Q_{(X^+)}$ or $Q_{(R^+)}$	$Q_{(X^+)}/Q_{(X^o)}$ or $Q_{(R^+)}/Q_{(R^o)}$	Ionization Energy	$K_{(X^o \rightarrow X^+)}$ [a] $K_{(R^o \rightarrow R^+)}$
Mn	6.281	7.536	1.200	59960	.130E 14
Au	2.347	1.085	.462	74410	.545E 11
Mo	8.377	7.124	.850	57260	.214E 14
Cd	1.001	2.000	1.999	72539	.423E 12
Ca	1.241	2.137	1.713	49305	.520E 15
Fe	26.46	41.75	1.578	63700	.531E 13

[a] .130E 14 is read as $.130 \times 10^{14}$.

proportional to the intensity ratio. Table 10 summarizes the values of the partition function ratio for the three element pairs at two temperatures which lie on either side of the range actually profiled and the percentage change in the intensity ratio due to this quantity alone. It is seen that a large difference exists between the element pairs.

The primary physical process which accounts for the observed profiles is ionization. Calculations using the model program indicate, for example, that manganese is 94% ionized while gold is only 12% ionized at 5500 °K (assuming a sample/argon ratio of 0.01 ml/10 l). This means that the sharp increase in intensity ratio with plasma height shown

Table 10. Partition function ratio change and its effect on the intensity ratio

Element Pair (X/R)	$Q_{(R^o)}/Q_{(X^o)}$		$\Delta\frac{I_{(X^o)}}{I_{(R^o)}}$ (%)
	3600 °K	6400 °K	
Mn/Au	.356	.311	-12.7
Mo/Cd	.135	.0696	-48.6
Ca/Fe	22.8	5.91	-74.1

in Figure 21 is primarily due to recombination of the manganese ion. This would increase the number of manganese neutral atoms relative to the number of gold neutral atoms and, thus, produce the increase in intensity ratio.

The Mo I/Cd I line pair is similar in its behavior, except that there is less difference between the Saha-Eggert equilibrium constants in this case. At 5500 °K and the same sample/argon ratio, molybdenum is 96% ionized while cadmium is 53% ionized. The observed profile results from the difference in the recombination rates of the two elements.

The Ca I/Fe I line pair represents a somewhat different situation. Calculations with the model program indicate that at 5500 °K, calcium is 99% ionized while iron is 80% ionized. On this basis, profiling to a region of lower temperature should produce a rapid drop in the intensity ratio due to a more rapid recombination reaction for iron than calcium.

The gradual slope actually observed in the 10 to 35 mm region (see Figure 23) results because of an opposing change in the partition function ratio as noted in Table 10. The positive slope observed in the profile beyond 35 mm is caused by an increase in the rate of recombination of the calcium ions relative to the iron ion recombination rate.

In order to confirm the above observations and interpretations, an alternate group of three line pairs was selected with similar Saha-Eggert equilibrium constants, partition function ratio behaviors and excitation energy mismatches. The properties of these additional examples are outlined in Table 11. Comparison with the data found in Tables 9 and 10 indicates that behaviors parallel to those of the first three examples would be expected. The experimental behaviors of the three line pairs are shown in Figure 24 and illustrate changes with similar magnitudes and directions as those shown in Figures 21, 22, and 23. Furthermore, the differences which are evident can be accounted for by normal day to day variations in experimental conditions.

The effects observed experimentally for the six line pairs discussed were primarily a result of ionization. In several of the examples, particularly Ca I/Fe I, there was also a partition function ratio change which modified the final results. In all cases, the excitation energies of the two lines making up each pair were closely matched.

Table 11. Properties of the alternate neutral atom line pairs

Element Pair (X/R)	Wave-length (Å)	$\Delta\frac{Q_{(R^o)}}{Q_{(X^o)}}$(%) 3600 to 6400 °K	Ionization Energy (cm^{-1})	$Q_{(X^+)}/Q_{(X^o)}$ or $Q_{(R^+)}/Q_{(R^o)}$ At 4600 °K	$K_{(X^o \rightarrow X^+)}$ or $K_{(R^o \rightarrow R^+)}$ At 4600 °K
Mg	2776.69	-12.4	61669	1.974	.125E 14
P	2553.28		84580	1.970	.278E 10
Cr	3804.80	-40.7	54570	.692	.405E 14
Sb	3232.52		69700	.676	.348E 12
Tl	2918.32	-39.0	49264	.402	.123E 15
Co	3730.48		63438	1.123	.409E 13

If this had not been true, additional modification of the final profile would have been observed.

Ion Examples

The properties of the experimental ion line pairs chosen for consideration in this chapter are outlined in Table 12. In this case one would expect, by the traditional rules, similar behavior from the latter two line pairs which should differ from that of the first example. The first line pair shows matched excitation energies for the two lines and very nearly equal ionization energies. The latter two line pairs also have matched excitation energies, but the ionization energies differ by 12000 and 15000 cm^{-1} respectively.

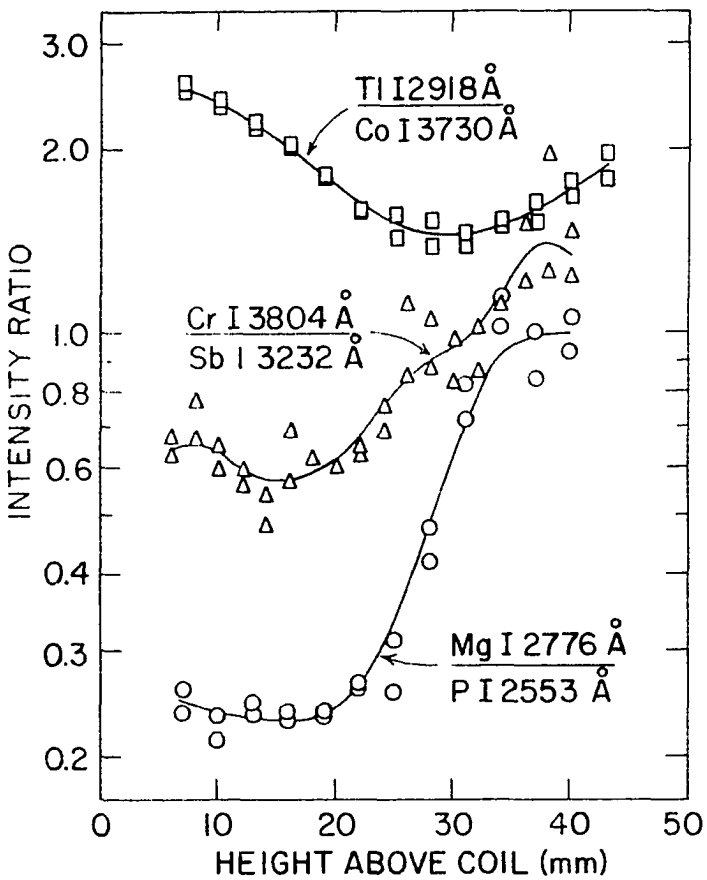

Figure 24. Experimental behaviors of the intensity ratios for the alternate neutral atom line pairs

Table 12. Characteristics of the ion line pairs

Element Pair	Wavelength (Å)	Energy Levels	Ionization Energy
Mg	2790.79	35669 - 71491	61669
Mn	2900.16	36274 - 70745	59960
Cu	2247.00	21929 - 66419	62317
Au[a]	2110.68	17639 - 65003	74410
Mo	3077.66	35406 - 67889	57260
Cd[b]	4415.63	46619 - 69259	72539

[a]Au II wavelength and energy levels from Platt and Sawyer (53).

[b]Cd II wavelength and energy levels from Shenstone and Pittenger (54).

Figures 25, 26, and 27 show the experimental results in each case. However, the profiles of the first two line pairs are similar while the third shows a markedly different behavior, opposite from the predicted result based on classical criteria.

In order to gain insight into the reasons for this apparent contradiction, it is instructive to consider the additional data outlined in Table 13. From these data and those in Table 12, the nearly ideal behavior of the Mg II 2790 Å/Mn II 2900 Å line pair is easily interpreted. The Saha-Eggert equilibrium constants for the two elements are almost equal, the excitation energies of the two lines are very nearly matched, and the partition function ratio of

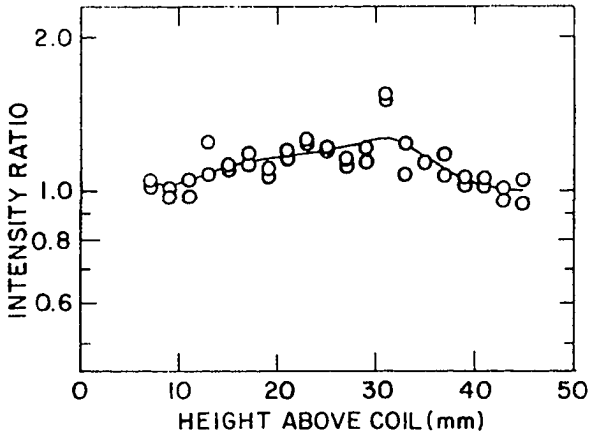

Figure 25. Experimentally observed behavior of the Mg II 2790 Å/Mn II 2900 Å line pair intensity ratio

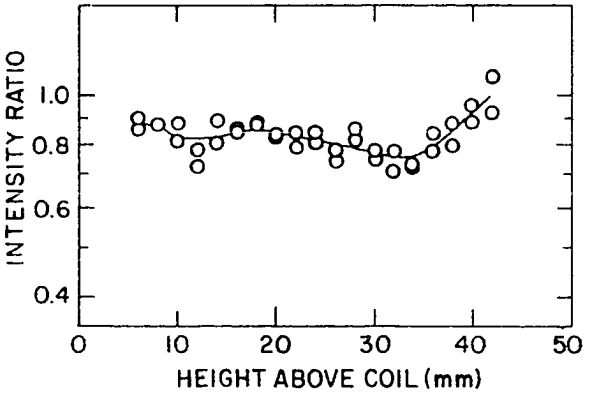

Figure 26. Experimentally observed behavior of the Cu II 2247 Å/Au II 2110 Å line pair intensity ratio

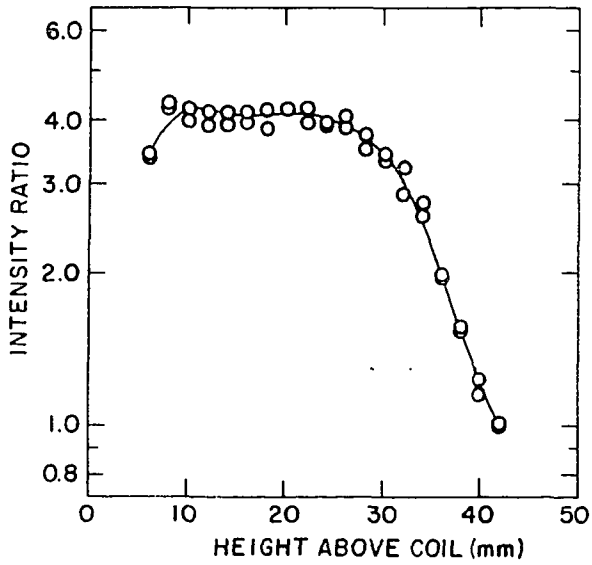

Figure 27. Experimentally observed behavior of the Mo II 3077 Å/Cd II 4415 Å line pair intensity ratio

Table 13. Partition functions, ionization energies and Saha-Eggert equilibrium constants for the ion line elements at 4600 °K

Element Pair (X/R)	$Q_{(X^o)}$ or $Q_{(R^o)}$	$Q_{(X^+)}$ or $Q_{(R^+)}$	$Q_{(X^+)}/Q_{(X^o)}$ or $Q_{(R^+)}/Q_{(R^o)}$	Ionization Energy	$K_{(X^o \rightarrow X^+)}$ or $K_{(R^o \rightarrow R^+)}$
Mg	1.013	2.000	1.975	61669	.125E 14
Mn	6.267	7.536	1.203	59960	.130E 14
Cu	2.249	1.014	.451	62317	.233E 13
Au	2.347	1.085	.462	74410	.544E 11
Mo	8.377	7.124	.850	57260	.214E 14
Cd	1.001	2.000	1.999	72539	.423E 12

Equation 31 shows a negligible variation. As a result, the intensity ratio will remain constant without regard to temperature or electron density changes.

The observed profiles for the other two line pairs are considerably more difficult to interpret. The data in Table 13 indicate that the two components of each line pair exhibit Saha-Eggert equilibrium constants differing by almost two orders of magnitude. This fact alone would suggest that a changing intensity ratio should be observed. Further, model program calculations show that at 5500 °K and a sample/argon ratio of 0.01 ml/10 l, molybdenum is 96% ionized while cadmium is 53% ionized; also, copper is 84% ionized compared with 20% ionization for gold. Thus, the change anticipated would be an increase in the intensity ratio because the denominator element in each pair has the lesser Saha-Eggert equilibrium constant. As regions of lower temperature are encountered, the denominator ion should recombine more readily than the numerator ion resulting in an increasing intensity ratio with height.

Instead of the predicted changes, the Cu II/Au II intensity ratio remained almost constant over the entire profile, while the Mo II/Cd II intensity ratio remained constant up to 30 mm above the induction coil before

beginning a steady decrease. At the present state of understanding concerning the processes occurring in the plasma, it is only possible to speculate concerning the reasons for these observed behaviors.

CONCLUSION

The foregoing examples--both theoretical and experimental--have provided confirmation that the choice of a good analysis line pair is more complex than implied by the traditional "rules". As a result, choosing ideal line pairs is really quite difficult because the process is more involved than matching numbers easily derived from tables. However, the probability for success has been enhanced as a result of a better understanding of some of the fundamental processes governing intensity ratio behavior in a spectral source.

A degree of compatibility has been demonstrated between the mathematical model and experimental results. The model successfully: (a) predicted the general trends of the neutral atom line pair intensity ratio behaviors; (b) provided parameters such as Saha-Eggert equilibrium constants which indicated differences between line pairs appearing, at first glance, equivalent; (c) integrated the present knowledge of line pair behavior in a plasma assumed to be in local thermodynamic equilibrium allowing predictions to be made; and (d) indicated areas of disagreement which will require further study.

In regard to this latter point, observations of line emission from the plasma indicate that the electron density

was higher and changed more rapidly than predicted by the equilibrium calculations. The reasons for this discrepancy are, at present, open to speculation. A geometrical factor may be partially responsible for the excess electron density. Low in the discharge, there is a steep, horizontal temperature gradient, but the "effective" temperature measured using Fe I lines will be biased toward the particular zone where the majority of the sample is located. In adjacent zones, there will be argon atoms which are at a higher temperature and, consequently, more highly ionized. Thus, the electron density could conceivably be higher than that calculated on the basis of the "effective" temperatures alone. In the upper regions of the plasma a more uniform sample distribution is achieved meaning the "effective" temperature should more accurately describe the physical situation. Other impurities, either from the tank argon or from the atmosphere, may be present and contribute to the electron density. In addition, the model assumes a constant sample/argon ratio. Any dilution which occurs will decrease the electron density with increasing height. Thus, it is apparent that there is still much to be learned concerning the phenomena occurring in the induction-coupled plasma.

The application of the principles and ideas discussed in this dissertation to other, more conventional sources

such as the dc arc or ac spark involves additional obstacles. In order to accurately calculate intensity ratio behavior, a knowledge of certain basic parameters such as chemical composition and electron density is necessary. For our plasma, the chemistry appeared sufficiently simple, allowing an approximation of these to be calculated for the various temperature-sample/argon ratio combinations considered. In addition, the induction-coupled plasma was relatively stable with time. In contrast, there are many more chemical reactions taking place in the plasma column of a dc arc or ac spark. These include reactions between the atmosphere, the electrode material, and the sample. Also, problems of selective vaporization can cause these conditions to change with time.

The most important variable in the temperature-sample/argon ratio domain examined in this study was ionization. Not only was it more complex in its behavior, being a function of both temperature and electron density, but its behavior was the most difficult to predict on the basis of numbers in the currently available tables. This supports the conclusion reached by Margoshes (7) for the dc arc, a spectral source with temperature characteristics similar to the induction-coupled plasma used for this study. Perhaps, if a table of Saha-Eggert equilibrium constants as a function of temperature were available, it would be possible to make a more

intelligent estimate of the compatibility of two elements as components of an ideal internal standard line pair. The one ideal line pair ratio considered--Mg II 2790 Å/Mn II 2900 Å--had equal equilibrium constants. For many of the examples studied, these equilibrium constants differed by two orders of magnitude or more. The ionization energies are not infallible guides because of the role played by the partition functions in determining the equilibrium constant behavior.

This investigation has demonstrated that it is possible to apply well accepted theoretical concepts to problems of atomic spectroscopy. To do so, however, requires extensive knowledge of the properties of the spectral source employed. Since much of this information is not readily available, an avenue for future research suggests itself. But, until more extensive knowledge of some of these parameters becomes available, it should be possible to apply many of these ideas in a qualitative manner to the problem of selecting good analysis line pairs.

LITERATURE CITED

1. Gerlach, W. Zur Frage der richtigen Ausführung und Deutung dur "quantitativen Spektralanalyse". Zeitschrift für Anorganische und Allgemeine Chemie 142: 383. 1925.

2. Ahrens, L. H. and S. R. Taylor. Spectrochemical analysis. 2nd ed. Reading, Mass., Addison-Wesley Publishing Co., Inc. 1961.

3. Harvey, C. E. Spectrochemical procedures. Glendale, Calif., Applied Research Laboratories, Inc. 1950.

4. Twyman, F. Metal spectroscopy. London, England, Charles Griffin and Company, Limited. 1951.

5. Smith, A. C. and W. C. Cummings. Factors affecting the choice of internal standards in emission spectrography. Publication du Groupement pour l'Avancement des Methodes Spectrographiques 1964, No. 4: 587. Oct.-Dec. 1964.

6. Boumans, P. W. J. M. Theory of spectrochemical excitation. London, England, Hilger and Watts, Ltd. 1966.

7. Margoshes, M. Excitation and ionization in arc and spark spectroscopic sources. Applied Spectroscopy 21: 92. 1967.

8. Greenfield, S., I. Ll. Jones and C. T. Berry. High-pressure plasmas as spectroscopic emission sources. Analyst 89: 713. 1964.

9. Wendt, R. H. and V. A. Fassel. Induction-coupled plasma spectrometric excitation source. Analytical Chemistry 37: 920. 1965.

10. Herzberg, G. Atomic spectra and atomic structure. New York, N.Y., Dover Publications. 1944.

11. Taylor, H. S. and S. Glasstone. A treatise on physical chemistry. 3rd ed. Vol. 1. New York, N.Y., D. van. Nostrand Co., Inc. 1942.

12. Mavrodineanu, R. and H. Boiteux. Flame spectroscopy. New York, N.Y., John Wiley and Sons, Inc. 1965.

13. Corliss, C. H. and W. R. Bozman. Experimental transition probabilities for spectral lines of seventy elements. National Bureau of Standards Monograph 53. 1962.

14. Reed, T. B. Induction-coupled plasma torch. Journal of Applied Physics 32: 821. 1961.

15. Griem, H. R. Plasma spectroscopy. New York, N.Y., McGraw Hill. 1964.

16. Pearce, W. J. Plasma-jet temperature measurement. In Dickermen, P. J., ed. Optical spectrometric measurements of high temperatures. Pp. 125-169. Chicago, Ill., The University of Chicago Press. 1961.

17. Aston, J. G. and J. J. Fritz. Thermodynamics and statistical thermodynamics. New York, N.Y., John Wiley and Sons. 1959.

18a. Moore, C. E. Atomic energy levels. National Bureau of Standards Circular 467, Vol. 1. 1949.

18b. Moore, C. E. Atomic energy levels. National Bureau of Standards Circular 467, Vol. 2. 1952.

18c. Moore, C. E. Atomic energy levels. National Bureau of Standards Circular 467, Vol. 3. 1958.

19. Drawin, H. W. and P. Felenbok. Data for plasmas in local thermodynamic equilibrium. Paris, France, Gauthier-Villars. 1965.

20. Drellishak, K. S., C. F. Knopp and A. B. Cambel. Partition functions and thermodynamic properties of argon plasma. Physics of Fluids 6: 1280. 1963.

21. Griem, H. R. High-density corrections in plasma spectroscopy. Physical Review 128: 997. 1962.

22. Olsen, H. N. Partition function cutoff and lowering of the ionization potential in an argon plasma. Physical Review 124: 1703. 1961.

23. Olsen, H. N. The electric arc as a light source for quantitative spectroscopy. Journal of Quantitative Spectroscopy and Radiative Transfer 3: 305. 1963.

24. Ecker, G. and W. Kröll. Lowering of the ionization energy for a plasma in thermodynamic equilibrium. Physics of Fluids 6: 62. 1963.

25. Olsen, H. N. Measurement of argon transition probabilities using the thermal arc plasma as a radiation source. Journal of Quantitative Spectroscopy and Radiative Transfer 3: 59. 1963.

26. Olsen, H. N. Thermal and electrical properties of an argon plasma. Physics of Fluids 2: 614. 1959.

27. Drellishak, K. S. Partition functions and thermodynamic properties of high temperature gases. U.S. Atomic Energy Commission Report AEDC-TDR-64-22 [Arnold Engineering Development Center, Tullahoma, Tenn.] 1964.

28. Dewan, E. M. Generalizations of the Saha equation. U.S. Atomic Energy Commision Report AFCRL-42 [Air Force Cambridge Research Laboratories, Bedford, Mass.] 1961.

29. Eggert, J. Über den Dissoziationszustand der Fixsterngase. Physikalische Zeitschrift 20: 570. 1919.

30. Saha, M. N. Ionization in the solar chronosphere. London, Edinburgh and Dublin Philosophical Magazine, Series 6, 40: 472. 1920.

31. Saha, M. N. Versuch einer Theorie der physikalischen Erscheinungen bei hohen Temperaturen mit Anwendungen auf die Astrophysik. Zeitschrift für Physik 6: 40. 1921.

32. Boumans, P. W. J. M. Fundamental source parameters--measurement, interpretation, and application in spectrochemical analysis. [To be published in Colloquium Spectroscopicum Internationale, 14th, Debrecen, 1967. London, England, Adam Hilger, Ltd. Ca. 1968.]

33. Diermeier, R. and H. Krempl. Thermische Anregungsfunktionen und Normtemperaturen von Atom- und Ionenlinien in Zweikomponentenplasmen. Zeitschrift für Physik 200: 239. 1967.

34. Kuhn, H. G. Atomic spectra. New York, N.Y., Academic Press. 1962.

35. ASTM Committee E-2 on Emission Spectroscopy. Methods for emission spectrochemical analysis. 4th ed. Philadelphia, Penna., American Society for Testing and Materials. 1964.

36. Greenfield, S., I. Ll. Jones, C. T. Berry, and L. G. Bunch. The high frequency torch: some facts, figures, and thoughts. Proceedings of the Society for Analytical Chemistry 2: 111. 1965.

37. Wendt, R. H. and V. A. Fassel. Atomic absorption spectroscopy with induction-coupled plasmas. Analytical Chemistry 38: 337. 1966.

38. Greenfield, S., C. T. Berry, and L. G. Bunch. Spectroscopy with a high frequency plasma torch. Des Plaines, Ill., Radyne International, Inc. U.S.A. Ca. 1966.

39. Hoare, H. C. and R. A. Mostyn. Emission spectrometry of solutions and powders with a high-frequency plasma source. Analytical Chemistry 39: 1153. 1967.

40. Fassel, V. A. and G. W. Dickinson. Continuous ultrasonic nebulization and spectrographic analysis of molten metals. Analytical Chemistry 40: 247. 1968.

41. Reed, T. B. Plasma torches. International Science and Technology, No. 6: 42. June 1962.

42. Fowler, R. H. and E. A. Milne. The intensities of absorption lines in stellar spectra and the temperatures and pressures in the reversing layers of stars. Monthly Notices of the Royal Astronomical Society 83: 403. 1923.

43. Johnson, P. D. Temperature and electron density measurements in an r. f. discharge in argon. Physics Letters 20: 499. 1966.

44. Gol'dfarb, V. M. and S. V. Dresvin. Optical investigation of the distribution of temperature and electron density in an argon plasma. High Temperature (translation of Teplofizika Vysokikh Temperatur) 3: 303. 1965.

45. Molinet, F. Étude de la répartition de la température électronique à l'intérier d'un plasma d'argon produit par un générateur h. f. Comptes Rendus de l'Academie des Sciences 262B: 1377. 1966.

46. Hughes, D. W. and E. R. Wooding. The temperature distribution in an h-mode r. f. plasma torch. Physics Letters 24A: 70. 1967.

47. Corliss, C. H. and B. Warner. Absolute oscillator strengths for Fe I. Astrophysical Journal, Supplement Series 8: 395. 1964.

48. Warner, B. Absolute oscillator strengths for once ionized elements of the iron group. Memoirs of the Royal Astronomical Society 70: 165. 1967.

49. Broida, H. P. and K. E. Shuler. Spectroscopic study of electronic flame temperatures and energy distributions. Journal of Chemical Physics 27: 933. 1957.

50. Cremers, C. J. and R. C. Birkebak. Application of the Abel integral equation to spectrographic data. Applied Optics 5: 1057. 1966.

51. Riemann, M. Ein stabilisierter Lichtbogen für die Lösungsspektralanalyse. In Ritschl, R. and G. Holdt, eds. Emissionsspektroskopie. Pp. 173-180. Berlin, Germany, Akademie-Verlag. 1964.

52. Meggers, W. F., C. H. Corliss and B. F. Scribner. Tables of spectral line intensities. National Bureau of Standards Monograph 32. 1961.

53. Platt, J. R. and R. A. Sawyer. New classifications in the spectra of Au I and Au II. Physical Review 60: 866. 1941.

54. Shenstone, A. G. and J. T. Pittenger. Cadmium spectra. Journal of the Optical Society of American 39: 219. 1949.

55. Scranton, D. G. Simplotter for B.P.S. [Basic Programming Support] Fortran. U.S. Atomic Energy Commission Ames Laboratory Computer Utilization Bulletin 23. Ca. 1965.

APPENDIX

The plasma simulation computer program written as part of this investigation was designed to predict the behavior of the intensity ratio of two spectral lines as a function of temperature at constant sample/argon ratio. The equations and assumptions imposed on the calculations have already been discussed in Chapter 3 of this dissertation. When it became desirable to study the effect of sample/argon ratio, several sets of calculations were carried out, each at a different sample/argon ratio, and the results correlated with the experimentally obtained results.

The program was written in FORTRAN IV specifically for the IBM 360 series of computers. The program was run successfully on both a model 50 and a model 65, approximately three times faster on the latter. Successful execution should be possible on any comparable machine with approximately 105000 bytes of memory space available. A Cal-Comp Digital Incremental Plotter was employed off-line to prepare the log intensity ratio versus temperature plots. In connection with the plotting portion of the program, two library subroutines (55), GRAPH and ORIGIN, were utilized.

For an installation without a Cal-Comp plotter or access to the library subroutines GRAPH and ORIGIN, the following

suggestions are offered:

1. Remove statements 51, 368, and 369 from routine MAIN. Discard subroutine FINISH which simply calls GRAPH and ORIGIN in the proper sequence.
2. Remove statements 48, 49, 58, and 59, from subroutine EXCITE. Subroutine EPLOT can now be discarded.
3. All calls to YSCALE have now also been eliminated so that this subroutine can be removed.

In this manner the program size is reduced and the plotting facility will no longer exist. If another plotting system is available, only FINISH and EPLOT must be written since all graphing is accomplished in these subroutines. Subroutine YSCALE may be suitable for use with rewritten subroutines FINISH and EPLOT for scaling the Y axis.

The contents of the data cards required for operation of this program are outlined in Table 14. The program was designed to operate completely from cards or to allow most of the data to be read from data sets on tape or disk. Card types 1 through 3c are always read from cards through FORTRAN unit 1. If IFT on card type 1 is not equal to 1, types 4a through 5d will be read as one data set from the specified FORTRAN unit number which must be defined by a system DD (data definition) control card. These data define the plasma being used and the temperature range to be covered.

Table 14. Data card requirements for the plasma simulation program

Type #	# Cards	Columns	Variable Name	Format	Remarks
1	1	1 - 10	XMIN	F10.0	Minimum temperature plotted
		11 - 20	XSF	F10.0	Temperature graph scale factor. If XSF = 0.0, graph scaled automatically.
		21 - 30	XWAY	F10.0	= +1.0, temperature plotted low to high. = -1.0, temperature plotted high to low. = 0.0, no plots produced.
		31 - 35	NTEMPS	I5	Number of temperatures - 30 maximum.
		36 - 40	IFT	I5	FORTRAN unit from which types 4 and 5 read. IFT = 1 indicates from cards.
2	NTEMPS	1 - 10	TEMP	F10.0	Temperature value (in °K)
		11 - 20	NE	E10.0	Electron density guess (number/cm^3)
3a	NTEMPS	16 - 25	Q2	F10.0	Partition function of argon first ion
		26 - 35	Q3	F10.0	Partition function of argon second ion
3b	NTEMPS				Same as 3a except for oxygen.
3c	NTEMPS				Same as 3a except for chlorine.
4a	1	21 - 30	V1	F10.0	First ionization energy of hydrogen.
		31 - 40	V2	F10.0	Second ionization energy (leave blank for hydrogen). Energies in cm^{-1}.
5a	1/level	11 - 15	J1	F5.0	J value of hydrogen energy level
		16 - 25	E1	F10.0	Energy of level in cm^{-1}.
Note: Repeat 5a for all levels (maximum of 500). Negative energy stops read.					
4b	1				Same as 4a except for argon.
5b	1/level				Same as 5a except for argon.

Table 14. (Continued)

Type	=	Cards	Columns	Variable Name	Format	Remarks
4c		1				Same as 4a except for oxygen.
5c		1/level				Same as 5a except for oxygen.
4d		1				Same as 4a except for chlorine.
5d		1/level				Same as 5a except for chlorine.

Note: If IFT $\neq$ 1 on card type 1, types 4 and 5 will be read as one data set of card images from tape or disk which must be defined by an appropriate system DD card.

Types 1 through 5d define the plasma and temperature range to be covered.

6	1	1 - 5	START	A4	Word "START" which acts as the initial control card.
7	1	1 - 10	NMETAL	I10	Number of elements (4 + number of metals)
		11 - 20	ARL	F10.0	Argon flow rate - liters/minutes
		21 - 30	SML	F10.0	Solution flow rate - ml/minute
		31 - 40	ATMP	F10.0	Atmospheric pressure - Torr
		41 - 60	DLAB1	5A4	Descriptive label
8	1	1 - 20	NAME	5A4	Element name or symbol and wavelength
		21 - 30	AW	F10.0	Atomic weight of element (gms/mole)
		31 - 40	OXNO	F10.0	Number of Cl^- per metal atom
		41 - 50	AMT	F10.0	Gms/100 ml of metal in solution
		51 - 60	EXCTA	F10.0	Excitation energy (cm^{-1}) of atom line
		61 - 70	EXCTI	F10.0	Excitation energy (cm^{-1}) of ion line
		71 - 80	IFT	I10	FORTRAN unit from which 9, 10a, 10b, and 10c read. IFT = 1 implies card reader.
9	1	1 - 20	ENAME	5A4	Name of element
		21 - 30	V1	F10.0	First ionization energy (cm^{-1})
		31 - 40	V2	F10.0	Second ionization energy (cm^{-1})

Table 14. (Continued)

Type	# Cards	Columns	Variable Name	Format	Remarks
		41 - 50	S1	F10.0	Spin momentum of ground state of first ion of element
		51 - 60	L1	F10.0	Orbital momentum of ground state of first ion of element
		61 - 70	NMIN	I10	Beginning principal quantum number for partition function approximation sum.
		71 - 80	IQ	I10	= 0, correction applied ≠ 0, correction skipped
Note:	Variables S1, L1, NMIN, and IQ are employed for the partition function correction approximation given by Griem (15, p. 140).				
10a	1/level	11 - 15	J1	F5.0	J value of energy level of atom
		16 - 25	E1	F10.0	Energy of level (cm^{-1})
10b	1/level	11 - 15	J2	F5.0	J value of energy level of first ion
		16 - 25	E2	F10.0	Energy of level (cm^{-1})
10c	1/level	11 - 15	J3	F5.0	J value of energy level of second ion
		16 - 25	E3	F10.0	Energy of level (cm^{-1})
Note:	Negative E1, E2, and E3 stops read of each set. Repeat 8 through 10c for each metal considered (up to 3). Type 9 through 10c can be read as one data set of card images from tape or disk as defined by a system DD card if IFT ≠ 1. The J values and energy levels read from card type 10 used for partition function calculations.				
11	1	1 - 5	NPLOTS	I5	Number of excitation energy differences to be considered by EXCITE (maximum of 4)

Table 14. (Continued)

Type #	# Cards	Columns	Variable Name	Format	Remarks
12	NPLOTS	1 - 10	DIFF	F10.0	Excitation energy of numerator element minus denomenator element (cm^{-1})
		11 - 30	LABEL	5A4	Descriptive lable (for graph use)
Note:	Repeat 11 and 12 as often as desired. When NPLOTS = 0, program stops this phase.				
13	1	1 - 4	STOP	A4	Word "STOP" acts as a control card
Note:	Types 6 through 13 can be repeated as often as desired.				
14	1	1 - 4	PLOT	A4	Word "PLOT" acts as a control card to end program and initiate SIMPLOTTER routines.

The remaining data defines the sample/argon ratio, the elements being considered, and their properties. Types 6 and 7 must be read from cards and serve to set up the experiment by defining the number of elements, flow rates and atmospheric pressure. Type 8 defines each element being considered, provides some basic parameters such as atomic weight, concentration, and the excitation energies of the lines being used. If the specified IFT equals 1, types 9 through 10c will be read from cards. If IFT equals some other FORTRAN unit, 9 through 10c will be read as one data set defined by another system DD card. It is especially convenient to have 9 through 10c on a tape or disk for all elements being considered because a large number of energy levels are frequently involved, especially for the transition elements. Also, if the same element is being used several times in a given run, having the energy levels on tape allows them to be reused without the necessity of duplicate decks of cards.

Card types 11 and 12 call into operation subroutine EXCITE; this segment calculates the behavior of the total intensity ratio for various mismatchings of the excitation energies of the lines of the analysis and internal standard element. This allows experimentation to determine the optimum excitation energy mismatch. "Optimum" would be defined as the mismatch producing the least amount of

change in intensity ratio over the temperature range of source operation.

Finally, types 13 and 14 simply act as control cards allowing additional simulations to be run as a batch. When type 14 is encountered, the program terminates. The operational mode of GRAPH and ORIGIN is to write an intermediate data set on a disk which is utilized by a master plot program following completion of the normal job. Thus, the PLOT control card terminates the simulation step and initiates the plotting step. A complete listing of the source statements is included as Program 1.

```
C     ****************************************************************
C     *                                                              *
C     * THIS PROGRAM IS A SIMULATION MODEL OF THE INDUCTION-COUPLED,  *
C     * ARGON PLASMA TORCH AND IS DESIGNED TO ITERATE TO A SELF-      *
C     * CONSISTANT SET OF SOURCE PARAMETERS.                         *
C     *                                                              *
C     ****************************************************************
C
C     THE PROGRAM WAS WRITTEN BY WILLIAM R. BARNETT AT IOWA STATE
C     UNIVERSITY, AMES, IOWA, AS PART OF A DISSERTATION STUDY ON THE
C     SELECTION OF ANALYTICAL LINE PAIRS FOR ATOMIC EMISSION ANALYSIS.
C
C     ****************************************************************
C     *                                                              *
C     *       THE ELEMENTS BEING CONSIDERED ARE NUMBERED AS FOLLOWS  *
C     *                                                              *
C     *    1. HYDROGEN (FROM WATER)                                  *
C     *    2. ARGON (MAIN PLASMA GAS)                                *
C     *    3. OXYGEN (FROM WATER)                                    *
C     *    4. CHLORINE (BEING CONSIDERED AS THE COMMON ANION)        *
C     *    5. FIRST METAL - TREATED AS THE NUMERATOR IN ALL RATIOS   *
C     *    6. SECOND METAL - DENOMINATOR IN ALL RATIOS               *
C     *    7. THIRD METAL - TO BE USED TO TEST ELECTRON SOURCE EFFECTS*
C     *                                                              *
C     ****************************************************************
C
C                  SOME OF THE SYMBOLS USED ARE DEFINED AS FOLLOWS
C
C          AMT = PER CENT (GMS/100 ML) OF METAL IN SOLUTION
C          ARL = LITERS/MINUTE OF ARGON GOING INTO PLASMA
C          ATMP = PRESSURE SURROUNDING THE PLASMA IN TORR
C          APTOT = TOTAL ARGON DENSITY (ATOMS + IONS)
C          AW = ATOMIC WEIGHT OF THE ELEMENTS CONSIDERED
C          C(I) = MOLES OF ELEMENT I INTERMS OF MOLES OF ARGON USED
C          COEF = 1.0E-05*ELECTRON DENSITY (USED FOR CONVERGENCE TESTING)
```

PROGRAM 1 - FORTRAN LISTING OF THE SOLUTION FED, ARGON PLASMA SIMULATION MODEL

```
C          DEBYE = THE DEBYE RADIUS IN CM
C          DELTA = THE LOWERING OF THE IONIZATION ENERGY
C          DIFF = ABSOLUTE DIFFERERNE BETWEEN NEW AND OLD ELECTRON
C                 DENSITY VALUES (USED FOR TESTING OF ITERATION
C                 CONVERGENCE)
C          DL1 , , DL6 = VARIOUS LABELS FOR THE GRAPHS
C          DLAB1 = DESCRIPTIVE LABEL FOR PRINTOUT AND GRAPHS
C          E1, E2, E3 = ENERGY LEVELS OF ATOM, FIRST AND SECOND ION
C                       (IN WAVENUMBERS)
C          EMAX = THE EFFECTIVE IONIZATION ENERGY
C          EXCTA, EXCTI = ATOM AND ION EXCITATION ENERGY (WAVENUMBERS)
C          EXPONA, EXPONI = THE EXPONENTIAL TERMS FOR TWO ATOM AND TWO
C                           ION LINES CALCULATED IN STATEMENTS 319 & 320
C          IFT = FORTRAN UNIT # FROM WHICH DATA SETS COME (IFT = 1 IF
C                ALL CARDS ARE BEING USED)
C          IMAX & IMIN = LIMITS OF PARTITION FUNCTION CORRECTION SUM
C          IMETAL = NUMBER OF SAMPLE METALS (NMETAL - 4)
C          IQ = THE PARTITION FUNCTION CORRECTION SWITCH:  IF ZERO, THE
C               THE CORRECTION APPLIED, IF NON-ZERO CORRECTION SKIPPED
C          J1, J2, J3 = J'S USED TO CALCULATE PARTITION FUNCTIONS
C          K1, K2 = THE SAHA-EGGERT EQUILIBRIUM CONSTANTS
C          L1 =  THE ORBITAL MOMENTUM OF THE GROUND STATE OF THE FIRST
C                ION OF THE SAMPLE ELEMENT
C          N1, N2, N3 = NUMBER OF ENERGY LEVELS OF ATOM, FIRST AND SECOND
C                       IONS
C          NA0, NA1, NA2 = FRACTION OR PERCENT OF EACH ELEMENT EXISTING
C                          IN EACH IONIZATION STATE
C          NAME = NAME OF METALS USED
C          NE = NUMBER DENSITY OF ELECTRONS
C          NEW = THE NEW CALCULATED VALUE OF ELECTRON DENSITY
C          NMETAL = TOTAL NUMBER OF ELEMENTS CONSIDERED (4 + # OF METALS)
C          NMIN & NMAX = IN PARTITION FUNCTION CALCULATIONS, THE RANGE
C                        OF PRINCIPLE QUANTUM NUMBERS OVER WHICH THE
C                        CORRECTION FACTOR IS CALCULATED
C          NPLOTS = NUMBER OF OVERPLOTS GENERATED BY EXCITE
```

PROGRAM 1 (CONTINUED)

```
C          NTEMPS = NUMBER OF TEMPERATURES USED
C          NTIMES, NGO = THE NUMBER OF ITERATIONS
C          NTOTAL = TOTAL PARTICLE DENSITY
C          OXNO = NUMBER OF CHLORIDES/METAL ATOM
C          PRESS = EFFECTIVE ATMOSPHERIC PRESSURE IN TORR
C          PO, P1, P2 = PARTICLES OF ATOM, FIRST ION, AND SECOND ION
C                       IN TERMS OF THE TOTAL NUMBER OF ARGON ATOMS
C          Q1, Q2, Q3 = PARTITION FUNCTIONS OF ATOM, 1ST AND 2ND IONS
C          QATOM, QION = PARTITION FUNCTION RATIO FOR ATOMS AND IONS
C          S1 = THE SPIN MOMENTUM OF THE GROUND STATE OF THE FIRST ION
C               OF THE SAMPLE
C          SAHAA, SAHAI = THE RATIO OF THE RESULTS OF CALCULATIONS
C                         USING THE SAHA-EGGERT EQUATION SHOWING
C                         RELATIVE CONCENTRATIONS OF ATOMS & IONS
C          SML = ML/MINUTE OF SOLUTION GOING INTO PLASMA
C          TEMP = TEMPERATURE (DEGREES K) BEING CONSIDERED
C          TOTALA, TOTALI = THE TOTAL INTENSITY RATIO FOR ATOM LINES
C                           AND ION LINES
C          V1, V2 = FIRST AND SECOND IONIZATION ENERGIES (CM-1)
C          WDIFF...ZDIFF = EXCITATION ENERGY DIFFERANCE USED BY
C                          SUBROUTINE EXCITE
C          XC, X1, X2 = NUMBER DENSITIES OF ATOM, FIRST ION AND SECOND
C                       ION EXPRESSED PER CC
C          XLAB, YLAB = THE X AND Y LABELS FOR THE GRAPHS
C          XMIN, YMIN = THE MINIMUM X AND Y VALUES WHICH ARE PLOTTED
C          XMOLE = MOLES/MINUTE ADDED TO PLASMA
C          XSF, YSF = THE X AND Y SCALE FACTORS FOR THE GRAPHS
C          XSIZE, YSIZE = THE LENGTH (IN INCHES) OF THE X AND Y AXES OF
C                         THE GRAPHS
C          XWAY = DETERMINES DIRECTION IN WHICH TEMPERATURE IS PLOTTED:
C                 +1.0 INDICATES TEMPERATURE IS PLOTTED LOW TO HIGH
C                 -1.0 INDICATES TEMPERATURE PLOTTED HIGH TO LOW
C                  0.0 INDICATES NO PLOTS PREPARED
C          XX, YY = THE POINTS REQUIRED TO PUT THE LINE ACROSS THE TOP
C                   AND ALONG THE RIGHT HAND SIDE OF THE GRAPHS
```

PROGRAM 1 (CONTINUED)

```
C
C     ****************************************************************
C
C         IN ADDITION TO THE MAIN PROGRAM, THERE ARE 6 SUBROUTINES - - -
C         FINISH, YSCALE, EXCITE, EPLOT, EWRITE AND REVIVE.
C
C         THE PROGRAM ALSO UTILIZES GRAPH AND ORIGIN WHICH ARE LIBRARY
C         SUBROUTINES AT THE IOWA STATE UNIVERSITY COMPUTATION CENTER
C         AND DVCHK (SUPPLIED BY IBM) FOR TROUBLE IDENTIFICATION
C         AND RECOVERY PURPOSES THROUGH SUBROUTINE REVIVE.
C
C     ****************************************************************
C     *                                                              *
C     *   ONLY FORTRAN UNITS #1 (CARD READER) AND #3 (THE PRINTER) ARE *
C     *   EMPLOYED UNLESS IFT SET TO SOME OTHER UNIT TO READ DATA SETS *
C     *   FROM TAPE OR DISK.  GRAPH AND ORIGIN REQUIRE UNIT # 14.      *
C     *                                                              *
C     ****************************************************************
C
      1      DIMENSION DLAB1(5),TPLOT(30), NAME5(3), NAME6(3), NAME7(3), AW(7),
     2AMT(7), XMOLE(7), TEMP(30), Q1(7,30), Q2(7,30), Q3(7,30),
     3E1(7,501), E2(3,501), E3(3,201), N1(7), N2(7), N3(7), V1(7),
     4V2(7), P0(7), P1(7), P2(7), C(7), X0(7, 30), X1(7,30), X2(7,30),
     5NTIMES(30), CXNO(7), EXCTI(7), EXCTA(7), QATOM(30), QION(30),
     6SAHAA(30), SAHAI(30), EXPONA(30), EXPONI(30), TOTALA(30), DL6(5),
     7TOTALI(30), S1(7), DELTA(30), DEBYE(30), NMIN(7), NMAX(30),IQ(7),
     8ENAME(7,5), Q201(6,30)
      2       REAL NE(30), J1(7, 501), J2(3, 501), J3(3, 201), K1(7, 30),
     2K2(7,30), NA0(7, 30), NA1(7, 30), NA2(7, 30), NTOTAL(30), NEW,
     3L1(7), KRATIO(30)
      3     100 FORMAT(I10, 3F10.0, 5A4)
      4     101 FORMAT (F10.0, E10.0)
      5     102 FORMAT (20X, 2F10.0)
      6     103 FORMAT (10X, F5.0, F10.0)
      7     104 FORMAT (5A4, 4F10.0, 2I10)
```

PROGRAM 1 (CONTINUED)

```
 8        105 FORMAT (1H1)
 9        106 FORMAT (1HO//   6X, 'TEMPERATURE =', I3, ',', 3I1, ' DEGREES K;',
             22X, 'IONIZATION POTENTIAL LOWERING =', E12.5, ' WAVE NUMBERS;',2X,
             3'DEBYE RADIUS =', F12.5, ' CM;' / 6X, 'TOTAL PARTICLE DENSITY =',
             4E12.5, ' PER CC;', 3X, 'ELECTRON DENSITY =', E12.5, ' PER CC;',
             52X, 'NUMBER OF ITERATIONS REQUIRED =', I3, ';')
10        107 FORMAT (1HO, 34X, 'NUMBER DENSITY', 27X, 'PER CENT', 17X,
             2'PARTITION FUNCTION'/9X, 'COMPONENT', 8X, 'X(0)', 11X, 'X(1)',
             311X, 'X(2)', 9X, 'NO', 8X, 'N+', 7X, 'N++', 8X, 'Q1', 8X, 'Q2',
             48X, 'Q3'/)
11        108 FORMAT (9X, 'HYDROGEN ', 3E15.5, 6F10.3/9X, 'ARGON    ', 3E15.5,
             26F10.3/9X, 'OXYGEN   ', 3E15.5, 6F10.3/9X, 'CHLORINE ', 3E15.5,
             36F10.3/)
12        109 FORMAT (1HO)
13        110 FORMAT (1HO,34X, 'ITERATION AT', F7.0, ' K WAS TERMINATED AFTER',
             2I3, ' ITERATIONS.')
14        111 FORMAT (35X, 'VALUES OBTAINED ARE QUESTIONABLE - - INSUFFICIENT IT
             2ERATIONS')
15        112 FORMAT (9X, 3A4, E12.5, 2E15.5, 6F10.3)
16        113 FORMAT (1HO//////////
             1              44X, 'INTENSITY RATIO BEHAVIOR OF TWO ION LINES'//
             233X, 3A4, ' IONIZATION POTENTIALS:  FIRST ', F8.0, ' WAVE NUMBERS'
             3/70X, 'SECOND', F8.0, ' WAVE NUMBERS'//33X, 3A4, ' IONIZATION POTE
             4NTIALS:  FIRST ', F8.0,' WAVE NUMBERS'/70X,'SECOND', F8.0, ' WAVE
             5NUMBERS'/)
17        114 FORMAT (33X, 65('-'))
18        115 FORMAT (65X, 'SAHA', 5X,'EXPONENTIAL', 4X, 'TOTAL'/36X, 'TEMPERATU
             2RE (K)', 4X, 'QRATIO', 4X, 'RATIO', 8X, 'TERM', 7X, 'RATIO')
19        116 FORMAT (5(32X, F14.0, F15.5, F10.5, 2F12.5/))
20        117 FORMAT (1HO//////////
             1              44X, 'INTENSITY RATIO BEHAVIOR OF TWO ATOM LINES'//
             233X, 3A4, ' IONIZATION POTENTIALS:  FIRST ', F8.0, ' WAVE NUMBERS'
             3/70X, 'SECOND', F8.0, ' WAVE NUMBERS'//33X, 3A4, ' IONIZATION POTE
             4NTIALS:  FIRST ',F8.0, ' WAVE NUMBERS'/70X, 'SECOND', F8.0,' WAVE
             5NUMBERS'/)
```

PROGRAM 1 (CONTINUED)

```
21        118 FORMAT (1H1////////
                     1           53X,   'PLASMA BEHAVIOR SIMULATION'/ 56X, 5A4/ 56X,
                     2'INITIAL ASSUMPTIONS')
22        119 FORMAT (1H0, 45X, 'ARGON FLOW RATE =', F8.4, ' LITERS/MINUTE'/47X,
                     2'SOLUTION FLOW RATE =', F8.4, ' ML/MINUTE')
23        120 FORMAT (1H0, 48X, 'CONCENTRATIONS OF METALS IN SOLUTION'/)
24        121 FORMAT (44X, 3A4, F8.5,' GRAMS/100 ML OF SOLUTION')
25        122 FORMAT (1H0, 49X, 'GUESS USED FOR ELECTRON DENSITY'//31X, 'TEMPERA
                     2TURE (K)', 3X, 'NE (NUMBER/CC)', 6X, 'TEMPERATURE (K)', 3X, 'NE (N
                     3UMBER/CC)'/)
26        123 FORMAT (5(30X, F11.0, E20.5, F18.0, E20.5/))
27        124 FORMAT (1H0, 47X, 'IONIZATION POTENTIALS OF THE METALS'/)
28        125 FORMAT (45X, 3A4, ' FIRST  =', F8.0, ' WAVENUMBERS'/58X, 'SECOND =
                     2', F8.0, ' WAVENUMBERS')
29        126 FORMAT (1H0, 43X, 'EXCITATION ENERGIES OF THE LINES CONSIDERED'/)
30        127 FORMAT (46X, 3A4, ' ATOM =', F8.0, ' WAVENUMBERS'/58X, ' ION  =',
                     2F8.0, ' WAVENUMBERS')
31        128 FORMAT (3F10.0, 2I5)
32        129 FORMAT (10X, 5('*'), 'ERROR--DIMENSION LIMITS NUMBER OF TEMPERATUR
                     2ES TO 30 OR LESS.')
33        130 FORMAT (6X, 'PARTITION FUNCTION CORRECTION SUMMATION CARRIED TO A
                     2PRINCIPLE QUANTUM NUMBER OF', I4, ';', 2X, 'EXTERNAL PRESSURE ='
                     3F6.1, ' MM OF HG;')
34        131 FORMAT (10X, 5('*'), 'ERROR--FORTRAN REQUIRES AT LEAST 1 EXICUTION
                     2 OF EACH DO LOOP----THEREFORE AT LEAST 1 SAMPLE ELEMENT REQUIRED')
35        132 FORMAT (10X, 5('*'), 'ERROR--DIMENSION AND PROGRAM CONSTRUCTION LI
                     2MIT NUMBER OF SAMPLE ELEMENTS TO 3 OR LESS.')
36        133 FORMAT (10X, 5('*'), 'ERROR--THERE WERE TOO MANY J VALUES AND ENER
                     2GY LEVELS OF UN-IONIZED ELEMENT #',I2, '.  LIMIT IS 500.')
37        134 FORMAT (10X, 5('*'), 'ERROR--THERE WERE TOO MANY J VALUES AND ENER
                     2GY LEVELS OF THE FIRST ION OF #', I2, '.  LIMIT IS 500.')
38        135 FORMAT (10X, 5('*'), 'ERROR--THERE WERE TOO MANY J VALUES AND ENER
                     2GY LEVELS OF THE SECOND ION OF #', I2, '.  LIMIT IS 200.')
39        136 FORMAT(1HC//////////          42X, 'SAHA IONIZATION EQUILIBRIUM CON
                     2STANT BEHAVIOR'/43X, 'FOR THE REACTION:  ATOM --> ION + ELECTRON'/
```

PROGRAM 1 (CONTINUED)

```
            3)
40        137 FORMAT(55X, '#1', 14X, '#2', 11X, 'RATIO'/33X, 'TEMPERATURE (K)',
             24X, 3A4, 3X, 3A4, 5X, '#1/#2')
41        138 FORMAT(5(33X, F11.0, 4X, E15.5, E15.5, F11.4/))
42        139 FORMAT (3A4, 8X, 5F10.0, I10)
43        140 FORMAT (A4)
44        141 FORMAT (10X, 10('*'),'PERMANENT DATA IN ERROR.'/20X, 'CHECK ORDER
             2OF ALL CARDS AND BE SURE IONIZATION POTENTIALS EXPRESSED IN WAVENU
             3MBERS.')
45        142 FORMAT (10X, 10('*'),'XWAY MUST HAVE VALUES OF +1.C, -1.0 OR 0.0 O
             2NLY.')
46        143 FORMAT (1H0//////////          35X, 'PARTITION FUNCTION RATIO BEHAVI
             2OR (Q2/Q1) FOR ', 3A4//)
47        144 FORMAT (33X, 'TEMPERATURE (K)', 9X, 'Q1', 13X, 'Q2', 10X, 'Q2/Q1')
48        145 FORMAT (5(33X, F11.0, F17.3, F15.3, F13.4/))
49            DATA PLOT/'PLOT'/, START/'STAR'/, HALT/'STOP'/
50            DATA TEMP/30*0.0/, NE/30*0.0/
51            CALL ORIGIN (0.0, 2.5, 1)
          C
          C     THE PROGRAM BEGINS BY READING IN INFORMATION WHICH DEFINES THE
          C     PLASMA UNDER CONSIDERATION AND THE TEMPERATURES BEING CONSIDERED.
          C
52            READ(1, 128) XMIN, XSF, XWAY, NTEMPS, IFT
53            IF(IFT .LE. 0)  IFT = 1
54            IF(NTEMPS .LE. 30) GO TO 1
55            WRITE (3, 129)
56            STOP 30
57          1 IF(XWAY .EQ. +1.0)  GO TO 4
58            IF(XWAY .EQ. -1.0)  GO TO 803
59            IF(XWAY .EQ. 0.0)  GO TO 4
60            WRITE(3, 141)
61            STOP 40
62        803 XMIN = -XMIN - 6.0*XSF
63          4 IPLOT = IFIX(ABS(XWAY)) + 1
          C
```

PROGRAM 1 (CONTINUED)

```
      C     THE TEMPERATURES, NE GUESS VALUES, AND Q2 AND Q3 FOR AR, O,
      C     AND CL ARE READ IN.
      C
 64         READ(1, 101) (TEMP(I), NE(I), I=1, NTEMPS)
 65         DO 7  I=2,4
 66       7 READ(1, 102) (Q2(I, J), Q3(I, J), J=1,NTEMPS)
 67         DO 40  I=1, NTEMPS
 68         Q2(1, I) = 1.00
 69      40 Q3(1, I) = 0.00
      C
      C     IONIZATION ENERGIES AND NEUTRAL ATOM ENERGY LEVELS OF F, AR, O,
      C     AND CL ARE READ IN AND CHECKED TO ASSURE LEGITIMATE VALUES.
      C
 70         DO 8   I=1, 4
 71         READ(IFT,102)V1(I), V2(I)
 72         DO 11  J=1, 501
 73         READ(IFT,103)J1(I,J), E1(I,J)
 74         IF(E1(I,J) .GE. 0.0)  GO TO 11
 75         N1(I) = J - 1
 76         GO TO 8
 77       11 CONTINUE
 78         WRITE(3, 133) I
 79         STOP 50
 80       8 CONTINUE
 81         IF(IFT .GT. 3)  REWIND IFT
 82       901 DO 909  I=2,4
 83         IF(V1(I) .LT. 30000.0)  GO TO 905
 84         IF(V2(I) .GT. 30000.0)  GO TO 909
 85       905 WRITE(3, 141)
 86         STOP 60
 87       909 CONTINUE
      C
      C     THE FIRST CONTROL CARD FOR THE PROGRAM IS READ IN AND UTILIZED.
      C
 88       600 READ(1, 140) CHECK
```

PROGRAM 1 (CONTINUED)

```
      IF(CHECK .EQ. PLOT)  STOP 999
      IF(CHECK .EQ. START)  GO TO 675
      CALL REVIVE (1, IGO, 1, NMETAL, V1, V2, EXCTA, EXCTI, AW)
      GO TO 600
C
C     ONE CARD READ IN WHICH DESCRIBES THE EXPERIMENT TO BE SIMULATED.
C
  675 READ(1, 100) NMETAL, ARL, SML, ATMP, DLAB1
C
C     NUMBER OF ELEMENTS CHECKED TO ASSURE THAT THEY ARE WITHIN THE
C     CORRECT RANGE FOR PROPER PROGRAM OPERATION.
C
      IF(NMETAL .GT. 4) GO TO 2
      WRITE (3, 131)
      CALL REVIVE (1, IGO, 1, NMETAL, V1, V2, EXCTA, EXCTI, AW)
      GO TO 600
    2 IF(NMETAL .LT. 8) GO TO 3
      WRITE (3, 132)
      CALL REVIVE (1, IGO, 1, NMETAL, V1, V2, EXCTA, EXCTI, AW)
      GO TO 600
C
C     INFORMATION NEEDED TO DESCRIBE EACH SAMPLE ELEMENT READ IN.
C
    3 DO 15   I = 5, NMETAL
      JCL = I - 4
      GO TO (50, 51, 52), JCL
   50 READ(1, 139) NAME5, AW(5), OXNO(5), AMT(5), EXCTA(5), EXCTI(5),IFT
      GO TO 53
   51 READ(1, 139) NAME6, AW(6), OXNO(6), AMT(6), EXCTA(6), EXCTI(6),IFT
      GO TO 53
   52 READ(1, 139) NAME7, AW(7), OXNO(7), AMT(7), EXCTA(7), EXCTI(7),IFT
   53 IF(IFT .LE. 0)  IFT = 1
      READ(IFT, 104) (ENAME( I,JJ),JJ=1,5),  V1(I), V2(I), S1(I),
     2L1(I), NMIN(I), IQ(I)
      DO 18  J=1, 501
```

PROGRAM 1 (CONTINUED)

```
113             READ(IFT,103)J1(I,J), E1(I,J)
114             IF(E1(I,J) .GE. 0.0)  GO TO 18
115             N1(I) = J - 1
116             GO TO 19
117          18 CONTINUE
118             WRITE(3, 133) I
119             CALL REVIVE (1, IGO, IFT, NMETAL, V1, V2, EXCTA, EXCTI, AW)
120             GO TO 600
121          19 M = I - 4
122             DO 21  J=1, 501
123             READ(IFT,103)J2(M,J), E2(M,J)
124             IF(E2(M,J) .GE. 0.0)  GO TO 21
125             N2(I) = J - 1
126             GO TO 22
127          21 CONTINUE
128             WRITE(3, 134)  I
129             CALL REVIVE (1, IGO, IFT, NMETAL, V1, V2, EXCTA, EXCTI, AW)
130             GO TO 600
131          22 DO 24  J=1, 201
132             READ(IFT,103)J3(M,J), E3(M,J)
133             IF(E3(M,J) .GE. 0.0)  GO TO 24
134             N3(I) = J - 1
135             IF(IFT .GT. 3)  REWIND IFT
136             GO TO 15
137          24 CONTINUE
138             WRITE(3, 135)  I
139             CALL REVIVE (1, IGO, IFT, NMETAL, V1, V2, EXCTA, EXCTI, AW)
140             GO TO 600
141          15 CONTINUE
          C
          C     INITIAL CONDITIONS AND ASSUMPTIONS WRITTEN OUT.
          C
142             WRITE(3, 118) CLASI
143             WRITE(3, 119) ARL, SML
144             GO TO (401, 401, 401, 401, 402, 402, 402), NMETAL
```

PROGRAM 1 (CONTINUED)

```
145         402 WRITE(3,120)
146             WRITE(3,121) NAME5, AMT(5)
147             GO TO (401, 401, 401, 401, 410, 403, 403), NMETAL
148         403 WRITE(3,121) NAME6, AMT(6)
149             GO TO (401, 401, 401, 401, 410, 410, 404), NMETAL
150         404 WRITE(3,121) NAME7, AMT(7)
151         410 WRITE (3, 124)
152             WRITE (3, 125) (ENAME(5,JJ),JJ=1,3), V1(5), V2(5)
153             GO TO(401, 401, 401, 401, 401, 408, 408), NMETAL
154         408 WRITE (3, 125) (ENAME(6,JJ),JJ=1,3), V1(6), V2(6)
155             GO TO (401, 401, 401, 401, 407, 407, 409), NMETAL
156         409 WRITE (3, 125) (ENAME(7,JJ),JJ=1,3), V1(7), V2(7)
157         407 WRITE(3, 126)
158             WRITE(3, 127) NAME5, EXCTA(5), EXCTI(5), NAME6, EXCTA(6),
                2EXCTI(6)
159         401 IHALF = (NTEMPS + 1)/2
160             WRITE(3, 122)
161             WRITE(3, 123) (TEMP(I), NE(I), TEMP(I + IHALF), NE(I + IHALF),
                2I=1, IHALF)
162             WRITE(3, 105)
            C
            C     CERTAIN KEY PARAMETERS ARE CHECKED TO ASSURE THAT THEY FALL
            C     WITHIN A LEGITIMATE RANGE OF VALUES.
            C
163             CALL REVIVE (2, IGO, 1, NMETAL, V1, V2, EXCTA, EXCTI, AW)
164             GO TO (625, 600), IGO
            C
            C     THE PLASMA COMPOSITION IS CALCULATED.
            C
165         625 XMOLE(2) = ARL/22.4136
166             XMOLE(3) = SML/18.016
167             XMOLE(1) = 2.0*XMOLE(3)
168             DO 5  I=5,NMETAL
169           5 XMOLE(I) = 0.01*SML*AMT(I)/AW(I)
170             XMOLE(4) = 0.0
```

PROGRAM 1 (CONTINUED)

```
171             DO 12  I=5, NMETAL
172          12 XMOLE(4) = XMOLE(4) + XMOLE(I)*UXNO(I)
173             DO 6  I=1,NMETAL
174           6 C(I) = XMOLE(I)/XMOLE(2)
          C
          C     PRELIMINARY (NON-ITERATED) CALCULATIONS OF Q2 AND Q3 FOR THE
          C     METALS PERFORMED.  ALSO K2 FOR ALL ELEMENTS CALCULATED.
          C
          C     TEMPERATURE LOOP BEGINS AT THIS POINT.
          C
175             DO 200  IT=1, NTEMPS
176             DEBYE(IT) = 4.762309*SQRT(TEMP(IT)/NE(IT))
177             DELTA(IT) = 2.322768E-03/DEBYE(IT)
178             DO 210  J = 5, NMETAL
179             M = J - 4
180             Q3(J, IT) = 0.0
181             KK = N3(J)
182             DO 210  K = 1, KK
183             L = 1 + N3(J) - K
184             IF(E3(M, L)) 211, 211, 212
185          211 Q3(J, IT) = Q3(J, IT) + 2.0*J3(M, L) + 1.0
186             GO TO 210
187          212 Q3(J, IT) = Q3(J, IT) + (2.0*J3(M,L) + 1.0)*EXP(-E3(M,L)/(TEMP(IT)
                2*.6950293))
188          210 CONTINUE
189             DO 220 J=5, NMETAL
190             M = J - 4
191             Q2(J, IT) = 0.0
192             KK = N2(J)
193             EMAX = V2(J) - DELTA(IT)
194             DO 220 K =1, KK
195             L = 1 + N2(J) - K
196             IF(EMAX - E2(M, L)) 220, 221, 221
197          221 IF(E2(M,L)) 222, 222, 223
198          222 Q2(J, IT) = Q2(J, IT) + 2.0*J2(M,L) + 1.0
```

PROGRAM 1 (CONTINUED)

```
199             GO TO 220
200           223 Q2(J, IT) = Q2(J, IT) + (2.0*J2(M,L) + 1.0)*EXP(-E2(M,L)/(TEMP(IT)
                 2*.6950293))
201           220 CONTINUE
202             DO 230  J=2,NMETAL
203             EMAX = V2(J) - DELTA(IT)
204           230 K2(J, IT) = 4.8250E+15*(Q3(J,IT)/Q2(J,IT))*TEMP(IT)**1.5*
                 2EXP(-EMAX/(TEMP(IT)*.6950293))
205             K2(1, IT) = 0.0
              C
              C     ACTUAL ITERATION BEGUN AT THIS POINT.
              C
206             DO 300  NGO=1, 35
207             DEBYE(IT) = 4.762309*SQRT(TEMP(IT)/NE(IT))
208             DELTA(IT) = 1.161384E-03/DEBYE(IT)
              C
              C     Q1 FOR ALL ELEMENTS CALCULATED.
              C
209             XMAX = SQRT(109095.0/DELTA(IT))
210             NMAX(IT) = IFIX(XMAX)
211             DO 325  J=1, NMETAL
212             Q1(J, IT) = 0.0
213             KK = N1(J)
214             EMAX = V1(J) - DELTA(IT)
215             DO 320  K=1, KK
216             L = 1 + N1(J) - K
217             IF(EMAX - E1(J,L)) 320, 321, 321
218           321 IF(E1(J,L)) 320, 322, 323
219           322 Q1(J, IT) = Q1(J, IT) + 2.0*J1(J,L) + 1.0
220             GO TO 320
221           323 Q1(J, IT) = Q1(J,IT) + (2.0*J1(J,L) + 1.0)*EXP(-E1(J,L)/(TEMP(IT)
                 2*.6950293))
222           320 CONTINUE
              C
              C     FOR THE SAMPLE ELEMENTS, AN APPROXIMATION FOR MISSING LEVELS IS
```

PROGRAM 1 (CONTINUED)

```
C      CALCULATED AND ADDED UNLESS IQ DOES NOT EQUAL ZERO.  THE PARTITION
C      FUNCTIONS OF THE PERMANENT MEMBERS OF THE PLASMA ARE COMPLETE
C      WITHOUT THIS ADDITION.
C
223          IF(J .LE. 4) GO TO 325
224          IF(IQ(J) .NE. 0)  GO TO 325
225          QEXTRA = 0.0
226          IMIN = NMIN(J)
227          IMAX = NMAX(IT)
228          DO 324  N=IMIN, IMAX
229        324 QEXTRA = QEXTRA + 2.0*N*N*EXP((109095.0/(N*N) -V1(J))/(.6950293*
            2TEMP(IT)))
230          QEXTRA = (2.0*S1(J) + 1.0)*(2.0*L1(J) + 1.0)*QEXTRA
231          Q1(J, IT) = Q1(J, IT) + QEXTRA
232        325 CONTINUE
C
C      K1 FOR ALL ELEMENTS CALCULATED.
C
233          DO 330  J=1,NMETAL
234          EMAX= V1(J) - DELTA(IT)
235        330 K1(J, IT) = 4.8250E+15*(Q2(J,IT)/Q1(J,IT))*TEMP(IT)**1.5*
            2EXP(-EMAX/(TEMP(IT)*.6950293))
C
C      FRACTION OF EACH ELEMENT IN EACH STAGE OF IONIZATION CALCULATED.
C
236          DO 340  J=1, NMETAL
237          NA0(J,IT) = 1.0/(1.0 + K1(J,IT)/NE(IT) + K1(J,IT)*K2(J,IT)/(NE(IT)
            2*NE(IT)))
238          NA1(J,IT) = K1(J,IT)/NE(IT)*NA0(J,IT)
239        340 NA2(J,IT) = K2(J,IT)/NE(IT)*NA1(J,IT)
C
C      THE COEFFICIENTS (P0, P1, AND P2) ARE NOW CALCULATED.
C
240          DO 350  J=1, NMETAL
241          P0(J) = NA0(J,IT)*C(J)
```

PROGRAM 1 (CONTINUED)

```
242             P1(J) = NA1(J,IT)*C(J)
243         350 P2(J) = NA2(J,IT)*C(J)
            C
            C       THE CORRECTED PRESSURE, NEW NE AND DENSITIES OF ALL PARTICLES
            C       ARE CALCULATED.
            C
244             PRESS = ATMP  -(1.373361E-21/DEBYE(IT)**3)*TEMP(IT)
245             NTOTAL(IT) = (9.657276E+18/TEMP(IT))*PRESS
246             PTOTAL = 0.0
247             DO 351  J=2,NMETAL
248         351 PTOTAL = PTOTAL + 3.0*P2(J)
249             DO 352  J=1,NMETAL
250         352 PTOTAL = PTOTAL + 2.0*P1(J)
251             DO 353  J=1,NMETAL
252         353 PTOTAL = PTOTAL + P0(J)
253             ARTOT = NTOTAL(IT)/PTOTAL
254             NEW = 0.0
255             DO 354  J=2, NMETAL
256         354 NEW = NEW + 2.0*P2(J)*ARTOT
257             DO 355  J=1, NMETAL
258         355 NEW = NEW + P1(J)*ARTOT
259             DO 356  J=1, NMETAL
260             X0(J,IT) = P0(J)*ARTOT
261             X1(J,IT) = P1(J)*ARTOT
262         356 X2(J,IT) = P2(J)*ARTOT
            C
            C       NE TESTED FOR CONVERGENCE OF ITERATION.
            C
263             COEF = 1.0E-05*NE(IT)
264             DIFF = ABS(NE(IT) - NEW)
265             IF(DIFF - COEF) 360, 360, 370
            C
            C       IF THE ITERATION HAS CONVERGED, THE TEMPERATURE AND NUMBER OF
            C       ITERATIONS ARE WRITTEN OUT.  IF X2<1.0, X2 IS SET EQUAL TO 0.0.
            C
```

PROGRAM 1 (CONTINUED)

```
266          360 WRITE(3, 110) TEMP(IT), NGO
267              NTIMES(IT) = NGO
268              DO 358  J=2, NMETAL
269          358 IF(X2(J, IT) .LE. 1.0)  X2(J, IT) = 0.0
270              GO TO 200
             C
             C       IF THE ITERATION HAS NOT CONVERGED, THE NE GUESS FOR THE NEXT
             C       ROUND IS CALCULATED.
             C
271          370 IF(NE(IT) - NEW) 371, 371, 372
272          371 NE(IT) = NE(IT) + .75*DIFF
273              GO TO 373
274          372 NE(IT) = NEW + 0.25*DIFF
275          373 NTIMES(IT) = NGO
276          300 CONTINUE
             C
             C       IF THE ITERATION DOES NOT CONVERGE AFTER THE ALLOWED NUMBER OF
             C       PASSES, A WARNING MESSAGE IS GENERATED.
             C
277              WRITE(3, 110) TEMP(IT), NTIMES(IT)
278              WRITE(3, 111)
279          200 CONTINUE
             C
             C       FRACTIONS IN EACH ION STATE ARE CONVERTED TO PERCENT AND RESULTS
             C       OF THE ITERATIONS ARE WRITTEN OUT.
             C
280              CALL DVCHK (ICODE)
281              GO TO (630, 635), ICODE
282          630 CALL REVIVE (1, IGO, 1, NMETAL, V1, V2, EXCTA, EXCTI, AW)
283              GO TO 600
284          635 IMETAL = NMETAL -4
285              DO 425  IT=1,NTEMPS
286              DO 357  J=1, NMETAL
287              NA0(J, IT) = 100.0*NA0(J, IT)
288              NA1(J, IT) = 100.0*NA1(J, IT)
```

PROGRAM 1 (CONTINUED)

```
289         357 NA2(J, IT) = 100.0*NA2(J, IT)
290             INDEX = IT - (IT/3)*3 + 1
291             GO TO (426, 427, 426, 426), INDEX
292         427 WRITE(3, 105)
293         426 ITEMP = IFIX(TEMP(IT))
294             IT1 = ITEMP/1000
295             IT2 =(ITEMP - IT1*1000)/100
296             IT3 = (ITEMP - IT1*1000 - IT2*100)/10
297             IT4  = ITEMP - IT1*1000 - IT2*100 - IT3*10
298             WRITE(3, 106) IT1, IT2, IT3, IT4, DELTA(IT), DEBYE(IT), NTOTAL(IT)
               2, NE(IT), NTIMES(IT)
299             WRITE(3, 130) NMAX(IT), ATMP
300             WRITE(3, 107)
301             WRITE(3, 108) (X0(J,IT), X1(J,IT), X2(J,IT), NA0(J,IT), NA1(J,IT),
               2NA2(J,IT), Q1(J,IT), Q2(J,IT), Q3(J,IT), J=1,4)
302             IF(IMETAL) 435, 425, 435
303         435 WRITE(3, 112) NAME5, X0(5, IT), X1(5,IT), X2(5,IT), NA0(5,IT),
               2NA1(5,IT), NA2(5,IT), Q1(5,IT), Q2(5,IT), Q3(5,IT)
304             GO TO (425, 430, 430),IMETAL
305         430 WRITE(3, 112) NAME6, X0(6,IT), X1(6,IT), X2(6,IT), NA0(6,IT),
               2NA1(6,IT), NA2(6,IT), Q1(6,IT), Q2(6,IT), Q3(6,IT)
306             GO TO (425, 425, 431), IMETAL
307         431 WRITE(3, 112) NAME7, XC(7,IT), X1(7,IT), X2(7,IT), NAC(7,IT),
               2NA1(7,IT), NA2(7,IT), Q1(7,IT), Q2(7,IT), Q3(7,IT)
308             WRITE(3, 109)
309         425 CONTINUE
            C
            C     VARIOUS INTENSITY RATIOS ARE CALCULATED AND NORMALIZED TO 1.0 AT
            C     THE LOWEST TEMPERATURE CONSIDERED.
            C
310             GO TO (997, 500, 500), IMETAL
311         500 DO 510  I=1,NTEMPS
312             DO 540  J=5,6
313         540 Q2Q1(J,I) = Q2(J,I)/Q1(J,I)
314             KRATIO(I) = K1(5,I)/K1(6,I)
```

PROGRAM 1 (CONTINUED)

```
315             QATOM(I) = Q1(6,I)/Q1(5,I)
316             QION(I) = Q2(6,I)/Q2(5,I)
317             SAHAA(I) = NA0(5,I)/NA0(6,I)
318             SAHAI(I) = NA1(5,I)/NA1(6,I)
319             EXPONA(I) =  EXP((EXCTA(6)-EXCTA(5))/(.6950293*TEMP(I)))
320         510 EXPONI(I) =  EXP((EXCTI(6)-EXCTI(5))/(.6950293*TEMP(I)))
321             QA = QATOM(1)
322             QI = QION(1)
323             EA = EXPONA(1)
324             EI = EXPONI(1)
325             SA = SAHAA(1)
326             SI = SAHAI(1)
327             DO 520  I=1,NTEMPS
328             QATOM(I) = QATOM(I)/QA
329             QION(I) = QION(I)/QI
330             SAHAA(I) = SAHAA(I)/SA
331             SAHAI(I) = SAHAI(I)/SI
332             EXPONA(I) = EXPONA(I)/EA
333             EXPONI(I) = EXPONI(I)/EI
334             TOTALA(I) = QATOM(I)*SAHAA(I)*EXPONA(I)
335         520 TOTALI(I) = QION(I)*SAHAI(I)*EXPONI(I)
            C
            C     RESULTS OF THE INTENSITY RATIO CALCULATIONS ARE WRITTEN OUT.
            C
336             WRITE(3,105)
337             WRITE(3, 113) NAME5, V1(5), V2(5), NAME6, V1(6), V2(6)
338             WRITE(3, 114)
339             WRITE(3, 115)
340             WRITE(3, 114)
341             WRITE(3, 116) (TEMP(I), QION(I), SAHAI(I), EXPONI(I), TOTALI(I),
                2I=1, NTEMPS)
342             WRITE(3, 114)
343             WRITE(3, 105)
344             WRITE(3, 117) NAME5, V1(5), V2(5), NAME6, V1(6), V2(6)
345             WRITE(3, 114)
```

PROGRAM 1 (CONTINUED)

```
346             WRITE(3, 115)
347             WRITE(3, 114)
348             WRITE(3, 116) (TEMP(I), QATOM(I), SAHAA(I), EXPONA(I), TOTALA(I),
               2I=1, NTEMPS)
349             WRITE(3, 114)
350             DO 535  J=5,6
351             WRITE(3, 105)
352             WRITE(3, 143) (ENAME(J,JJ), JJ=1,3)
353             WRITE(3, 114)
354             WRITE(3, 144)
355             WRITE(3, 114)
356             WRITE (3, 145) (TEMP(I), Q1(J,I), Q2(J,I), Q2Q1(J,I), I=1,
               2NTEMPS)
357         535 WRITE(3, 114)
358             WRITE(3, 105)
359             WRITE(3, 136)
360             WRITE(3, 114)
361             WRITE(3, 137) NAME5, NAME6
362             WRITE(3, 114)
363             WRITE(3, 138) (TEMP(I), K1(5,I), K1(6,I), KRATIO(I), I=1,NTEMPS)
364             WRITE(3, 114)
365             DO 530  I=1, NTEMPS
366         530 TPLOT(I) = XWAY*TEMP(I)
367             CALL EXCITE (NTEMPS, TEMP, QATOM, QION, SAHAA, SAHAI, DLAB1,
               2XMIN, XSF, TPLOT, IPLOT)
368             GO TO (997, 533), IPLOT
369         533 CALL FINISH (DLAB1, QATOM, QION, SAHAA, SAHAI, EXPONA, EXPONI,
               2TOTALA, TOTALI, NTEMPS,TPLOT, XMIN, XSF)
370         997 READ(1, 140) CHECK
371             IF(CHECK .EQ. HALT)  GO TO 600
372             CALL REVIVE(1, IGO, NMETAL, V1, V2, EXCTA, EXCTI, AW)
373             GO TO 600
374             END
```

PROGRAM 1 (CONTINUED)

```
 1              SUBROUTINE FINISH (DLAB1, QATOM, QION, SAHAA, SAHAI, EXPONA,
               2EXPONI, TOTALA, TOTALI, NTEMPS, TEMP, XMIN, XSF)
 2              DIMENSION DLAB1(5), QATOM(30), QION(30), SAHAA(30), SAHAI(30),
               2EXPONA(30), EXPONI(30), TOTALA(30), TOTALI(30), XLAB(5),
               3YLAB(5), DL1(5), DL2(5), DL3(5), DL4(5), DL5(5), DL6(5),
               4XX(3), YY(3), TEMP(30)
         C
         C      LOG VALUES OF ALL RATIOS ARE CALCULATED AND THE RESULTS ARE
         C      PLOTTED AS LOG INTENSITY RATIO VERSUS TEMPERATURE.
         C
 3              DO 530  I=1, NTEMPS
 4              QATOM(I) = ALOG10(QATOM(I))
 5              QION(I) = ALOG10(QION(I))
 6              SAHAA(I) = ALOG10(SAHAA(I))
 7              SAHAI(I) = ALOG10(SAHAI(I))
 8              EXPONA(I) = ALOG10(EXPONA(I))
 9              EXPONI(I) = ALOG10(EXPONI(I))
10              TOTALA(I) = ALOG10(TOTALA(I))
11          530 TOTALI(I) = ALOG10(TOTALI(I))
12              DATA XLAB/'TEMP', 'ERAT', 'URE ', '(K) ', '    '/,YLAB/'LOG ',
               2'INTE', 'NSIT', 'Y RA', 'TIO '/, DL6/'TOTA', 'L RA', 'TIO ',
               3'    ', '    '/
13              DATA DL1/'EXPO', 'NENT', 'IAL ', 'TERM', '    '/, DL2/'ICNI', 'ZAT
               2I', 'ON T', 'ERM ', '    '/,DL3/'PART', 'ITIO', 'N FU', 'NCTI',
               3'ON  '/,DL4/'TWO ', 'ICN ', 'LINE', 'S   ', '    '/, DL5/'TWO ',
               4'ATOM', ' LIN', 'ES  ', '    '/
14              XSIZE = 6.0
15              XX(1) = XMIN
16              XX(2) = XMIN +XSIZE*XSF
17              XX(3) = XX(2)
18              CALL YSCALE(EXPONA, SAHAA, QATOM, TOTALA, YSIZE, YMIN, YSF,
               2NTEMPS)
19              YY(1) = YMIN + YSIZE*YSF
20              YY(2) = YY(1)
21              YY(3) = YMIN
```

PROGRAM 1 (CONTINUED)

```
      800 CALL ORIGIN (10., 0.0, 1)
          CALL GRAPH (3, XX, YY, 2, 4, XSIZE, YSIZE, XSF, XMIN, YSF, YMIN,
     1XLAB, YLAB, DLAB1, DL5)
          CALL GRAPH (NTEMPS, TEMP, EXPONA, 1, 103, 0, 0, 0, 0, 0, 0, 0, 0,
     20, DL1)
          CALL GRAPH (NTEMPS, TEMP, SAHAA, 10, 103, 0, 0, 0, 0, 0, 0, 0, 0,
     20, DL2)
          CALL GRAPH (NTEMPS, TEMP, QATOM,  4, 103, 0, 0, 0, 0, 0, 0, 0, 0,
     20, DL3)
          CALL ORIGIN(10.0, 0.0, 1)
          CALL GRAPH (3, XX, YY, 2, 4, XSIZE, YSIZE, XSF, XMIN, YSF, YMIN,
     2XLAB, YLAB, DLAB1, DL5)
          CALL GRAPH (NTEMPS, TEMP, TOTALA, 1, 103, 0, 0, 0, 0, 0, 0, 0, 0,
     20, DL6)
          CALL YSCALE (EXPONI, SAHAI, QION, TOTALI, YSIZE, YMIN, YSF,
     2NTEMPS)
          YY(1) = YMIN + YSIZE*YSF
          YY(2) = YY(1)
          YY(3) = YMIN
      900 CALL ORIGIN(10.0, 0.0, 1)
          CALL GRAPH (3, XX, YY, 2, 4, XSIZE, YSIZE, XSF, XMIN, YSF, YMIN,
     2XLAB, YLAB, DLAB1, DL4)
          CALL GRAPH (NTEMPS, TEMP, EXPONI, 1, 103, 0, 0, 0, 0, 0, 0, 0, 0,
     20, DL1)
          CALL GRAPH (NTEMPS, TEMP, SAHAI, 10, 103, 0, 0, 0, 0, 0, 0, 0, 0,
     20, DL2)
          CALL GRAPH (NTEMPS, TEMP, QION, 4, 103, 0, 0, 0, 0, 0, 0, 0, 0, 0,
     2DL3)
          CALL ORIGIN (10.0, 0.0, 1)
          CALL GRAPH (3, XX, YY, 2, 4, XSIZE, YSIZE, XSF, XMIN, YSF, YMIN,
     2XLAB, YLAB, DLAB1, DL4)
          CALL GRAPH (NTEMPS, TEMP, TOTALI, 1,  103, 0, 0, 0 , 0, 0, 0, 0,
     20, 0, DL6)
          RETURN
          END
```

PROGRAM 1 (CONTINUED)

```
  1            SUBROUTINE YSCALE (W, X, Y, Z, YSIZE, YMIN, YSF, N)
               C
               C     THE PURPOSE OF THIS SUBROUTINE IS TO DETERMINE THE Y-AXIS SCALING
               C     FOR THE LOG IRATIO VERSUS TEMPERATURE PLOTS.
               C
  2            DIMENSION W(30), X(30), Y(30), Z(30)
  3            XBIG = 0.0
  4            XLIT = 0.0
  5            YSIZE = 6.0
  6            YSF = 1.0
  7            DO 25  I=1, N
  8            IF(XBIG - X(I)) 1, 2, 2
  9          1 XBIG = X(I)
 10          2 IF(XBIG - Y(I)) 3, 4, 4
 11          3 XBIG = Y(I)
 12          4 IF(XBIG - Z(I)) 5, 6, 6
 13          5 XBIG = Z(I)
 14          6 IF(XBIG - W(I)) 7, 8, 8
 15          7 XBIG = W(I)
 16          8 IF(XLIT - X(I)) 10, 10, 9
 17          9 XLIT = X(I)
 18         10 IF(XLIT - Y(I)) 12, 12, 11
 19         11 XLIT = Y(I)
 20         12 IF(XLIT - Z(I)) 14, 14, 13
 21         13 XLIT = Z(I)
 22         14 IF(XLIT - W(I)) 25, 25, 15
 23         15 XLIT = W(I)
 24         25 CONTINUE
 25            DIFF = XBIG - XLIT
 26            IF(DIFF - 4.0)  75, 40, 40
 27         75 YSF = 0.8
 28            IF(DIFF - 3.5) 70, 40, 40
 29         70 YSF = 0.7
 30            IF (DIFF - 3.0) 50, 40, 40
 31         50 YSF = 0.6
```

PROGRAM 1 (CONTINUED)

```
      IF(DIFF - 2.5) 80, 40, 40
   80 YSF = 0.5
      IF(DIFF - 2.0) 60, 40, 40
   60 YSF = 0.4
      IF(DIFF - 1.5) 30, 40, 40
   30 YSF = 0.3
      IF (DIFF - 1.0) 35, 40, 40
   35 YSF = 0.2
   40 ILIT = IFIX(XLIT*10.0)
      YMIN = FLOAT(ILIT)/10.0 - 0.1
      RETURN
      END
```

PROGRAM 1 (CONTINUED)

```
1            SUBROUTINE EXCITE (NTEMPS, TEMP, QATOM, QION, SAHAA, SAHAI, GLAB,
            2XMIN, XSE, TPLOT, IPLOT)
      C
      C     THE PURPOSE OF THIS SUBROUTINE IS TO EXAMINE THE EFFECT OF VARIOUS
      C     EXCITATION ENERGY MISMATCHES ON INTENSITY RATIO BEHAVIOR.
      C
      C     DIFF VALUES ARE TREATED AS EXCITATION ENERGY OF NUMERATOR ELEMENT
      C     MINUS EXCITATION ENERGY OF DENOMINATOR ELEMENT.
      C
2            DIMENSION TEMP(30), QATOM(30), QION(30), SAHAA(30), SAHAI(30),
            2XLAB(5), YLAB(5), DLATOM(5), DLION(5), GLAB(5), DLW(5), DLX(5),
            3DLY(5), DLZ(5), W(30), X(30), Y(30), Z(30), ZTERM(30), XTERM(30),
            4WTERM(30), YTERM(30), TPLOT(30)
3         100 FORMAT (I5)
4         101 FORMAT (F10.0, 5A4)
5         102 FORMAT(10X, 5('*'), 'ERROR---NUMBER OF PLOTS PER GRAPH CAN NOT EXC
            2EED 4 - - - THIS PHASE OF PROGRAM ABANDONED')
      C
      C     THE RCUTINE BEGINS BY SETTING UP SOME OF THE LABELS, READING THE
      C     NUMBER OF OVERPLOTS (MAXIMUM OF 4) AND INITIALIZING THE RATIO
      C     ARRAYS TO ZERO.
      C
6            DATA XLAB/'TEMP', 'ERAT', 'URE ',  '(K) ', '    '/, YLAB/'LOG ',
            2'INTE', 'NSIT', 'Y RA', 'TIO'/, DLATOM/'TWO ', 'ATOM', ' LIN',
            3'ES  ', '    '/, DLION/'TWO ', 'ION ', 'LINE', 'S   ', '    '/
7          50 READ (1, 100) NPLOTS
8             IF(NPLOTS .LE. 0)  RETURN
9             IF(NPLOTS .LE. 4) GO TO 52
10            WRITE(3, 102)
11            RETURN
12         52 DO 51 I=1,30
13            W(I) = 0.0
14            X(I) = 0.0
15            Y(I) = 0.0
16         51 Z(I) = 0.0
```

PROGRAM 1 (CONTINUED)

```
C
C     THE ROUTINE READS IN THE ENERGY LEVEL DIFFERANCE AND DESCRIPTIVE
C     LABEL (USED FOR GRAPH) FOR EACH.
C
      GO TO (10, 20, 30, 40), NPLOTS
   40 READ (1, 101) ZDIFF, DLZ
   30 READ (1, 101) YDIFF, DLY
   20 READ (1, 101) XDIFF, DLX
   10 READ (1, 101) WDIFF, DLW
C
C     THE EXPONENTIAL TERMS ARE CALCULATED AND NORMALIZED TO ONE AT THE
C     LOWEST TEMPERATURE VALUE.
C
      DO 150  I=1, NTEMPS
      GO TO (110, 120, 130, 140), NPLOTS
  140 ZTERM(I) = EXP(-ZDIFF/(.6950293*TEMP(I)))
  130 YTERM(I) = EXP(-YDIFF/(.6950293*TEMP(I)))
  120 XTERM(I) = EXP(-XDIFF/(.6950293*TEMP(I)))
  110 WTERM(I) = EXP(-WDIFF/(.6950293*TEMP(I)))
  150 CONTINUE
      ZNORM = ZTERM(1)
      YNORM = YTERM(1)
      XNORM = XTERM(1)
      WNORM = WTERM(1)
      DO 175  I=1, NTEMPS
      GO TO (190, 180, 170, 160), NPLOTS
  160 ZTERM(I) = ZTERM(I)/ZNORM
  170 YTERM(I) = YTERM(I)/YNORM
  180 XTERM(I) = XTERM(I)/XNORM
  190 WTERM(I) = WTERM(I)/WNORM
  175 CONTINUE
C
C     THE INTENSITY RATIOS FOR TWO ATOM AND TWO ION LINES ARE NOW
C     CALCULATED, WRITTEN OUT (USING EWRITE), AND PLOTTED (USING
C     EPLOT).
```

PROGRAM 1 (CONTINUED)

```
      C
40          DO 200  I=1, NTEMPS
41          GO TO (210, 220, 230, 240), NPLOTS
42        240 Z(I) = SAHAA(I)*QATOM(I)*ZTERM(I)
43        230 Y(I) = SAHAA(I)*QATOM(I)*YTERM(I)
44        220 X(I) = SAHAA(I)*QATOM(I)*XTERM(I)
45        210 W(I) = SAHAA(I)*QATOM(I)*WTERM(I)
46        200 CONTINUE
47            CALL EWRITE(NTEMPS, NPLOTS, TEMP, W, X, Y, Z, ZDIFF, YDIFF, XDIFF,
             2WDIFF, GLAB, 1)
48            GO TO (410, 405), IPLOT
49        405 CALL EPLOT (NTEMPS, NPLOTS,TPLOT, W, X, Y, Z, XLAB, YLAB, GLAB,
             2DLATOM, DLW, DLX, DLY, DLZ, XMIN, XSF)
50        410 DO 300  I=1, NTEMPS
51            GO TO (310, 320, 330, 340), NPLOTS
52        340 Z(I) = SAHAI(I)*QION(I)*ZTERM(I)
53        330 Y(I) = SAHAI(I)*QION(I)*YTERM(I)
54        320 X(I) = SAHAI(I)*QION(I)*XTERM(I)
55        310 W(I) = SAHAI(I)*QION(I)*WTERM(I)
56        300 CONTINUE
57            CALL EWRITE(NTEMPS, NPLOTS, TEMP, W, X, Y, Z, ZDIFF, YDIFF, XDIFF,
             2WDIFF, GLAB, 2)
58            GO TO (420, 415), IPLOT
59        415 CALL EPLOT (NTEMPS, NPLOTS,TPLOT, W, X, Y, Z, XLAB, YLAB, GLAB,
             2DLION, DLW, DLX, DLY, DLZ, XMIN, XSF)
60        420 GO TO 50
61            END
```

PROGRAM 1 (CONTINUED)

```
 1            SUBROUTINE EWRITE(NTEMPS, NPLOTS, TEMP, W, X, Y, Z, ZDIFF, YDIFF,
             2XDIFF, WDIFF, GLAB, ITYPE)
 2            DIMENSION TEMP(30), W(30), X(30), Y(30), Z(30), GLAB(5), DL1(5),
             2DL2(5)
       C
       C     THIS SUBROUTINE WRITES OUT THE DATA FROM EXCITE.
       C
 3         100 FORMAT (1H1//////)
 4         102 FORMAT (30X, 5A4, 20X, 5A4/)
 5         103 FORMAT (30X, 60('-'))
 6         104 FORMAT (60X, 'TOTAL RATIO BEHAVIOR'/34X, 'TEMPERATURE (K)',
              2F10.0, 3F9.0)
 7         105 FORMAT (60X, 'TOTAL RATIO BEHAVIOR'/34X, 'TEMPERATURE (K)',
              2F10.0, F13.0, F14.0)
 8         106 FORMAT (60X, 'TOTAL RATIO BEHAVIOR'/34X, 'TEMPERATURE (K)',
              26X, F9.0, F17.0)
 9         107 FORMAT (60X, 'TOTAL RATIO BEHAVIOR'/34X, 'TEMPERATURE (K)',
              213X, F10.0)
10         108 FORMAT (5(35X, F9.0, F15.3, 3F9.3/))
11         109 FORMAT (5(35X, F9.0, F15.3, F13.3, F14.3/))
12         110 FORMAT (5(35X, F9.0, 11X, F9.3, F17.3/))
13         111 FORMAT (5(35X, F9.0, 16X, F12.3/))
14             WRITE(3,100)
15             DATA DL1 /'    ', '  TW', 'O AT', 'OM L', 'INES'/
16             DATA DL2 /'    ', '   T', 'WO I', 'ON L', 'INES'/
17             GO TO (10, 20), ITYPE
18          10 WRITE(3, 102) GLAB, DL1
19             GO TO 25
20          20 WRITE(3, 102)  GLAB, DL2
21          25 WRITE (3,103)
22             GO TO (31, 32, 33, 34), NPLOTS
23          34 WRITE (3,104) WDIFF, XDIFF, YDIFF, ZDIFF
24             GO TO 35
25          33 WRITE (3,105) WDIFF, XDIFF, YDIFF
26             GO TO 35
```

PROGRAM 1 (CONTINUED)

```
27          32 WRITE (3,106) WDIFF, XDIFF
28             GO TO 35
29          31 WRITE (3,107) WDIFF
30          35 WRITE (3,103)
31             GO TO (210, 220, 230, 240), NPLOTS
32         240 WRITE(3,108) (TEMP(I), W(I), X(I), Y(I), Z(I), I=1,NTEMPS)
33             GO TO 250
34         230 WRITE(3,109) (TEMP(I), W(I), X(I), Y(I), I=1,NTEMPS)
35             GO TO 250
36         220 WRITE(3,110) (TEMP(I), W(I), X(I), I=1,NTEMPS)
37             GO TO 250
38         210 WRITE(3,111) (TEMP(I), W(I), I=1,NTEMPS)
39         250 WRITE(3,103)
40             RETURN
41             END
```

PROGRAM 1 (CONTINUED)

```
1            SUBROUTINE EPLOT (NTEMPS, NPLOTS, TEMP, W, X, Y, Z, XLAB, YLAB,
            2GLAB, DLAB, DLW, DLX, DLY, DLZ, XMIN, XSF)
      C
      C      THE PURPOSE OF THIS SUBROUTINE IS TO CALCULATE THE LOGS OF THE
      C      INTENSITY RATIOS GENERATED IN SUBROUTINE EXCITE AND PLOT THEM.
      C
2            DIMENSION W(30), X(30), Y(30), Z(30), TEMP(30), XX(3), YY(3),
            2XLAB(5), YLAB(5), DLAB(5),GLAB(5),DLW(5), DLX(5), DLY(5), DLZ(5)
3            XSIZE = 6.0
4            XX(1) = XMIN
5            XX(2) = XMIN + XSIZE*XSF
6            XX(3) = XX(2)
7            DO 5 I=1, NTEMPS
8            GO TO (1, 2, 3, 4), NPLOTS
9          4 Z(I) = ALOG10(Z(I))
10         3 Y(I) = ALOG10(Y(I))
11         2 X(I) = ALOG10(X(I))
12         1 W(I) = ALOG10(W(I))
13         5 CONTINUE
14           CALL YSCALE (W, X, Y, Z, YSIZE, YMIN, YSF, NTEMPS)
15           YY(1) = YMIN + YSIZE*YSF
16           YY(2) = YY(1)
17           YY(3) = YMIN
18           CALL ORIGIN (10.0, 0.0, 1)
19           CALL GRAPH (3, XX, YY, 2, 4, XSIZE, YSIZE, XSF, XMIN, YSF, YMIN,
            2XLAB, YLAB, GLAB, DLAB)
20           GO TO (10, 20, 30, 40), NPLOTS
21        40 CALL GRAPH (NTEMPS, TEMP, Z,  1, 103, 0,0,0,0,0,0,0,0,0, DLZ)
22        30 CALL GRAPH (NTEMPS, TEMP, Y, 10, 103, 0,0,0,0,0,0,0,0,0, DLY)
23        20 CALL GRAPH (NTEMPS, TEMP, X,  4, 103, 0,0,0,0,0,0,0,0,0, DLX)
24        10 CALL GRAPH (NTEMPS, TEMP, W,  2, 103, 0,0,0,0,0,0,0,0,0, DLW)
25           RETURN
26           END
```

PROGRAM 1 (CONTINUED)

```
      SUBROUTINE REVIVE (IACT, IGO, IFT, NMETAL, V1, V2, EXCTA, EXCTI,
     2AW)
C
C     THE PURPOSE OF THIS SUBROUTINE IS TO CHECK CERTAIN VARIABLES TO
C     INSURE PROPER VALUES AND TO PROVIDE A MEANS FOR THE
C     PROGRAM TO RECOVER IF A BAD DATA SET IS PRESENT AMONG A BATCH.
C
      DIMENSION EXCTA(7), EXCTI(7), AW(7), V1(7), V2(7)
  100 FORMAT (1H0, 9X, 90('*')/10X, 'AN ERROR HAS BEEN DETECTED IN THE D
     2ATA FOR THIS SIMULATION RUN'/10X, 'IF SEVERAL EXAMPLES ARE BEING R
     3UN IN A BATCHED MODE, AN ATTEMPT TO RECOVER HAS BEEN MADE'/10X,
     490('*'))
  101 FORMAT (A4)
  102 FORMAT (1H0, 9X, 'ERROR DETECTED WHICH INDICATES THAT THE INPUT DA
     2TA IS PROBABLY ARRANGED INCORRECTLY'/10X, 'ALSO CHECK TO BE CERTAI
     3N THAT ALL ENERGIES ARE IN WAVENUMBERS.')
      DATA HALT/'STOP'/
      GO TO (200, 10), IACT
   10 DO 20 I=5, NMETAL
      IF(V1(I) .LE. 30000.0)  GO TO 300
      IF(V2(I) .LE. 30000.0)  GO TO 300
      IF(AW(I) .LE. 0.0) GO TO 300
   20 CONTINUE
      ISTOP = 5
      IF(NMETAL .GT. 5) ISTOP = 6
      DO 30  I=5, ISTOP
      IF(EXCTA(I) .LE. 5000.0)  GO TO 300
      IF(EXCTI(I) .LE. 5000.0)  GO TO 300
      IF(EXCTA(I) .GT. 5.0E+05) GO TO 300
      IF(EXCTI(I) .GT. 5.0E+05) GO TO 300
   30 CONTINUE
      IGO = 1
      RETURN
C
C     IF AN IMPROPER DATA SET IS DETECTED, THE SUBROUTINE CHECKS ALL
```

PROGRAM 1 (CONTINUED)

```
C      DATA CARDS UNTIL THE "STOP" CONTROL CARD IS FOUND.  CONTROL THEN
C      PASSES TO STATEMENT 600 IN THE MAIN PROGRAM.
C
   300 WRITE (3, 102)
   200 WRITE(3, 100)
       IGO = 2
   210 READ(1, 101) CHECK
       IF(CHECK .NE. HALT)  GO TO 210
       IF(IFT .LT. 4)  RETURN
       REWIND IFT
    25 RETURN
       END
```

PROGRAM 1 (CONTINUED)

ACKNOWLEDGMENTS

During the period of metamorphosis of the investigation described in this dissertation from a few vague ideas to its present status, many individuals provided the author with assistance which is greatly appreciated. Those deserving of special mention are:

Dr. Velmer A. Fassel who originally suggested the study and provided valuable guidance during the course of the investigation;

Other members of the spectrochemistry group, especially Mr. Richard Kniseley and Mr. George Dickinson, whose discussions and ideas contributed much to the final completion of this study; and

Mr. Gary Wells and his fine group of craftsmen who aided in the design and construction of much of the experimental equipment employed in the investigation.